TAMPEREEN TEKNILLINEN YLIOPISTO
TAMPERE UNIVERSITY OF TECHNOLOGY

TEPPO NORONEN

LONG-WAVELENGTH MODE-LOCKED BISMUTH FIBER LASERS

Master of Science thesis

Examiner: Academy Postdoctoral Researcher Regina Gumenyuk
Examiner and topic approved by the Faculty Council of the Faculty of Natural Sciences
on 4th May 2016

ABSTRACT

TEPPO NORONEN: Long-Wavelength Mode-Locked Bismuth Fiber Lasers
Tampere University of technology
Master of Science Thesis, 62 pages, 12 Appendix pages
May 2016
Master's Degree in Science and Engineering
Major: Technical Physics
Examiner: Academy Postdoctoral Researcher Regina Gumenyuk

Keywords: fiber laser, bismuth, ultrafast optics, mode-locking

Ultrafast lasers producing short, intense pulses are of great interest for both optical science community and laser industry. The applications of ultrafast lasers range from medicine and optical communications to material processing. At present, especially ultrafast fiber lasers have attracted considerable amount of interest as a result of their superior beam quality, straightforward optical alignment and effortless cooling. However, the wavelength range of current fiber lasers is limited, due to the absence of suitable gain materials. Today, fiber devices mainly operate at ~1 μm (ytterbium lasers), ~1.55 μm (erbium lasers) and ~2 μm (thulium and holmium lasers).

In this thesis, novel active fibers based on bismuth-doped glasses were exploited for the generation of ultrashort pulses at 1450 nm and 1730 nm. These spectral regions are not covered by the more well-established gain fibers. However, these new wavelengths are extremely interesting because of their potential for optical communications, medical applications and gas detection systems.

At 1450 nm wavelength, a bismuth fiber system capable of producing 240 fs optical pulses was designed and demonstrated. These are the shortest optical pulses generated by bismuth-doped fiber lasers to date. The achieved pulse energy was 0.75 nJ after careful dispersion management and amplification in separate power amplifier. At 1730 nm wavelength, a bismuth-doped fiber laser delivered 1.65 ps and 1.2 ps pulses in anomalous and normal dispersion regimes, respectively. This 1700 nm spectral region is novel for ultrafast pulse generation and has not been demonstrated before to the best of author's knowledge.

TIIVISTELMÄ

TEPPO NORONEN: Long-Wavelength Mode-Locked Bismuth Fiber Lasers
Tampereen teknillinen yliopisto
Diplomityö, 62 sivua, 12 liitesivua
Toukokuu 2016
Teknis-luonnontieteellinen tutkinto-ohjelma
Pääaine: Teknillinen fysiikka
Tarkastaja: Tutkijatohtori Regina Gumenyuk

Avainsanat: kuitulaser, vismutti, ultranopea optiikka, muotolukitus

Lyhyitä optisia pulsseja tuottavia lasereita käytetään nykyisin laajasti sekä tutkimuksessa että teollisuudessa. Sovelluskohteita ovat esimerkiksi lääketiede, optinen tiedonsiirto sekä materiaalien työstö. Viime aikoina erityisesti kuitulaserit ovat saavuttaneet suurta huomiota helppokäyttöisyytensä ansiosta. Kuitulasereissa valo kulkee valokuidun sisällä, jolloin vältytään erilaisilta kohdistusongelmilta, joita esiintyy monimutkaisia linssisysteemejä sisältävissä lasereissa. Lisäksi kuitulasereista saatava säteen laatu on erinomainen, ja niiden tuottaman lämmön hallinta on helppoa valokuidun ominaisuuksien ansiosta. Valokuidun pinta-ala on suuri suhteessa sen tilavuuteen, ja tämän vuoksi sen jäähdytys on verrattain helppoa. Nykyisillä kuitulasereilla saavutettavat aallonpituusalueet ovat kuitenkin rajoitettuja saatavilla olevien niin sanottujen aktiivisten kuitujen vuoksi. Aktiivisia kuituja käytetään kuitulasereissa vahvistinmateriaalina. Tällä hetkellä kuitulaserit toimivat lähinnä noin 1 μm:n (ytterbium-laserit), noin 1,55 μm:n (erbium-laserit) ja noin μm:n (tulium- ja holmium-laserit) aallonpituusalueilla.

Tässä työssä tarkoituksena oli kehittää vismuttikuituun perustuvia, lyhyitä pulsseja tuottavia lasereita 1450 ja 1730 nanometrin aallonpituuksille. Näitä aallonpituuksia ei saavuteta käyttäen perinteisiä aktiivikuituja, mutta kyseisten aallonpituuksien potentiaaliset sovelluskohteet ovat kuitenkin huomattavat. Esimerkiksi noin 1450 nanometrin aallonpituus on luonnollinen laajennus nykyiseen tiedonsiirrossa käytettyyn optiseen kaistaan, joka rajoittuu käytännössä noin 1530–1560 nanometrin alueelle. Pidemmällä 1730 nanometrin aallonpituudella toimivan laserin sovelluskohteita ovat esimerkiksi lääketiede, erilaiset kaasupitoisuuksien mittalaitteet, sekä lasereihin perustuva etäisyysmittaus.

Työssä kehitettiin 1450 nanometrin aallonpituudella toimiva vismutti-kuituun perustuva laser, sekä erillinen kuituvahvistin. Näiden yhdistelmällä saavutettiin tälle aallonpituudelle ja vismutti-kuiduille ennätyksellisiä 240 femtosekunnin pulsseja, joiden energia oli vahvistuksen jälkeen 0,75 nanojoulea. Myös pidemmällä 1730 nanometrin aallonpituudella saavutettiin lyhyitä, 1,2 pikosekunnin mittaisia pulsseja. 1730 nanometrin aallonpituus on täysin ainutlaatuinen kuitulasereille, eikä tällä aallonpituudella toimivia pulsseja tuottavia kuitulasereita ole aiemmin tutkittu.

PREFACE

This work has been carried out at Optoelectronics Research Centre (ORC) in Tampere University of Technology.

I would like to thank the administration of ORC for giving me the opportunity to work in world class, highly academic environment at ORC. Especially I would like to thank Pekka Savolainen and Anne Viherkoski for their help during the unpredicted circumstances at the final stage of this thesis.

I want to thank Regina Gumenyuk for her help in the laboratory and for many helpful discussions. She has offered me invaluable help especially during the start of my research career. Moreover, I want to thank her for acting as an examiner of this thesis on such a short notice.

As well, I would want to thank Esa Saarinen and Antti Saarela for their help regarding semiconductor disk lasers which were used as a pump source in this work. I also want to thank other people of Ultrafast and intense optics -group for their help and support.

I thank Fiber Optic Research Centre (FORC) of the Russian Academy of Sciences and research group of Professor E. M. Dianov for providing us the bismuth-doped optical fibers. Without these fibers, the experimental part of this work would have not been possible.

In memory of Professor Oleg Okhotnikov, my previous supervisor, who unfortunately was not able to see the final version of this thesis.

Tampere, 13.5.2016

Teppo Noronen

CONTENTS

LIST OF SYMBOLS AND ABBREVIATIONS

β_2	Second-order dispersion
β_3	Third-order dispersion
β_3	Nonlinear parameter
λ	Optical wavelength
ν	Optical frequency
ω	Oscillation frequency
σ	Transition cross-section
τ	Lifetime
a	Radius of the fiber core
A	Pulse envelope
c	Speed of light in vacuum
E	Energy
f	Thermal occupation of energy level
F	Fluence
h	Planck's constant
k_0	Wave number
L	Cavity length
n	Index of refraction
N	Number of ions
r	Pump rate
T	Time
V	V-parameter
q	Quantum efficiency
z	Distance

2-D	Two dimensional
BDFA	Bismuth-doped fiber amplifier
Bi	Bismuth
CFBG	Chirped fiber Bragg grating
CNT	Carbon nanotube
CO_2	Carbon dioxide
CPA	Chirped pulse amplification
CW	Continuous wave (laser)
DBR	Distributed Bragg reflector
DCF	Dispersion compensating fiber
EDFA	Erbium-doped fiber amplifier
Er	Erbium
ESA	Excited state absorption
FBG	Fiber Bragg grating
FWM	Four-wave mixing
GaAs	Gallium arsenide
GeO_2	Germanium dioxide
Ho	Holmium
InGaAs	Indium gallium arsenide
LASER	Light Amplification by Stimulated Emission of Radiation
LIDAR	Light Detection and Ranging, or portmanteau of “light” and “radar”
MCVD	Modified chemical vapor deposition
MOPA	Master oscillator – power amplifier
MUX-DEMUX	multiplexer-demultiplexer, technique used in telecom systems
Nd	Neodymium
NIR	Near-infrared
NLPR	Nonlinear polarization rotation
ODC	Oxygen-deficiency center
OSA	Optical spectrum analyzer
QW	Quantum-well
RFA	Raman fiber amplifier
SDL	Semiconductor disk laser
SESAM	Semiconductor saturable absorber
SiC	Silicon carbide
SiO_2	Silicon dioxide, silica
SMF	Single mode fiber
SMF-28	Standard fiber in telecom systems, brand of Corning
SPM	Self-phase modulation
SWNT	Single-walled carbon nanotube
Tm	Thulium
UV	Ultraviolet
WDM	Wavelength division multiplexer
XPM	Cross-phase modulation
Yb	Ytterbium

1. INTRODUCTION

Ultrafast lasers producing intense light pulses, with pulse durations as short as few femtoseconds, have been widely studied and used for research and applications over the few last decades. For scientists, ultrafast lasers have allowed observing of different non-linear phenomena and exotic pulse dynamics, which were difficult to obtain before. Ultrafast lasers are also suitable for many applications, including for example medicine and micromachining. Typically the repetition rates of pulsed fiber lasers are order of 1-100 MHz, although at least in principle this can be adjusted fairly easily by changing the design parameters of the laser cavity. The pulse energies can range from few pico-joules up to even millijoule range, providing a great diversity of potential applications. Because of energetic pulses with extremely short pulse durations, the ultrafast lasers can easily provide optical peak powers in megawatt-level, and in extreme cases even up to petawatts. The high peak power is preferred in many applications. One example is laser ablation, a method which uses high-intensity laser pulses to convert solids directly to plasma.

In this thesis, the discussion of lasers will be mainly limited to the one member of the laser family: fiber lasers. Fiber lasers and amplifiers, as well as optical fibers in overall, are a great interest also in information technology in addition to the before mentioned industrial and medical applications. Indeed, optical fibers have revolutionized the worldwide data transmission, enabling our modern everyday life. However, the current telecommunication is relying virtually only on erbium-doped fiber amplifiers (EDFAs) that provide signal amplification in a fairly narrow wavelength region between 1530 – 1610 nm. This sets the limit for the wavelength range that can be used for decoding and transmitting information, resulting in limit of the rate of data transfer.

So far the problems encountered as a result of increased demands for data transfer rates have been solved by increasing the number of data channels using a technique called *wavelength division multiplexing* (WDM). This means that increased amount of information can be carried in a single fiber by transmitting multiple signals at different wavelengths (i.e. channels) simultaneously, and separating the different channels in the receiver end (MUX-DEMUX). However, the gain bandwidth of EDFAs sets a practical limit for this technique, since the channels cannot be extended outside of this wavelength range. On the other hand, the channels should have some sufficient separation in frequency domain, so that different channels remain separable in the receiver. Alternative solutions to EDFAs, such as Raman fiber amplifiers (RFAs) are available, but their efficiencies are an order of magnitude lower than those of EDFAs, making them an undesirable solution for commercial applications.

In recent years, bismuth-doped fibers and bismuth-doped fiber amplifiers (BDFAs) have received much attention because of their promising properties that could be suitable for broadband amplification and pulse generation. By using different types of bismuth-doped fibers, optical gain in the wavelength range of 1100 – 1800 nm has been demonstrated. Indeed, since the discovery of near-infrared emission from bismuth-doped glasses, various different optical devices, such as optical amplifiers and fiber lasers have been developed.

The aim of this thesis was to realize bismuth-doped fiber lasers and demonstrate pulse generation at long wavelengths using gain fibers optimized for ~1450 nm and ~1700 nm wavelengths. These wavelengths are not covered efficiently by erbium-doped fiber lasers and amplifiers, but match the low-loss window of silica-glass used in optical fibers. Therefore, in the market there would be a great demand for reliable, highly efficient pulsed laser sources and optical amplifiers at these wavelength regions.

In Chapter 2, first the basic principles of laser light generation are considered. Fiber lasers, which are the main focus of this thesis, are discussed in more detail together with different gain media used in fiber lasers. Especially bismuth-doped fibers are discussed thoroughly, since the experimental part of this work is focused to bismuth-doped fibers.

Chapter 3 includes the detailed discussion of pulsed fiber lasers, focusing mainly on mode-locked lasers. Different types of saturable absorbers are discussed, especially carbon-based saturable absorbers, such as carbon nanotubes and graphene. The effect of cavity dispersion on pulse dynamics of the fiber lasers is discussed, as well as the basic principles of energy scaling using fiber amplifiers.

Chapter 4 includes the detailed experimental results and insights of two mode-locked bismuth fiber laser lasers. First, the experimental work accomplished for achieving pulse generation at 1440 nm is discussed in detail. This includes the cavity design and laser characterization in anomalous and normal dispersion regimes. Power scaling in normal dispersion regime is demonstrated with a dual-purpose BDFA providing both amplification and compression of the pulse. Finally, pulse generation is realized at long wavelength edge of 1730 nm using novel bismuth-doped fibers. The performed experimental work as well as the obtained results are shown and discussed. Finally, Chapter 5 summarizes the work and the results, together with some discussion of the future prospects.

2. LASERS AND GAIN MEDIA

In this chapter, the basic principles of laser action are discussed. More detailed discussion is focused on fiber lasers and gain media used in fiber lasers. Especially, bismuth-doped fibers are considered in high detail. Finally, a brief review of bismuth fiber lasers is given.

2.1 Principle of lasers

Lasers need essentially three elements: gain medium, pumping process to excite the atoms inside the gain medium to achieve population inversion, and reflectors which provide the optical feedback to the laser cavity (Figure 2.1). The word “laser” is actually derived originally from an acronym LASER (Light Amplification by Stimulated Emission of Radiation). The *stimulated emission* is a phenomenon, where an incoming photon with a proper energy is triggering the emission of another photon with same energy. Moreover, the photon created by stimulated emission will acquire same phase as the incident photon, giving raise to the special properties of laser light, such as narrow bandwidth, high coherence and high brightness [1].

For stimulated emission to occur, an occasion called *population inversion* is needed inside the gain medium. Population inversion is a state of the system, where the majority (> 50%) of the atoms or ions of the active medium are located in an excited energy state. Therefore the occasion of population inversion deviates from the state of equilibrium, and additional energy is needed to force the medium to this kind of state. Energy is delivered to the system by exciting, or *pumping*, the atoms to higher energy levels. In case of semiconductor laser diodes the laser is pumped by direct electrical current. On the other hand, for solid-state lasers and especially for fiber lasers, the optical pumping is the most common method. In optical pumping the atoms are excited by pumping them with another light source, usually another laser such as a high-power laser diode.

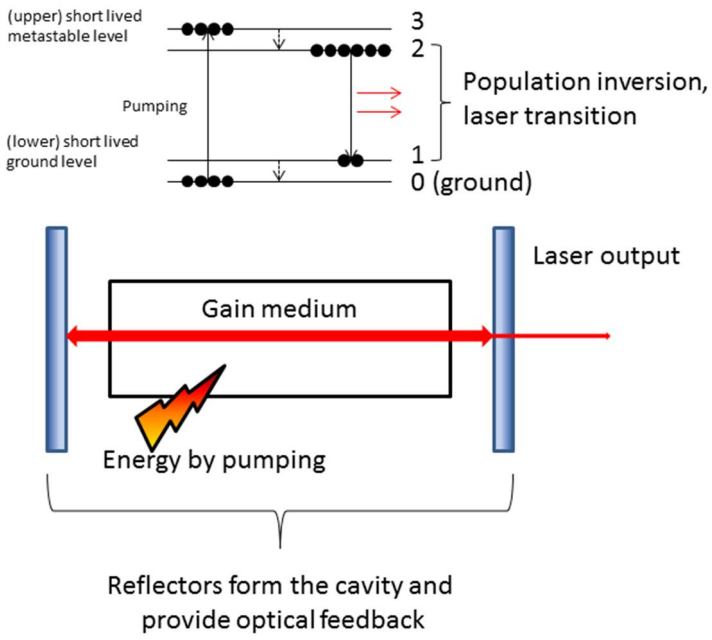

Figure 2.1: *The principle of a laser based on a four-level gain medium. The energy is provided by the pumping process, which excites the atoms from ground state to excited state 3. Level 3 is quickly depopulated to the underlying level 2 with slightly lower energy and longer lifetime. The laser transition occurs when this level is relaxed to the level 1 above the ground state. The population inversion is achieved easily, since the level 1 is quickly relaxed to ground-state 0. Therefore level 1 remains essentially unpopulated.*

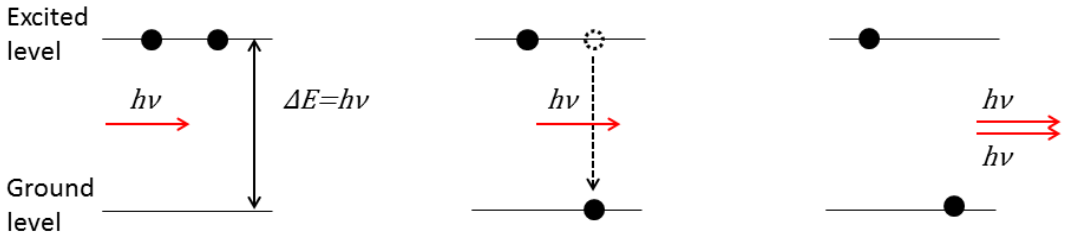

Figure 2.2: *The principle of stimulated emission and population inversion. The excited energy level is populated with atoms or ions. The incident photon of a suitable energy is triggering the emission of another photon, which acquires the same phase as the incident photon.*

The simplest case of a laser system is a two level energy system as shown in Figure 2.2. The atoms at the ground state are pumped to a higher energy state by using the energy provided by the pump source. From the higher energy level the stimulated emission can occur as a result of incoming photon, the energy of which is matching to the energy difference between the energy levels of the gain medium. When the energy is suitable, the incoming photon triggers the emission of another photon, and the atom is relaxing back to its ground state. The emitted photons propagate inside the gain medium and laser cavity, and reflect back from the mirror or other reflectors at the end of the laser

cavity. Therefore, inside the cavity there are photons oscillating back and forth, which are triggering the emission of subsequent photons and leading to laser oscillation. Finally, suitable amount of photons is taken out via the other partially reflective mirror, and this provides the output of the laser light.

However, although being intuitive as an example, two energy levels are not sufficient for real world lasers, since in case of only two energy levels the condition of population inversion cannot be achieved. Instead, at best, an equal population in ground state and excited state is possible, resulting in optical transparency but still being insufficient to provide optical amplification.

Three more realistic, yet still simplified systems are shown in Figure 2.3. In three-level system Figure 2.3(a), the pumping process is exciting the atoms to energy level E_3, from which the atoms are quickly relaxed to a lower metastable energy level E_2 by a fast non-radiative relaxation. The laser transition is observed between the energy levels E_2 and E_1 (ground state). If the lifetime of transition $E_3 \rightarrow E_2$ is significantly shorter than the lifetime of transition $E_2 \rightarrow E_1$, the level E_3 remains essentially unpopulated and practically all the excited atoms are located in level E_2. The population inversion is achieved if over half of the atoms can be excited by the pump radiation. Therefore a sufficiently strong pumping is required to be applied to the gain medium. Moreover, signal reabsorption on the laser transition in weakly pumped regions of the gain medium is significant because of high remaining population on the ground level. As a result, three level gain media are rather inefficient for laser light generation [1][2].

The first laser was demonstrated in 1960 by using ruby as a gain medium. Although ruby forms a three-level system [3], most of the practical modern lasers are based either on quasi-three-level or four-level systems. The principle of the four-level system is shown in Figure 2.3(b). The atoms or ions are pumped to the excited state E_3, from which they decay to level E_2 by a fast non-radiative relaxation. The laser transition occurs between the level E_2 and short-lived level E_4, which is significantly above the ground level so that the thermal occupation of E_4 is vanishing. From level E_4 the atoms are once again decaying rapidly to the ground level, so that during the laser operation the level E_4 remains practically empty. Therefore, in the four-level systems achieving population inversion is easy due to the empty lower laser transition level. As a result, the four-level lasers are more efficient than three-level lasers, and signal reabsorption in weakly pumped parts of the gain medium is minimal [1][2].

An intermediate case between the three- and the four-level systems is a so called quasi-three-level system (Figure 2.3 (c)). In the quasi-three level systems, the level E_4 is only slightly above the ground level, so that a notable population of level E_4 is present in thermal equilibrium. Therefore, the properties of quasi-three-level systems are somewhere between the actual three- and four-level systems. In practice, many laser gain media act as the quasi-three-level system.

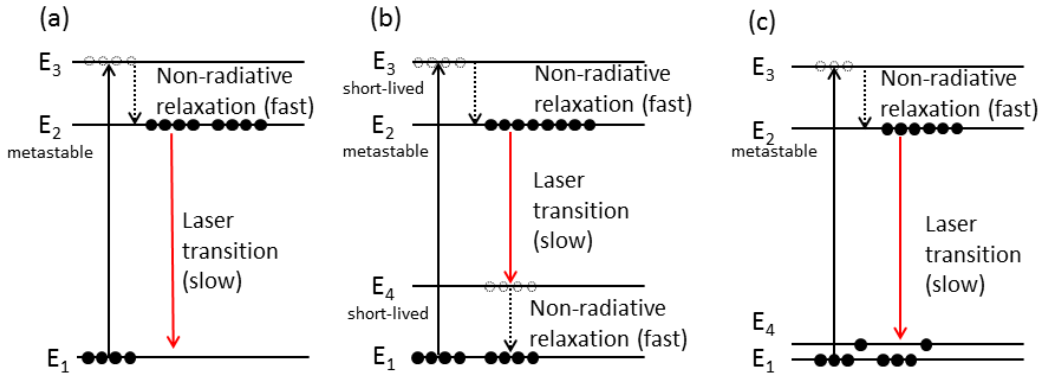

Figure 2.3: *(a) A three-level system (b) a four-level system and (c) a quasi-three-level system.*

In all types of gain media, so called *quantum defect* sets the fundamental limit for the efficiency of the conversion from pump light to laser light [2]. This is because the frequency of a pump photon is higher than that of a signal photon and therefore part of the energy is lost because of non-radiative transitions, such as heating of the gain media. Often, the quantum defect is described as the difference between the energies of the pump and signal photon, so that

$$q = h\nu_{pump} - h\nu_{signal} = h\nu_{pump}\left(1 - \frac{\lambda_{pump}}{\lambda_{signal}}\right), \quad (1)$$

where h is the Planck constant, ν is the frequency of a photon and λ is the wavelength of a photon. From (1) it is seen that when the pump and signal wavelength are close to each other, the quantum defect becomes small. However, when the wavelengths are too close to each other, it unavoidably leads to quasi-three-level behavior of the system.

2.2 Optical fibers

The optical fiber is a type of a *waveguide,* which structure guides electromagnetic radiation. In case of optics, the waveguide i.e. optical fiber is based on the total internal reflection of the light on the boundary of two materials having different index of refraction. The first practical optical fibers were produced in 1950s, when the use of the cladding layer in optical fibers was introduced [4]. A simple optical fiber consists of a glass core which is surrounded by the cladding with larger diameter. The refractive indices of the cladding is made slightly lower than that of the core, introducing the change of refractive index at the core-cladding interface. In simple terms this enables the total internal reflection at the interface, confining the light inside the fiber. The cladding is surrounded by the protective layers of polymer, known as the buffer and jacket.

The schematic of a common single-mode fiber is shown in Figure 2.4 The core of the single-mode fiber is small, usually < 10 µm, whereas in case of multimode fibers the size of the core can be at least several tens of microns, even 100 µm. The size of the

cladding is most commonly 125 μm for both the single- and the multi-mode fibers. Single-mode fibers are used in long distance communication, mainly because the lack of modal dispersion. Modal dispersion is a distortion caused by different propagation velocities of different modes, which leads to pulse broadening effects and limits the achievable data transfer rate in long-haul communication systems. However, in local area short distance communications multi-mode fibers are preferred because of their lower price and easier use.

For the optical fibers so called V-parameter is defined so that

$$V = k_0 a (n_1^2 - n_2^2)^{\frac{1}{2}}, \qquad (2)$$

where $k_0 = 2\pi/\lambda$, a is the radius of the core and n_1, n_2 are the refractive indices of the core and cladding, respectively [5]. It can be shown, that the V-parameter determines how many different propagating modes the fiber can support, so that if V < 2.405 only one mode is supported. In that case, the fiber acts as a single-mode fiber for given wavelength. If the V-parameter is larger, the fiber supports the propagation of multiple modes. The detailed discussion related to the fiber modes requires considerable algebra using Maxwell equations and is beyond the scope of this thesis. Detailed discussion can be found for example in [5]. However, to illustrate the concept of modes, Figure 2.5 shows the simulation of the mode intensities inside a step-index optical fiber. Only the fundamental mode LP_{01} is guided in single-mode fibers. In multi-mode fibers, the number of the propagating modes is increased, and as a result the intensity profile becomes very complex compared to the Gaussian intensity profile of the LP_{01} mode.

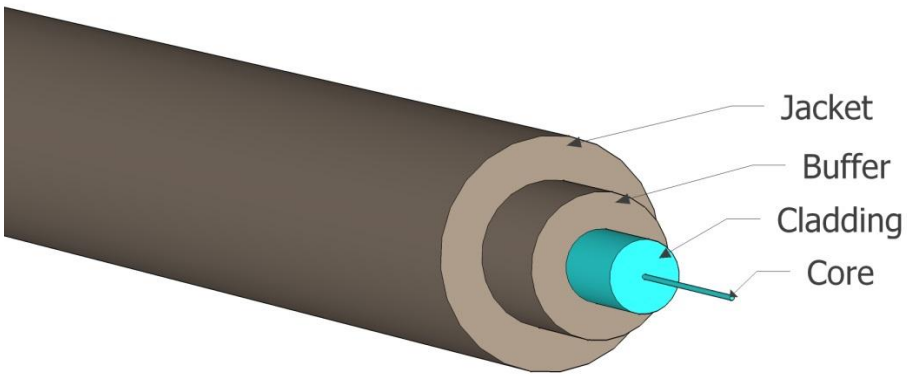

Figure 2.4: *A schematic of a single-mode fiber (in scale). The small core is surrounded by a larger glass volume called the cladding. The glass regions are protected by the polymer layers known as buffer and jacket.*

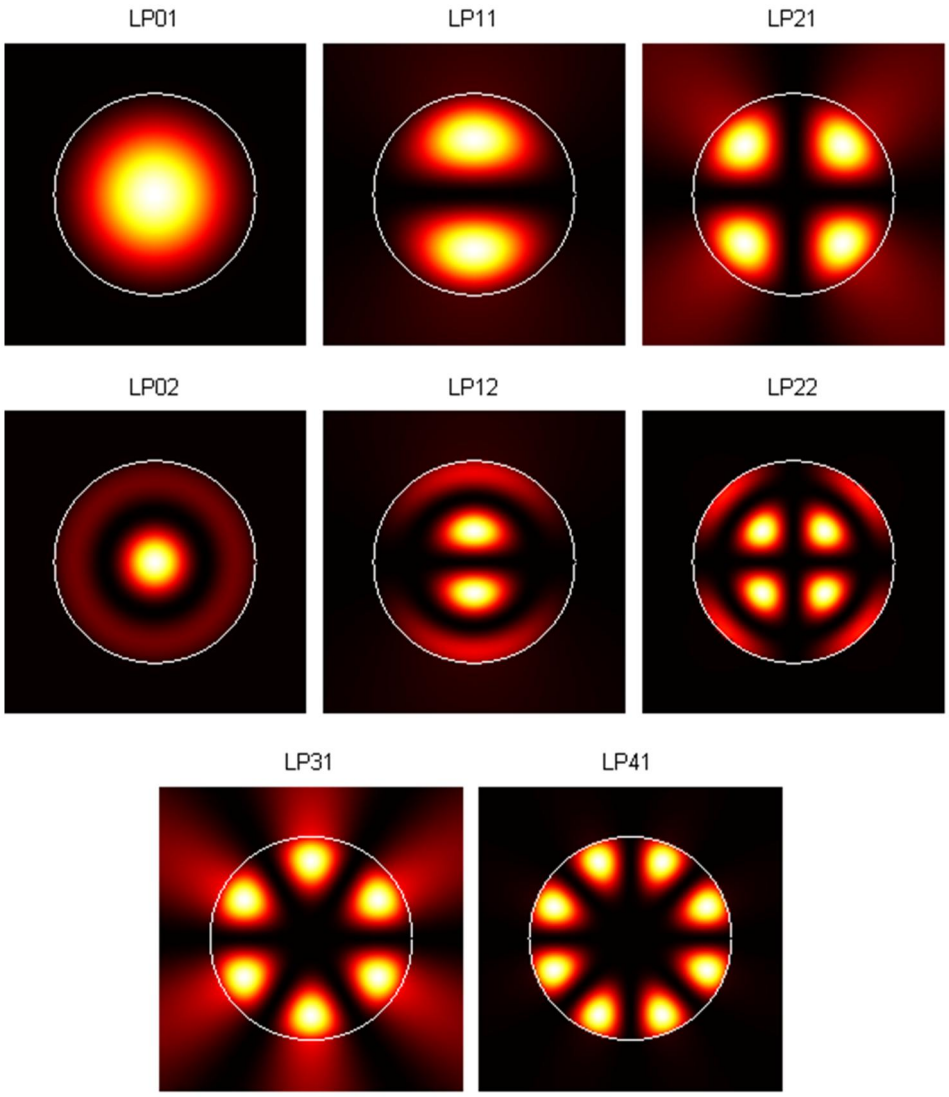

Figure 2.5: *Simulation of a few modes for the light propagating inside an optical fiber. Only the fundamental mode LP_{01} is guided in the singe-mode fiber, whereas in the multimode fibers enable the propagation of other modes.*

2.3 Fiber lasers

One type of solid-state lasers and the main focus in this thesis are fiber lasers. In the fiber lasers, the gain media is based on so called *active fiber*, an optical fiber doped by suitable active elements. The doping elements are chosen based on the desired wavelength of the laser operation. Different types of active fibers and doping elements will be discussed in more detail in the following section.

Figure 2.6 shows a typical fiber laser with a simple linear cavity. The pump light is launched inside the cavity using a pump combiner or wavelength-division-multiplexer (WDM). The pump light then propagates through the active fiber, where the emission at the desired signal wavelength occurs. The cavity is formed by adding suitable reflectors on the both sides of the active fiber. A great variety of different methods and combinations of components can be used to implement a working laser and few of them are shown in Figure 2.7. The output of the laser can be taken through a separate fiber coupler or with the aid of a partial reflector, such as a fiber loop mirror, a fiber Bragg grating (FBG) or a dichroic mirror. In case of fiber lasers, the length of the gain medium can be relatively long, from meters to few tens of meters or sometimes even longer. Therefore, the gain inside the cavity can be remarkable high, which enables high output coupling percentages in fiber lasers. Often a suitable output coupler can be achieved by using a fiber end with a straight cleave, which gives ~ 4 % Fresnel reflection from the air-glass surface of the bare fiber end. Compared to other solid-state lasers, which can often tolerate only losses of few percent, achieving laser operation in fiber lasers is often relatively easy. It should be noted, however, that for example the optimization of fiber length and output coupling is not a trivial task, since the design parameters are not independent but affect each other and therefore should be optimized together. Furthermore, changing fiber length inside the cavity changes other parameters than the gain of the laser as well. Such parameters are for example dispersion and nonlinearity, which are often very important in case of pulsed fiber lasers.

The fiber lasers provide a few benefits compared to other types of lasers. The laser light is already confined inside the optical fiber, and additional coupling into a delivery fiber is not needed. The beam quality of the fiber lasers is excellent because of the waveguiding properties of the fiber. Moreover, since the gain medium is based on a flexible optical fiber, long length of the gain material can be coiled into a relatively small volume, enabling compact design of the fiber lasers. Also the cooling of the fiber lasers is relatively easy, since surface area to volume ratio of the fiber lasers is high because of the shape of the fibers.

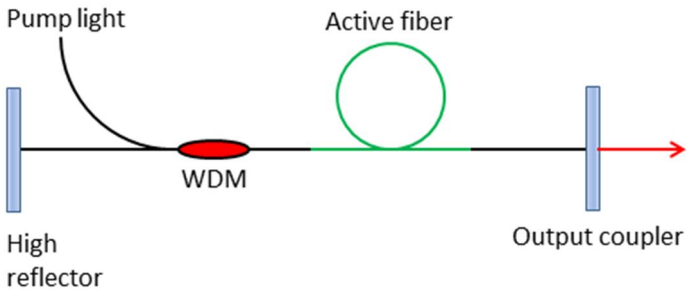

Figure 2.6: *A schematic of a simple linear fiber laser cavity. This picture demonstrates the basic principle of a fiber laser, although there are great amount of variations even in linear cavity scheme only. Especially the output coupling can be implemented in many ways, depending on the specific needs, available components or practical issues.*

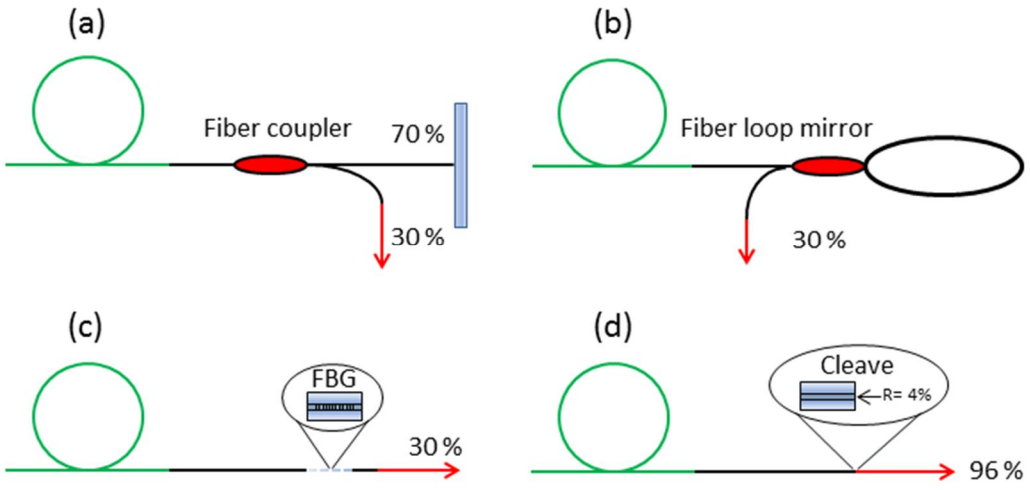

Figure 2.7: *A few practical realizations of output coupling for a fiber laser. (a) A separate fiber coupler combined with a reflective element, such as a mirror or FBG. (b) A fiber loop mirror, the reflectivity of which can be adjusted by adjusting the coupling ratio. (c)Output taken through a FBG with a suitable reflectivity. (d) A straight cleave in fiber end providing 4 % feedback to the cavity because of Fresnel reflection from the glass-air interface. In (a)-(c) 30% output coupling is used as an example but can be freely selected depending on the application and design parameters of the laser.*

2.4 Gain media and active fibers

In previous section the gain media were introduced as simplified energy-level systems which enable the population inversion and therefore laser light generation. In this section real gain media are considered, focusing on the common gain media used in fiber lasers.

The gain medium can be implemented in multiple ways in any state of material, and is commonly used to divide lasers to different categories based on their gain mechanism. Commonly lasers are divided for example to solid-state lasers, dye lasers and gas lasers by the state of the gain medium. Beyond that, the categories include fiber lasers, disk lasers and so on, based on the more detailed description of the gain material or mechanism [1]. Fiber lasers, which are the main interest in this thesis, are solid-state lasers that use optical fiber as a gain medium. This gain medium, active fiber, is realized by doping optical fibers with additional elements that provide absorption and emission at their characteristic wavelengths. The atoms, or ions, of the doping element are excited (pumped) to upper energy levels by using an appropriate wavelength of the pump light. Most often in case of fiber lasers the pump source is another laser, for example a laser diode or another fiber laser. In this sense, fiber lasers can be thought as wavelength and brightness converters, since the wavelength and the brightness of the output laser beam are usually different than those of the pumping laser beam [2]. Brightness in laser technology is understood as a parameter describing the beam quality, better brightness meaning better beam quality and ability to focus the beam into a smaller spot, which is important in many applications.

The most common gain media used in fiber lasers at the moment are ytterbium (Yb) emitting in ~1 µm range wavelength and erbium (Er) emitting at ~1.55 µm [2]. In addition, thulium, holmium and thulium/holmium co-doped fibers are used for the 2 µm optical applications. Erbium is extremely important for telecommunication industry, since erbium-doped amplifiers (EDFAs) form the backbone of current information technology, amplifying the optical signals and therefore compensating the losses between the data links. Ytterbium on the other hand is a common choice for high-power needs of the industry because of the high efficiency and output power of ytterbium-doped devices. Recently, novel active fibers based on bismuth have received significant amount of interest due to their extremely broadband emission wavelength range.

2.4.1 Rare-earth active fibers

Ytterbium

Ytterbium is a rare earth metal providing gain at 1 µm spectral region. In silica fibers, the most common choice for optical fibers, Yb-doping is deployed as trivalent Yb^{3+} ions [6]. First reports of laser oscillation in ytterbium doped silicate glass date back to 1962 [7]. This was followed by a demonstration of a CW-laser using single-mode ytterbium fibers as a gain element in 1988 [8]. Today, ytterbium medium is used in a wide variety of fiber systems, acting as a highly efficient gain material.

The absorption band of Yb-doped fibers extends from 800 nm to 1000 nm, with absorption cross section peaking at ~975 nm, although the details of the absorption and emission spectra are dependent on the host glass. The ytterbium fibers do not exhibit excited state absorption (ESA), since only two optically relevant energy manifolds, $^2F_{7/2}$ (ground-state) and $^2F_{5/2}$ (excited state) exist. These manifolds are divided into four and three sublevels. At shorter wavelengths near 975 nm, ytterbium acts as a three-level system, whereas for longer wavelengths the four-level behavior is observed, leading to better efficiency and straightforward optimization of the active fiber length because of low signal reabsorption [6].

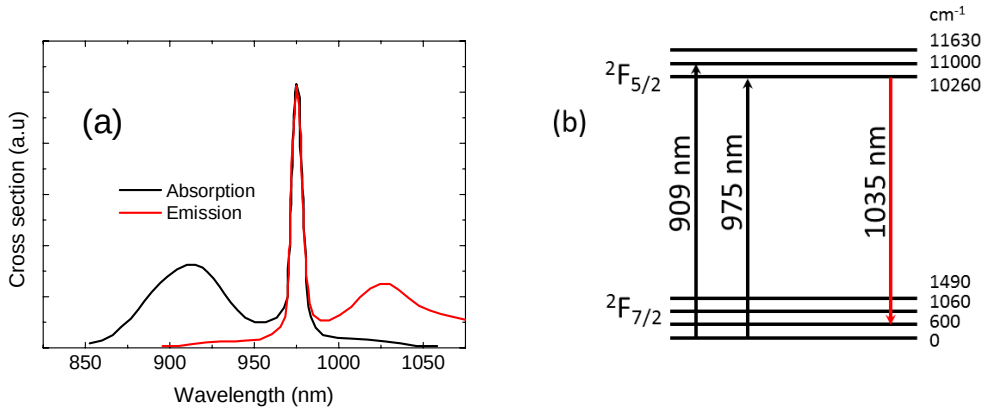

Figure 2.8: *(a) Absorption and emission cross-section of Yb^{3+} (b) Energy level diagram of Yb^{3+}. Modified representation based on the data from reference [9].*

Erbium

Another important rare-earth metal widely in use is erbium (Er). Since the fabrication of first Er-doped fibers in 1985 [10] and subsequent demonstration of first EDFA in 1988 [11], EDFAs have enabled modern telecommunication by providing optical gain within the low-loss window of optical fibers. Originally introduced as a third alternative to Raman fiber amplifiers and semiconductor laser amplifiers, EDFA is now the standard amplifier for the telecommunication industry.

The absorption bands of the erbium-doped fibers are sparsely positioned from visible light to near infrared, and all of them can be used to successfully pump erbium-doped fibers. The most widely used absorption bands are those matching commercially available diode lasers, such as 980 nm and 1480 nm. These are the standard pump wavelengths of EDFAs and erbium fiber lasers ensuring the highest small-signal gain efficiencies for EDFAs.

Erbium behaves as a quasi-three-level system, which can be confirmed by measuring the relaxation oscillations of erbium-doped fibers [2], [12]. Absorption at 980 nm corresponds to the transition of Er^{3+} ions from $^4I_{15/2}$ level to $^4I_{11/2}$ level, providing high absorption cross-sections and high conversion efficiencies. For the best performance, special care should be taken to match the pump light to the absorption peak, the location of which depends slightly on the composition of the host glass. This requirement of fine-tuning the pump wavelength is less prominent with 1480 nm resonant pumping, which has become the major technique for pumping EDFAs. 1480 nm pumping corresponds to a direct transition of Er^{3+} to $^4I_{13/2}$ metastable state changing erbium-doped fiber virtually to two-level system. However, gain is still obtained because of the absorption and emission spectra are shifted as a consequence of Stark effect [13].

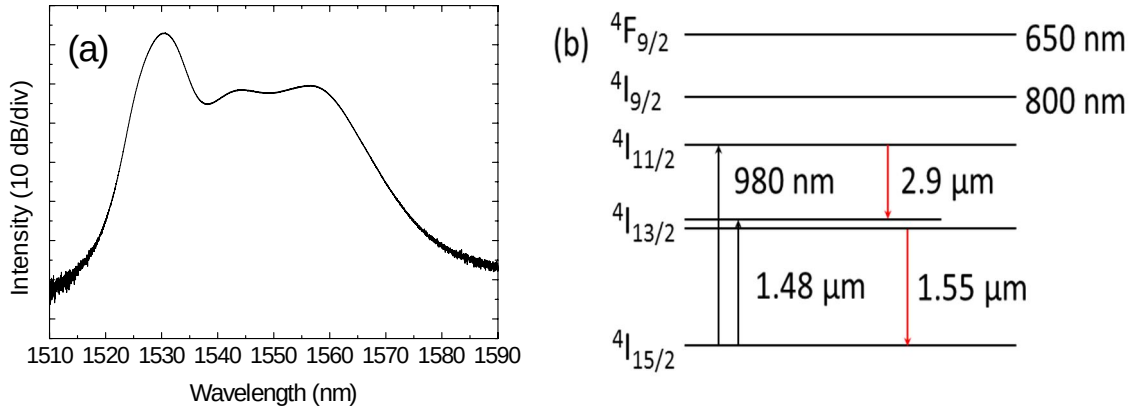

Figure 2.9: *(a) A typical spontaneous emission of Er-doped fiber pumped at 980 nm. (b) Simplified energy level diagram of erbium based on references [2] and [13].*

The emission spectrum of erbium extends from 1500 nm to 1600 nm, providing gain values over 20 dB between 1530 and 1560 nm. A typical amplified spontaneous emission (ASE) spectrum of the erbium-doped fiber pumped by a 980 nm laser diode is shown in Figure 2.9. For mode-locked fiber lasers erbium-doped fiber is often a desirable choice as a gain medium, since the dispersion of the standard optical fibers at signal wavelength (~1550 nm) is anomalous, supporting the soliton operation of the laser. Dispersion and its main influences on the mode-locked fiber lasers are discussed in detail in Section 3.3.

Thulium, holmium, and thulium-holmium

Gain of the erbium-doped fibers is limited below 1600 nm, but extension of the spectral range of fiber lasers has been achieved using thulium (Tm) -doped fibers. The emission spectrum of Tm-doped fibers is located at ~2μm, allowing first demonstration of 1.88-1.96 μm thulium fiber laser in 1988, by same group and same year than the first demonstration of ytterbium fiber laser [14]. For thulium active media, the most used pump wavelengths are 0.8 μm, 1.15 μm and 1.55 μm. Pumping at 0.8 μm allows the use of widely available high-power pump diodes. Pumping at 1.55 μm on the other hand, is possible exploiting erbium-doped fiber lasers with single-mode output, which allow direct core pumping of the thulium doped fibers. The peak of the absorption is seen at ~1700 nm, but pumping of thulium this wavelength is not commonly used due to lack of suitable pump sources.

Another gain element suitable for long-wavelength operation at near 2 μm is holmium. Holmium is often used as a co-dopant of thulium, improving the efficiency of the lasers at longer (> 2 μm) wavelengths compared to fibers containing thulium alone. The main absorption bands of thulium-holmium doped fibers are the same as those of pure thulium-doped fibers [15]. Fiber lasers doped with purely holmium have been demonstrated as well, illuminated at wavelengths of 2.0 - 2.2 μm [16]. Another emission band of holmium occurs at 2.9 μm, which can be exploited for ultra-long-wavelength fiber lasers at ~3 μm [17]. Long-wavelength lasers are used for example in eye-safe LIDAR applications [18], medicine [19] and in spectroscopy especially for detection of CO_2 [20].

2.4.2 Bismuth active fibers

Near-infrared (NIR) luminescence of bismuth-doped silica glass was discovered in 1999, revealing luminescence spectrum with peak at 1140 nm when using 500 nm excitation wavelength [21]. This was later followed by observation of optical amplification at 1300 nm using bismuth-doped silica glass [22]. Few years after that, in 2005, the first bismuth-doped optical fibers and a fiber laser operating in CW regime were demonstrated in 2005 [23]-[25]. The laser operation was obtained in spectral region between 1150 and 1300 nm using aluminosilicate glass fibers fabricated by modified chemical vapor deposition (MCVD). Soon it was noticed that the wavelength of the laser transition is

dependent on the host glass matrix, which allowed to tailor the operation wavelength of bismuth-doped devices by varying the composition of the host glass.

At present, bismuth doped fibers have been demonstrated to be able to provide gain within a broad spectral region between 1150 nm and 1800 nm [26], [27]. This spectral region is a particular interest, since it includes the whole low-loss window of optical fibers, desirable for telecommunication purposes. To date, demands for optical data transmission have increased from 30% to 100% per year [28]. This sets increasing challenge for telecommunication devices, such as amplifiers and optical fibers. One of the major limiting factors in the current systems is the limited bandwidth of EDFAs, providing practical gain only in a relatively narrow spectral range between 1530 and 1560 nm. Optical amplifiers operating outside this region are low-efficiency alternatives, such as Raman amplifiers. In order to increase the data rates by extending the bandwidth, highly efficient optical amplifiers should be developed for the whole wavelength region between 1300 and 1700 nm. One of the promising candidates is bismuth-doped fiber amplifier (BDFA). For comparison the emission wavelength regions from Bi- and rare-earth-doped fibers are shown in Figure 2.10.

The origin of NIR emission from Bi-doped materials remains controversial to date [26], [29]. Bismuth has four oxidation states: Bi^{5+}, Bi^{3+}, Bi^{2+} and Bi^{+}. The Bi^{3+} and Bi^{2+} ions have been confirmed to emit only at visible and UV-region of the spectrum, and hence they do not contribute to NIR-luminescence of the bismuth doped media. Different hypotheses for the origin of NIR-emission have been suggested, such as Bi^{5+} ions, Bi-clusters, Bi^{+}, BiO, Bi_2^{-}/Bi_2, Bi_2^{-}/Bi_2^{2-} , Bi_0 and point defects in the fibers. However, none of these hypotheses has been absolutely confirmed to date. During the fabrication of bismuth doped fibers, the bismuth ions stay in reduction/oxidation equilibrium in molten glass, as described by the equation

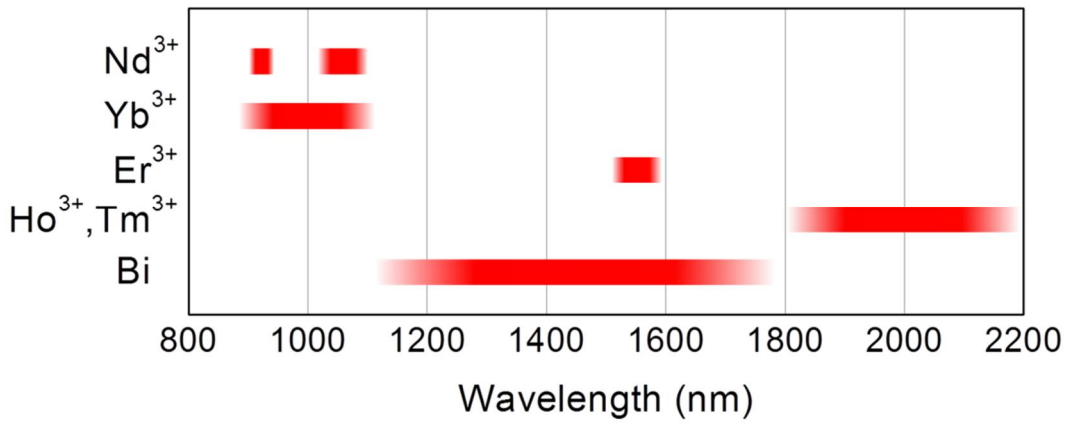

Figure 2.10: *The emission wavelength of few common rare-earth doped fibers and bismuth fibers.*

$$Me^{x+n} + \frac{n}{2}O^{2-} \Leftrightarrow Me^{x} + \frac{n}{4}O_2, \quad (3)$$

where Me^{x+n} and Me^{x} represent the polyvalent ions [26]. The equilibrium point of this equation is strongly dependent of the environmental parameters, such as temperature, pressure and composition of the host glass. When the temperature is increased Bi-ions are reduced to lower oxidation states, forming Bi clusters and $(Bi)_n$-colloids, making the determination of the exact valence state of bismuth extremely difficult. Experimentally it has been demonstrated, that NIR-emission in bismuth-doped glasses is caused by the reduction of Bi^{3+} to lower valence states, and that the NIR-emitting centers observed in crystals doped with isoelectronic ($6s^2$ $6p^1$) ions Ti^0 and Pb^+ are related to ions and adjacent anion vacancies [30], [31]. This suggests that the origin of NIR-emission of bismuth active centers (BACs) could be Bi-ion and an adjacent oxygen-deficiency defect of the host glass. In recent experiments it was shown that the emission and absorption of bismuth-doped fibers were greatly reduced after 244 nm irradiation dose. This may indicate that there is a relationship between BACs and oxygen-deficiency centers (ODCs) of SiO2-GeO2 glasses. Moreover, it was suggested that only the ODC(ii) center is significant for BACs. [27].

2.5 Review of bismuth-doped fiber lasers

Although the detailed explanation of the NIR-emission of bismuth-doped media remains unclear, bismuth doped fiber devices have been studied extensively in recent years. The first bismuth fiber lasers performed operation at ~1.15 μm wavelength. This has been followed by demonstration of BDFAs [32], [33] and high-power CW lasers in spectral region of 1100-1550 nm [34] - [37]. Recently, CW bismuth fiber lasers were demonstrated to operate in 1600-1800 nm wavelength region [27] and be able to deliver watt-level output power with 33 % slope efficiency [38]. Therefore, to date bismuth fiber lasers have been demonstrated to cover the whole spectral region of 1100-1800 nm. In addition to CW bismuth fiber lasers and amplifiers, various pulsed devices have been presented. Similar to CW experiments, the early demonstrations of mode-locked bismuth fiber lasers following the developing of efficient active fiber were focused on the short wavelength side of the gain provided by aluminosilicate bismuth doped fibers. Mode-locking is a technique used widely to obtain generation of ultrashort optical pulses. The details of this and other techniques for pulse generation are discussed more in Chapter 3.

The first mode-locked bismuth laser was published in 2007, two years after the first CW laser [39]. This laser operated at 1160 nm wavelength, delivering 50 ps pulses with 13 MHz repetition rate and producing average output power of ~2 mW. In 2009, Bi-doped fiber laser operating in anomalous dispersion regime and producing soliton pulses was demonstrated [40]. This laser used a linearly chirped fiber Bragg grating (CFBG) for dispersion compensation, introducing large anomalous dispersion to the cavity. The

laser was able to deliver 1.9 ps pulses at 1165 nm. In both of the above-mentioned lasers, the authors used semiconductor saturable absorber mirrors (SESAMs) as a mode-locker. In 2010, Kelleher et al. demonstrated mode-locking of a bismuth doped fiber laser in both normal and anomalous dispersion regimes, using carbon nanotubes (CNTs) as a saturable absorber [41]. The laser produced 558 ps and 4.7 ps pulses in normal and net anomalous dispersion regimes, respectively. Similar to [41], the authors used a chirped fiber Bragg grating for changing the cavity dispersion to net anomalous regime. In addition to passive mode-locking using saturable absorbers, Luo et al. used nonlinear polarization rotation technique to achieve pulsed operation of a bismuth laser at ~1160 nm wavelength region [42]. The authors obtained generation of 21 ps pulses, together with tunable and switchable dual-wavelength mode-locked operation.

Following the development of bismuth doped CW lasers and amplifiers, after the first demonstrations of mode-locking at ~1150 nm wavelength the research of mode-locked bismuth fiber lasers was shifted towards the longer wavelengths. In 2013, a mode-locked bismuth fiber laser which operated at wavelength of 1320 nm in both anomalous and normal dispersion regimes was demonstrated [43]. The laser was capable of producing 2.51 ps and 25.5 ps pulses in anomalous and normal dispersion regimes, respectively. The pulses in normal dispersion regime could be compressed to 580 fs. Later, in 2014, a mode-locked bismuth fiber laser at wavelength of ~1450 nm was reported [44]. This publication was mainly focused on absorption recovery and its effect on soliton grouping phenomena observed in the laser.

The aim of this thesis was to develop mode-locked bismuth doped fiber lasers for ultrashort pulse generation at long wavelengths of 1450 nm and 1700 nm. For 1450 nm, the aim was further development of the previous work done by our research group in [44] and improvement of the performance of the laser in terms of pulse energy, pulse duration and peak power. For 1700 nm, the aim of the experimental work was to realize mode-locked devices based on bismuth-doped fiber operating in the 1700 nm wavelength range. The detailed investigation of the laser behavior and the output parameters tailoring was employed.

3. PULSED FIBER LASERS

In many applications a pulsed operation of the laser is favored instead of continuous-wave output. In this chapter the discussion of fiber lasers is extended to cover the most common pulsed fiber devices such as Q-switched and mode-locked fiber lasers. Principle of power scaling using a master oscillator – power amplifier (MOPA) system is introduced and finally the role of dispersion and nonlinearity on pulse formation is considered.

3.1 Q-switching

The term Q-switching is derived from the cavity Q-factor (quality factor), which essentially is defined as the ratio between the energy stored inside the cavity to the energy dissipated per cavity roundtrip. The Q-factor of the cavity can be modulated by time-varying the resonator losses, hence the term Q-switching.

In Q-switched operation of the laser the resonator losses are sharply rising up by external action, preventing the laser oscillations inside the cavity and therefore enabling development of higher population inversion inside the gain medium [1]. Then, after the buildup of large population inversion the cavity losses are quickly changed, or switched, to a lower value enabling the laser oscillation to occur again. As a result, an intense laser pulse is formed, releasing the extra energy which was stored inside the cavity during the higher losses of the resonator. After that the high loss level of the cavity is restored and the energy starts to accumulate again. Typically the pulse durations for Q-switched pulses are order of tens of nanoseconds. Peak power of the pulse can be orders of magnitudes higher than the CW power level available from a cavity with similar gain characteristics Figure 3.1.

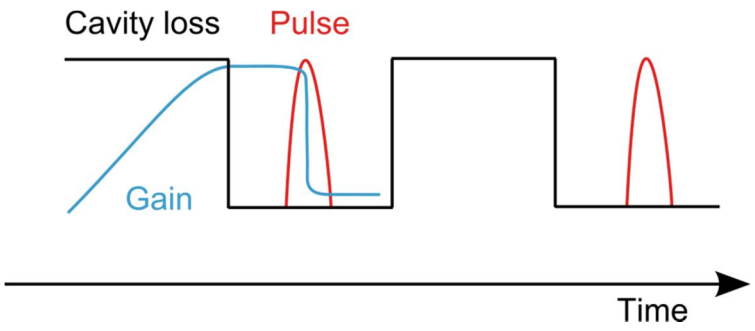

Figure 3.1: *The principle of Q-switched pulse generation. The pulse is emitted during the low cavity loss window, quickly consuming the energy stored inside the cavity during the high resonator losses.*

One of the most straightforward ways to modulate the losses of a laser cavity is to incorporate a rotating end-mirror inside the resonator. This was one of the earliest ways to achieve Q-switched operation of the laser. However, this method is relatively slow, and suffers from alignment problems and timing instabilities because of the deviations in mirror rotation. In practice, modern Q-switching is usually implemented by incorporating either an electro- or acousto-optic modulator inside the cavity, or by using saturable absorbers. Q-switching using modulators is regarded as active Q-switching, since the modulators need external driving voltage to be applied to them. In addition, Q-switching can be achieved by using passive components similar than the ones used for passive mode-locking. These are discussed in Section 3.2.2.

Typically the pulse duration of Q-switched laser is order of nanoseconds, whereas the repetition rates are 1-100 kHz. The repetition rate is usually dependent on the energy inside the cavity, i.e. it is dependent on the pump power. Q-switched lasers are used in applications where high pulse energy is necessary, but the pulses do not need to be ultrashort (<1 ps) but rather in range of few nanoseconds. The applications of Q-switched lasers vary from laser cutting and medicine to range-finding devices [45]-[47].

3.2 Mode-locking

Typically the pulse durations from Q-switched fiber lasers are limited to nanosecond range. Still shorter pulse durations can be generated by mode-locked lasers producing sub-picosecond pulses. In extreme cases the pulse duration can be only several femtoseconds, order of few optical cycles [48]. Compared to Q-switched lasers, the repetition rates of mode-locked lasers are higher, whereas the pulse energies are usually lower. The repetition rate of a mode-locked fiber laser is defined by the cavity length, and typically varies from 1-100 MHz, although more extreme cases outside of this typical region have been demonstrated as well [49], [50]. Similar to Q-switched lasers, mode-locking can be achieved using either active or passive techniques.

3.2.1 Active mode-locking

Active mode locking, similar to active Q-switching, refers to mode-locking with an active element inside the cavity, such as an electro- or acousto-optic modulator [1]. The drive frequency of the modulator is matched with the cavity round-trip frequency, and in time-domain it is reasonable to consider the modulator as a switch, which opens an optical path for a pulse circulating inside the cavity, giving to it the maximal transmission. In frequency-domain, active mode-locking is described by considering the axial modes of the laser cavity. The modulator is driven with a frequency $n \times \omega_m$ close to the cavity frequency ω_c or one of its multiples. The modulation sidebands are therefore matching the other axial modes of the laser resonator, forcing them to lock with the adjacent modes, which leads to the term of mode-locking. In active mode-locking, the

speed of the modulator and its control devices are usually the limiting factor for the pulse duration, restricting it to the order of 1 ps.

3.2.2 Passive mode-locking

To overcome the limitations in response times of modulators and controlling electronics, different passive mode-locking techniques have been considered and demonstrated. Indeed, the shortest laser pulses to date have been generated with passively mode-locked laser resonators [48]. In passively mode-locked lasers, a nonlinear element is included inside the cavity, initiating the pulsed operation without any applied external modulation. The nonlinear element is called a saturable absorber, which characterizes intensity-dependent transmission losses. The saturable absorber has high optical transmission losses at low optical intensities but becomes transparent as the optical intensity is increased.

In practice, the saturable absorber can be implemented as a real optical element, such as semiconductor saturable absorber mirror (SESAM) or carbon nanotube (CNT) saturable absorber. Another alternative is to use so called artificial saturable absorption, including for example the mode-locking based on nonlinear polarization rotation (NLPR) or Kerr-lens mode-locking [48].

Nonlinear polarization rotation

One of the most used passive methods relying on artificial saturable absorption is polarization rotation. NLPR mode-locking is based on the intensity-dependent change in polarization state, which is a combined effect of cross-phase modulation, self-phase modulation and birefringence of the optical fibers, caused by the imperfections in its symmetrical structure [51]. Commonly a polarization dependent isolator together with polarization controllers or waveplates is then included inside the cavity. The controllers are adjusted so that the transmission of the isolator (or the other polarizer) is maximized for the highest optical power, therefore acting as an artificial saturable absorber and triggering the pulsed operation of the laser [52].

NLPR mechanism is extremely fast, and therefore the pulse duration is typically below 100 fs. However, NLPR technique suffers from environmental instabilities, such as drifting of the optimal polarization state with temperature, which is limiting the practical use of it.

Semiconductor saturable absorbers

Developments in semiconductor growth technology and bandgap engineering in recent decades have enabled the design and manufacturing of semiconductor saturable absorbers for pulsed lasers. Today, semiconductor saturable absorber mirror (SESAM) as a passive mode-locker is the standard choice for commercial pulsed laser due to its bene-

fits over the other techniques. Compared to the other passive mode-locking techniques and saturable absorbers, optimized SESAMs offer high environmental stability and reliable self-starting mode-locked operation, which is very important property in many applications [53]. The parameters of the SESAM growth can be controlled well, and therefore the manufacturing of the SESAMs is highly repeatable. This is crucial for matching the quality control needs for the commercial lasers.

A typical SESAM consists of a semiconductor-based distributed Bragg reflector (DBR), accompanied by one or multiple quantum wells (QW) which provide the saturable absorption. Additional antireflection coating is often included on top of the structure to reduce the possible harmful reflections from the surface.

SESAMs and other saturable absorbers are characterized by few important parameters: operational wavelength, modulation depth (ΔR), saturation fluence (F_{sat}), recovery-time and nonsaturable losses (α_0), which all can be controlled by the choice of the material composition and design parameters. Figure 3.2 shows a typical nonlinear transmission curve of SESAM. The modulation depth is defined as a difference between the saturated and non-saturated transmission. The response and pulse shaping properties of the absorber are determined by the recovery time, dividing the absorbers to fast and slow types. Moreover, semiconductor absorbers have bitemporal response, fast response corresponding to the intraband thermalization and slow response corresponding to interband trapping and recombination processes [53]. Fast response of SESAM is important for stabilizing of short femtosecond pulses, whereas the slow response enables self-starting mode-locking and shapes longer pulses or pulse groups.

Self-starting pulse formation initiated by saturable absorbers can be explained as follows: the laser operates in CW-regime prior to starting of the pulsed operation. However, in CW-regime some random high-amplitude noise fluctuation always exists, which acquires lower losses due to partial bleaching of the saturable absorber. During multiple roundtrips inside the cavity, the absorber favors the buildup of this initially random spike. The spike eventually develops to an intense pulse, which is “burning” its way through the absorber. The absorber then continues to shape the observed pulse, giving the lowest losses for the pulse center and higher losses for the pulse wings as shown in Figure 3.3. Eventually a stable pulse is formed and the laser emits short pulses at the repetition rate which corresponds to the round-trip time of the laser cavity.

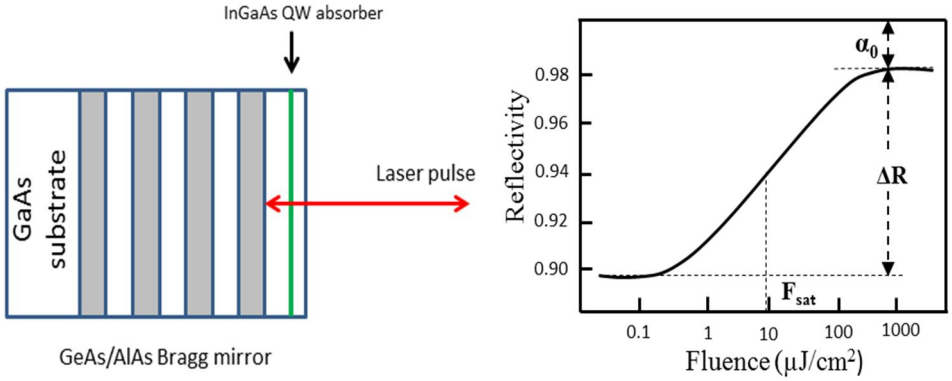

(a) (b)

Figure 3.2:: *(a) The schematic of a SESAM consisting of GaAs/AlAs DBR and InGaAs QWs providing saturable absorption. (b) A typical reflectance of a semiconductor saturable absorber mirror showing the basic parameters of the absorber.*

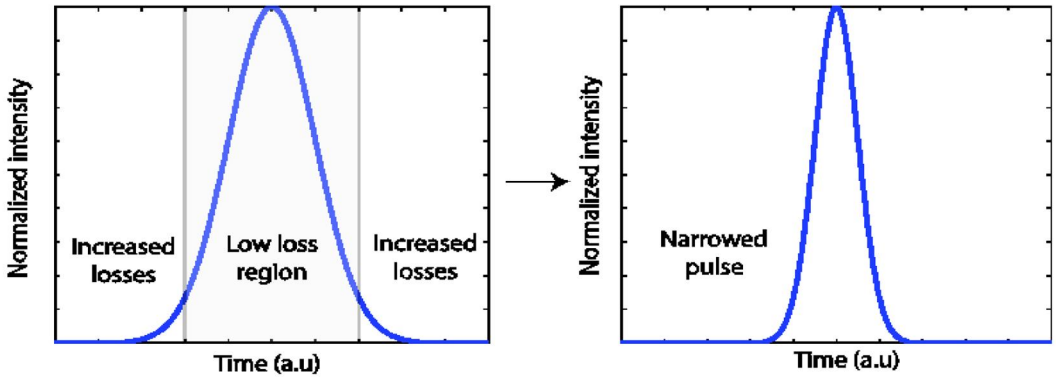

Figure 3.3: *The pulse shaping mechanism of a saturable absorber. The high-intensity part of the pulse acquires low losses, whereas the wings experience higher losses and the pulse duration decreases.*

Carbon nanotube saturable absorbers

In 2003, first mode-locked lasers utilizing single-walled carbon nanotubes (SWNT) were demonstrated [54], [55]. The authors achieved mode-locked operation using both ring and linear cavity schemes. Since then, considerable amount of research has been made using carbon nanotubes as saturable absorbers at different wavelength regions (See, for example, Ref. [56] and references therein). While SESAMs are most commonly used in reflection configuration since they are grown on a Bragg reflector, CNTs can be easily adopted to use in transmission which is beneficial for some cavity schemes. One of the most common methods to use CNTs in transmission configuration is to incorporate them sandwiched between two fiber connectors into a ring fiber laser.

Carbon nanotubes offer certain other advantages compared to traditional mode-locking with SESAMs. While fabrication of SESAMs requires costly semiconductor technologies such as molecular beam epitaxy, carbon nanotubes can be grown with relatively low costs by laser vaporization or arch discharge technique [57].The absorption characteristics of SWNT-absorber can be designed during fabrication process by controlling the nanotubes diameter. While SESAMs need to be designed for specific, narrow wavelength region, CNT saturable absorbers are broadband by nature because they include a distribution of nanotubes of different diameters. However, nanotubes with a diameter differing from the optimal for a given wavelength do not contribute much to the nonlinear properties but increase the linear non-saturable loss of the absorber.

Disadvantage of CNT absorbers is the relatively low ratio of nonlinearity to non-saturable losses. Usually for CNTs the ratio is ~ 1[56]. Therefore, achieving high nonlinearity with CNT absorber unavoidably leads to increase in linear losses as well. On the other and, especially with fiber lasers too low nonlinearity can lead to stability problems and parasitic CW oscillations in the laser because the lack of sufficient saturable absorption. In principle the modulation depth of the CNT-absorber can be typically increased by increasing the thickness of the CNT layer or stacking multiple layers of CNT on top of another. However, a balance between sufficient modulation depth and acceptable non-saturable losses should be reached for stable mode-locked operation.

Graphene saturable absorbers

Soon after the discovery of graphene in 2004 [58], first mode-locked lasers based on graphene saturable absorber were demonstrated independently by two groups in 2009 [59], [60]. Both used a sheet of graphene sandwiched between two fiber connectors to mode-lock an erbium-doped fiber laser with a ring cavity. The results were promising, since both obtained pulses with bandwidth of 5 nm and pulse durations of 713 fs and 1.17 ps.

Initially the graphene was produced by using so called Scotch-tape method, i.e. mechanical exfoliation of graphite [58]. Later, a variety of methods more suitable for mass production of graphene have been developed, including for example liquid-phase and thermal exfoliation, chemical vapor deposition and synthesis on SiC-wafers [61].The liquid-phase exfoliation is based on dispersing the graphite flakes in solvent, after which ultrasonification and centrifugation are used to separate few-layer and single-layer graphene flakes. Chemical vapor deposition on the other hand is one of the promising techniques for mass production of large areas of few-layer graphene.

Graphene is structured as sp^2 hybridized two dimensional (2-D) honeycomb-lattice, enabling its unique electrical and optical properties. The valence and conduction bands of graphene form a conical shape, which results in zero-bandgap. Despite its 2-D structure only one atomic layer thick, graphene absorbs a significant amount of incident

light, absorption of one layer being 2.3 %. The absorption is wavelength independent, since the dispersion relation of graphene is linear. Broad absorption wavelength region together with fast saturable absorption makes graphene an interesting alternative as a saturable absorber for pulsed laser applications.

Even though graphene has some definitely interesting properties for mode-locked applications, it suffers from relatively low optical damage threshold similar to CNT absorbers. In high power applications this is a serious problem, limiting the practical use of these saturable absorbers. Different methods for solving the problem have been developed, such as depositing graphene/CNT on waveguides to enable evanescent-field coupling to the absorber [62], [63].

Topological insulators

Among the novel saturable absorbers for pulsed laser applications are the absorbers based on topological insulators, such as Bi_2Se_3, which was demonstrated and successfully used to mode-lock an erbium-doped fiber laser [64], [65]. Other topological insulators, such as Bi_2Te_3 have been demonstrated as well to offer saturable absorption and be able to trigger mode-locked operation of a laser [66]. Similar to graphene, topological insulators have linear dispersion relation making them wavelength independent absorbers. So far, topological insulators are not studied thoroughly in optical applications compared to other saturable absorbers and mode-locking techniques.

Frequency-shifted feedback

Another standalone mode-locking technique is called frequency-shifted feedback (FSF). In this technique, a key component is a frequency-shifter is inserted inside the cavity. Usually this is done by using an acousto-optic modulator inside the cavity, which is providing frequency shift of the spectrum at each resonator roundtrip. Therefore, FSF laser does not allow conventional buildup of longitudinal modes inside the resonator. A mode-locked like behavior can be developed under sufficient conditions because of the interplay between self-phase modulation, frequency shifting and spectral filtering which is usually due to limited gain bandwidth [67], [68]. Because of the use of electrically driven acousto-optic modulator inside the cavity, some arguments against categorizing FSF mode-locking as a passive mode-locking technique could be justified. However, conventionally the concept of active mode-locking has been used for techniques which modulate directly the cavity losses, and therefore mode-locking using frequency-shifted feedback is often considered as a passive mode-locking technique.

3.3 Pulse dynamics and dispersion management

One of the important parameters defining the operation of the mode-locked fiber laser is the sign and value of the cavity dispersion. Even though a saturable absorber is typically

triggering the mode-lock operation of the laser and contributing to the pulse shaping, the total dispersion of the cavity has a strong influence on the properties of the pulse. Often in mode-locked fiber lasers the pulses are so called soliton pulses, which mathematically are steady state solutions to nonlinear Schrödinger equation [5]

$$\frac{\partial A}{\partial z} = \frac{i\beta_2}{2}\frac{\partial^2 A}{\partial T^2} + \frac{\beta_3}{6}\frac{\partial^3 A}{\partial T^3} + i\gamma|A|^2 A - i\gamma T_R A\frac{\partial |A|^2}{\partial T} - \frac{\gamma}{\omega_0}\frac{\partial}{\partial T}(|A|^2 A), \quad (4)$$

where A is the pulse envelope, z is the distance in the fiber, T is the pulse local time, β_2 is the second order dispersion of the laser medium, β_3 is the third order dispersion, γ is the nonlinear parameter, ω_0 is the carrier frequency and T_R is a parameters corresponding to the Raman effect of the medium. Essentially, in simple consideration the solitons are formed when the dispersion and Kerr nonlinearity of the cavity balance each other leading to a self-maintaining solitary pulse. For a medium with positive nonlinear coefficient (which is the case for most media) the formation of conventional solitons requires the chromatic dispersion to be anomalous. For standard telecom fibers, this essentially means that conventional soliton operation is easiest to obtain at longer wavelengths (>1300 nm) since the dispersion of the fiber is anomalous in that region (Figure 3.4).

The soliton mode-locking is an interesting phenomenon, since it enables one to use weak and relatively slow saturable absorber, still producing pulses significantly shorter than the recovery time of the absorber. Hence, in soliton operation the absorber has minimal contribution to pulse shaping which is almost solely determined by the interplay between the group delay dispersion and self-phase modulation due to Kerr-nonlinearity. In soliton mode-locked laser the purpose of the absorber is mainly to trigger the mode-locked operation and stabilize the pulses against development of parasitic CW-oscillations. Indeed, saturable absorbers with recovery time of 10 ps have been demonstrated to be able to produce 300 fs pulses [69].

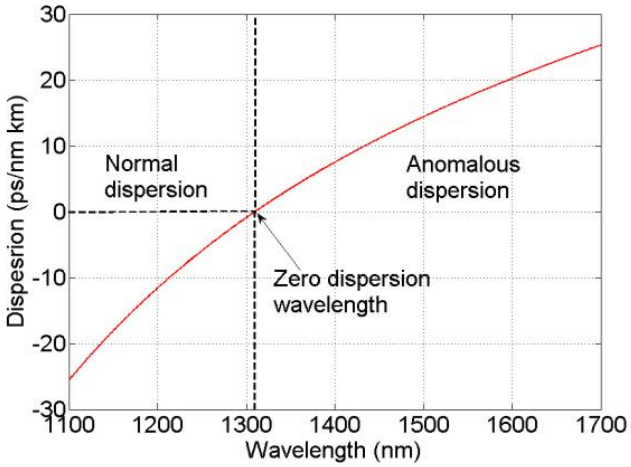

Figure 3.4: *Calculated dispersion curve for a standard telecommunication fiber Corning SMF-28 [70] . The zero-dispersion wavelength is assumed to be 1310 nm. The dispersion is anomalous at wavelengths longer than zero-dispersion wavelength.*

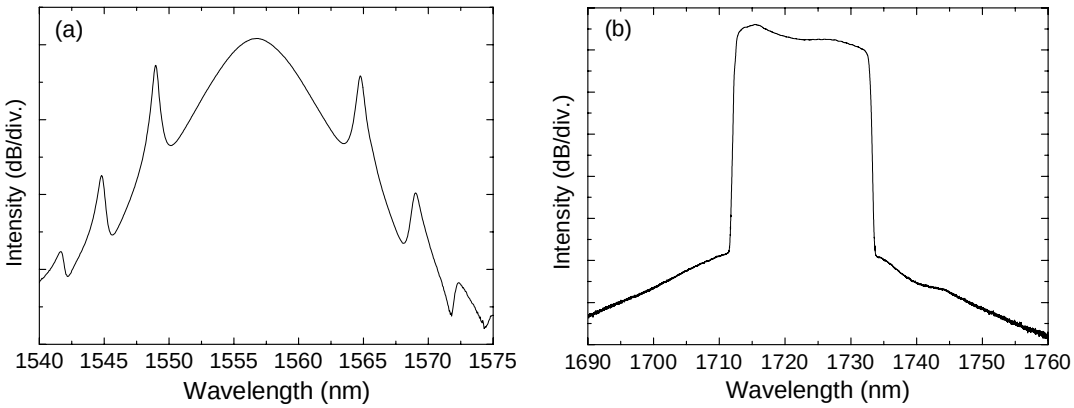

Figure 3.5: *(a) A typical spectrum for a soliton operation of the laser with a net anomalous dispersion cavity. (b) A typical spectrum of a dissipative soliton from a laser operating in normal dispersion regime.*

A typical spectrum characteristic for the soliton operation of the laser is shown in Figure 3.5 (a). The spectrum is Gaussian or hyperbolic secant shaped and contains additional superimposed narrow peaks, called Kelly sidebands. These sidebands are formed when the co-propagating dispersive wave is coupled to the soliton by periodical disturbances occurring inside the cavity [71]. The dispersive wave is a part of the pulse which is not properly developed into a soliton but remains as a background together with the actual soliton. The nonlinearity for this low-intensity background is not high enough to compensate the chromatic dispersion. The periodic disturbances are occurring because of discrete nature of chromatic dispersion and Kerr-nonlinearity and additionally because of periodical local losses and gain inside the laser cavity.

Different pulse dynamics are observed when the cavity dispersion is changed to normal dispersion regime. The resulting pulses are often called dissipative solitons. Compared

to conventional solitons described earlier, dissipative solitons are characterized by their continuous exchange of energy with the environment, accompanied by energy redistribution between the parts of the soliton itself [72].The main interest for dissipative solitons emerged at the beginning of 2000s, when scientist started to design cavities capable of delivering higher pulse energies. Mainly, the maximum pulse energy of a conventional soliton is fundamentally limited by accumulation of nonlinear phase shift which will eventually force the pulse to break into multiple pulses. Therefore, in recent years great amount of interest has been devoted to development of dispersion managed and all-normal dispersion lasers.

In dispersion-managed fiber lasers, the cavity is formed by including fibers or other components with both anomalous and normal dispersions, forming a so called dispersion map of the cavity. In case of dispersion-managed lasers, the pulse acquires strong breathing dynamics inside the cavity. The pulse is compressed and subsequently stretched when the sign of the dispersion is changed. The circulation of these highly stretched pulses enables higher pulse energies to be achieved, since the pulse breaking is suppressed as a result of reduced peak power and, therefore, reduced nonlinear phase shift [72]. Dispersion-managed fiber lasers can demonstrate both soliton-like and all-normal-dispersion like attributes depending on the net dispersion of the cavity in the average sense.

Further increase in pulse energy is possible by using cavities which comprise only fibers with normal dispersion at the signal wavelength. In all-normal-dispersion fiber lasers the pulse does not breathe during the round-trip, instead of this the pulse is formed as a balance between spectral filtering, nonlinearity and chromatic dispersion plus gain-loss characteristics of the laser medium. A typical spectrum of a pulse from a net normal dispersion cavity is shown in Figure 3.5 (b), displaying the characteristic rectangular or M-shaped spectrum with steep edges contrary to Gaussian-shaped spectra of conservative solitons (Figure 3.5 (a)). In all-normal-dispersion cavities the pulse is stretched even more than in dispersion-managed cavities operating in net normal dispersion regime. Therefore, in all-normal dispersion resonators the multiple pulse instabilities are well suppressed because of reduced nonlinear effects.

3.4 Pulse compression

The minimum pulse duration from a laser oscillator is dependent on the spectral bandwidth of the pulse. A pulse at this limit is called a transform limited pulse, and can be characterized by a parameter called the time-bandwidth product, a product of its duration and spectral width. For Gaussian-shaped pulses, transform-limited pulses have time-bandwidth product of 0.44, whereas for sech^2-shaped pulses the limit is 0.315. However, it is common that the time-bandwidth product of an optical pulse is considerably higher than the fundamental limit. Essentially this denotes that the temporal dura-

tion of the pulse is higher than the lowest possible value for a given spectral width, meaning that the peak power of the pulse is lower than in optimal case.

The deviations from the optimal time-bandwidth product are caused by a pulse property called chirp, which is understood as time-dependency of its instantaneous frequency. The chirp can be further categorized to up-chirp and down-chirp, where the instantaneous frequency rises or decreases as a function of time. In the absence of the chirp the pulse is transform-limited. The chirp can be superimposed on a pulse during propagation in a dispersive media or because of nonlinearities, such as self-phase modulation. In dispersion managed and all-normal-dispersion laser cavities the pulse acquires a strong chirp when stretching in time domain. This is exploited to reduce the nonlinear effects as described more detailed in previous section.

However, optimizing the peak power of the final output pulse is usually one of the main laser design goals, and therefore different methods for compressing chirped pulses have been developed. The most straightforward case is a pulse with a linear chirp, which can be compressed relatively easily by using dispersive elements, such as prisms or gratings external to the cavity. The use of external optical fiber for pulse compression is possible as well and is often preferred in case of fiber lasers due to its easy implementation, maintaining the all-fiber setup without bulk optical components. Unfortunately, the chirp is not always perfectly linear because of higher order dispersion, and therefore even after compression transform-limited quality cannot always be guaranteed.

3.5 Power scaling using MOPA-systems

The achievable pulse energy from a fiber laser cavity is often limited due to phenomena described in previous section. Furthermore, optical damage of the laser components, such as saturable absorbers, can be a serious problem when high pulse energies are present inside the cavity. Because of these fundamental and practical limitations, a fiber amplifier is often used together with the laser oscillator, forming a so called master oscillator – power amplifier (MOPA) architecture. In case of fiber lasers and amplifiers, the system is sometimes called MOFA (master oscillator – fiber amplifier) or MOPFA (master oscillator – power fiber amplifier). Here the general term MOPA is used.

Figure 3.6 shows the schematic of a MOPA. The pulse generator (master oscillator) is used to feed the amplifier with optical pulses. The amplifier should have a gain fiber suitable for efficient amplification of the pulse. Therefore, the gain bandwidth of the amplifier should be wide enough to provide efficient gain for the whole spectral region of the pulse, which in case of ultrashort pulses may be few or even tens of nanometers in width. In subsequent power amplifier, the pulses may be amplified to considerably higher power levels, up to 20 dB or 30 dB amplifications are not unusual.

An interesting approach to power scaling is to exploit stretching of the pulse to achieve high power pulsed operation. This method is called chirped pulse amplification (CPA), first demonstrated for optical pulses in the middle 1980s [73].

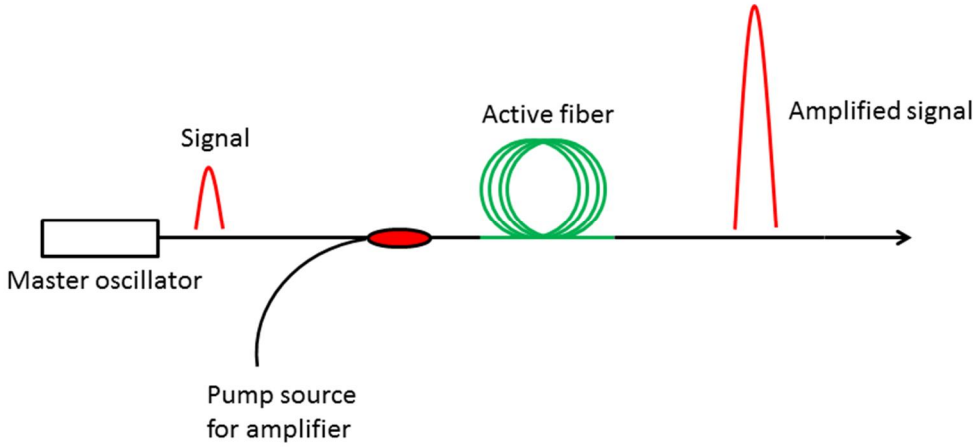

Figure 3.6: *The schematic of a principle for power scaling using a master oscillator – power amplifier configuration. The signal from the master oscillator is seeded to amplifier, which increases the signal power level in the presence of suitable pumping.*

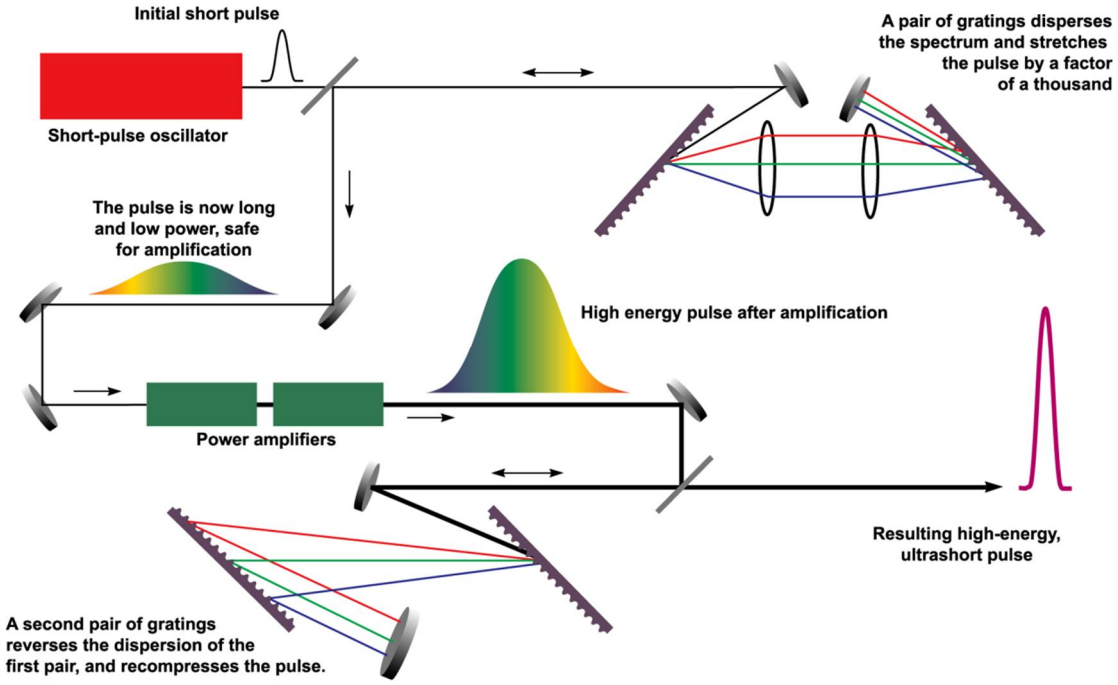

Figure 3.7: *The schematic of a CPA-system. Slightly modified figure taken under public domain from [74].*

Similar to laser resonators, in amplifiers there is a limit for the achievable peak power, after which the nonlinear effects become so dominant that the pulse quality is sacrificed. In CPA-technique the pulse from the master oscillator is stretched in time-domain before it enters the power amplifier. Similar to pulse dynamics in dispersion-managed and all-normal-dispersion cavities, the stretching of the pulse reduces the peak power and therefore restricts the nonlinear effects inside the amplifier medium. The stretched and highly chirped pulse is then propagating through the amplifier, enabling the pulse energy to grow possibly by few orders of magnitudes. After the amplifier, this high energy but relatively long pulse is then restored to its original temporal duration by a subsequent pulse compressor (Figure 3.7). Using the CPA-technique, short and energetic pulses can be generated without damaging the optical components inside the amplifier and without sacrificing the pulse quality because of nonlinear effects.

Different realizations of the pulse stretcher and compressor are possible. As described more detailed in previous section, it should be noted that lasers for generation of dissipative solitons are essentially acting as dual purpose devices, since they generate optical pulses and provide an intrinsic mechanism for pulse stretching simultaneously. If these dissipative solitons are then amplified with a fiber amplifier and possibly subsequently compressed, the system is essentially identical to CPA-system [72]. In addition to diffraction gratings, the compressor can be realized by adding a proper length of fiber with suitable sign of dispersion. Therefore, in some cases a fiber amplifier can act as both amplifier and pulse compressor if the dispersion of the amplifier gain fiber is chosen carefully.

4. DEVELOPMENT OF MODE-LOCKED BISMUTH FIBER LASERS

This chapter describes the experimental work accomplished for developing two different pulsed bismuth fiber laser systems operating at wavelengths of 1400 nm and 1700 nm. Both pulsed devices are implemented using passive mode-locking, exploiting the broad bandwidth of CNT saturable absorbers.

4.1 Carbon nanotube saturable absorber

In this work, carbon nanotubes were used as a saturable absorber. CNTs provide broadband absorption, and were a natural choice for experiments at novel wavelengths due to their ease of use compared to more complicated absorbers, such as SESAMs.

Carbon nanotube films were provided by Department of Physics in Aalto University. They were synthesized by a scale-up aerosol reactor using ferrocene as the catalyst precursor and CO as the carbon source. The reactor temperature was 880 °C. The total flow of the aerosol was 84 liter per minute of which 40 liters per minute was sucked from the side as shown schematically in Figure 4.1. The CNTs were collected on the nitrocellulose filter which was rolled inside the dilutor on the porous wall. The absorption spectrum for CNT was recorded with a double beam Perkin-Elmer Lambda 950 UV-Vis-NIR spectrometer equipped with two excitation sources of a deuterium lamp and a halogen lamp, which covered the working wavelength range from 175 to 3300 nm. The measured absorption spectrum is shown in Figure 4.2 (a).

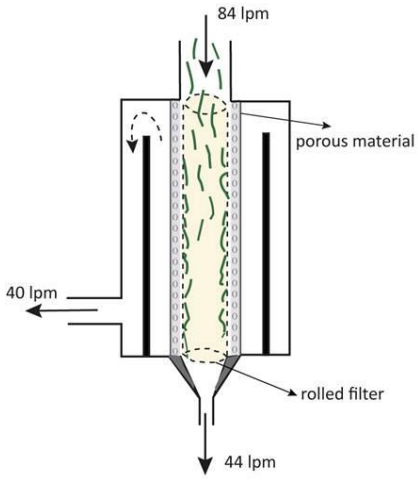

***Figure 4.1**: Schematic illustration of the inverse dilutor for collecting CNT-films. A filter collecting the CNTs was rolled inside the dilutor on the porous wall.*

The carbon nanotube film was then transferred onto a silver mirror by pressing the filter and SWNT-film (SWNT-film side down) against the mirror. The carbon nanotube film was strongly adhered on the mirror surface as a result of applied pressure, after which the remaining filter was peeled off leaving a pure SWNT-film on the mirror surface. As described in Section 3.2.2, major drawback of CNT-absorbers is their relatively high non-saturable losses and low ratio of modulation depth to the non-saturable loss. Particularly in case of fiber lasers, a stable mode-locking needs sufficient value of modulation depth, whereas considerable amount of non-saturable losses is admissible because of usually high values of gain. Therefore, multiple layers of carbon nanotube film were needed to increase the modulation depth of the absorber, although this unavoidably increased the non-saturable losses as well. At least two layers of SWNT-film were found to be vital in order to achieve stable mode- locked operation and suppress the parasitic continuous wave oscillations, which were encountered when using an absorber with just one layer of SWNT-film.

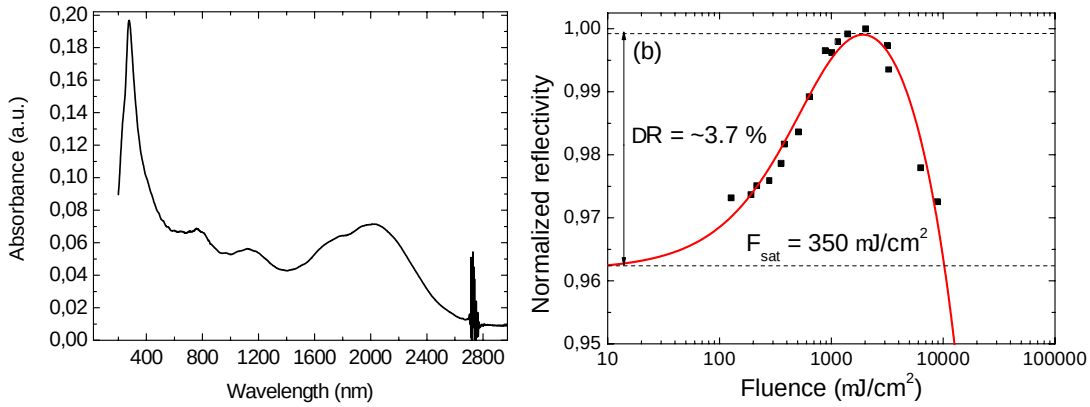

***Figure 4.2**: (a) The linear absorption of a single layer of CNT-film used as a saturable absorber. (b) The nonlinear absorption of two layers of CNT-film deposited onto a silver mirror.*

4.2 Bismuth fiber laser at 1450 nm

The experimental work was started with bismuth-doped fibers providing gain at 1400-1500 nm wavelength region, the gain peaking at ~1430 nm. Two different types of fibers were tested and used in these experiments. The active fibers were fabricated and kindly provided to our use by Fiber Optic Research Center (FORC) located in Moscow, Russia.

4.2.1 Fiber characterization

Two fiber types with different absorption and gain properties were characterized and used in the experiments. Both fiber preforms were made by the MCVD technique. High-absorption fiber (Bi-75) has higher bismuth weight concentration (≈ 0.3 %) in the fiber core compared to the low-absorption (Bi-203N) fiber (≈ 0.031%). Fibers have step index profiles with Dn ≈ 7×10^{-3} and Dn ≈ 9×10^{-3} formed by adding of 5 mol.% and 6.5 mol.% of germanium in high- and low-absorption fibers, respectively. The cut-off wavelength is ≈ 0.9 µm for both fibers.

Both of the fibers were excited using 1.32 µm semiconductor disk laser (SDL) as a pump source. SDL delivered near diffraction limited beam quality, essential for achieving efficient core pumping necessary for bismuth doped fibers. Absorption and gain spectra observed for excitation wavelength of 1320 nm are presented in Figure 4.3. The highest net gain of 4.4 dB/m for high-absorption fiber and 0.7 dB/m for low-absorption fiber peaking at 1420-1430 nm were measured for 350 mW of pump power at 1320 nm.

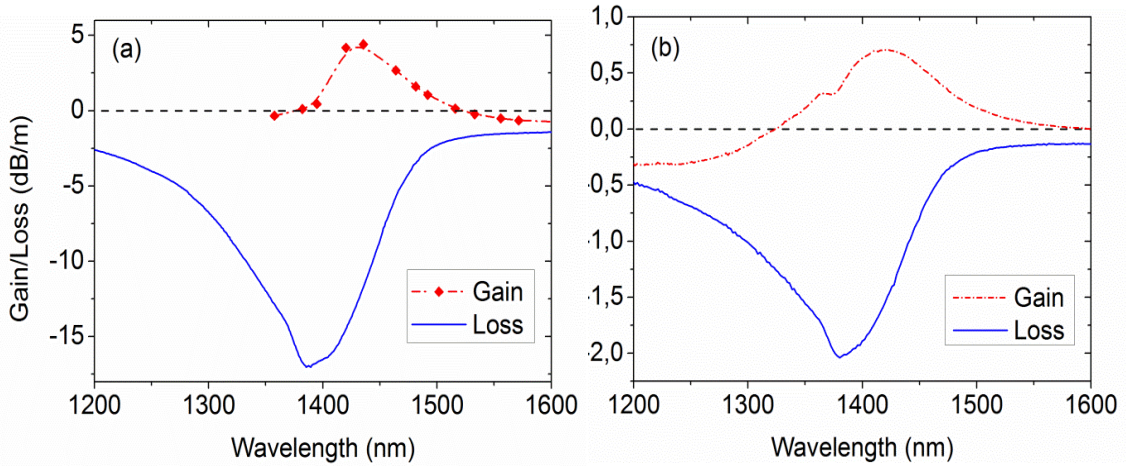

Figure 4.3: *The optical loss and gain for bismuth-doped fibers with (a) high absorption and (b) low absorption values.*

The energy transition mechanism of the fibers was determined by the method based on relaxation oscillations. These are small-amplitude oscillations, the frequency of which is dependent on the transition cross section, level degeneracy and partition functions of for both ground and excited energy levels [12].For three-level laser systems, the rate equations yield to a small-signal solution of relaxation oscillation frequency given by

$$\omega^2 = \frac{1}{\tau_C \tau_s}(1 + c\tau_c \sigma \eta f^l N)(r-1), \tag{5}$$

where N is the number of ions, c is the speed of light, σ is the transition cross section, and f^l is the thermal occupation of the lower energy level. τ_C and τ_s are the cavity and laser lifetimes and $\eta = l/[L + l(n-1)]$, where L is the total cavity length and n is the refractive index of the gain medium. r represents the normalized pump rate. For three-level laser systems frequency ω^2 is wavelength-dependent, since the transition cross-section is wavelength dependent and lower energy level has non-zero thermal occupation. On the other hand, for four-level systems the value of ω^2 is wavelength-independent, since the population on the lower laser transition level is negligible. Therefore $f^l = 0$ and the dependence of the wavelength via transition cross-section disappears from the equation.

The relaxation oscillation frequencies for both of the fibers were measured using a simple linear CW laser cavity scheme. The pumping was provided by a SDL through a pump combiner. A 3 nm tunable filter was incorporated inside the laser cavity in order to tune the wavelength of the laser. An additional free-space section inside the cavity was arranged by using lens coupling to a mirror, allowing a chopper to be placed in the

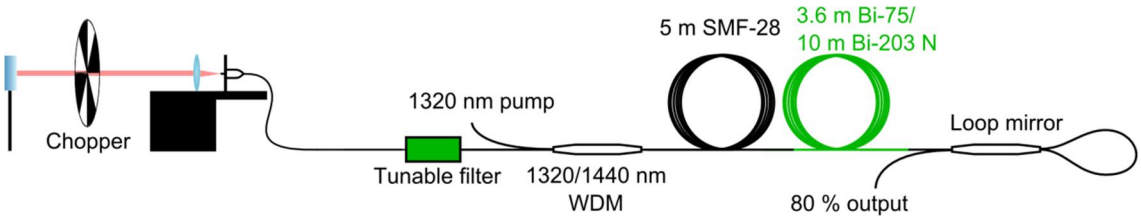

Figure 4.4: *The schematic of the setup for relaxation oscillation measurements. A chopper was placed in the free-space section of the laser to enable the observation of transient laser dynamics.*

free-space section (Figure 4.4). This enabled one to monitor the spectrally resolved transition oscillations of the laser by using an oscilloscope and an optical spectrum analyzer (OSA). Although the overall cavity length as well the active fiber length is affecting the absolute value of relaxation oscillation frequency ω^2, its wavelength dependence arises only from the non-negligible population on the terminal laser transition energy level, which does not appear as a function of fiber length. Therefore, reliable characterization of the laser system is possible using arbitrary fiber lengths.

Figure 4.5 shows a typical relaxation oscillation recorded with a digital oscilloscope. Figure 4.6 represents the obtained wavelength dependency of the relaxation oscillation frequencies for two tested bismuth-doped fibers. The relaxation oscillation frequency was determined from the strongly-damped, small-amplitude near sinusoidal oscillation visible in Figure 4.5.

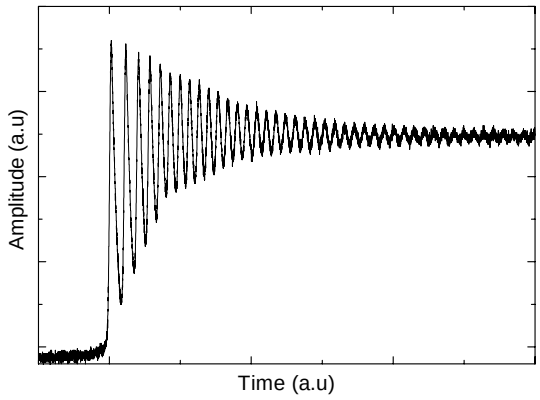

***Figure 4.5**: A typical relaxation oscillation from 1400 nm bismuth-doped fibers*

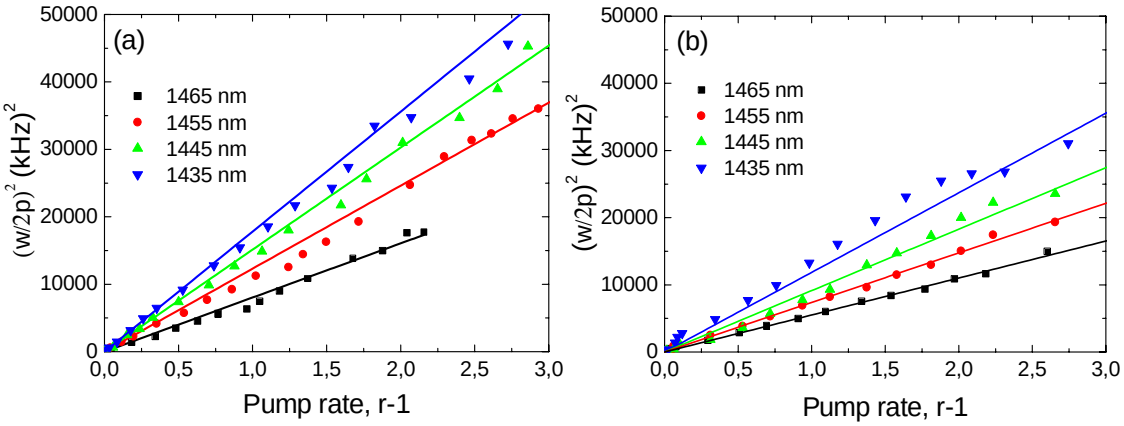

***Figure 4.6:** The wavelength-dependence of the relaxation oscillation frequency for (a) high-absorption and (Bi-75) (b) low-absorption (Bi-203N) bismuth-doped fibers.*

The wavelength dependence of the relaxation oscillation frequency indicates a three-level laser medium. Figure 4.6 clearly shows that the slope of the linear fitting is changed for different wavelengths, indicating that both bismuth-doped fibers are showing three-level laser system behavior. It should be noted, however, that the change of the slope is modest in case of low-absorption Bi fiber This can be interpreted so that low-absorption Bi-doped fiber acts as a quasi-three-level system, and the population at the terminal laser level is decreased compared to the high-absorption bismuth fiber.

4.2.2 Mode-locking in anomalous dispersion regime

After fabrication of the saturable absorber mirrors and characterization of the fibers a laser cavity supporting soliton operation in anomalous dispersion was designed and assembled. Both of the active fibers, Bi-75 and Bi-203N were tested as gain medium. The linear design was used as a cavity scheme. The schematic of the cavity is shown in Figure 4.7. Pump light provided by a 1.3 μm semiconductor disk laser (SDL) delivering near diffraction limited beam quality was coupled into a cavity by using a 1320/1440 pump combiner. The linear fiber cavity was terminated by a loop mirror with relatively high ~80% output coupling. The other end of the cavity was a CNT saturable absorber triggering mode-locked operation. The high output coupling was noticed to suppress effectively parasitic CW oscillations, which are often encountered when using CNT saturable absorbers with moderate nonlinearity. Essentially, the weak absorber is unable to suppress the CW oscillations if the energy inside the cavity is too high. For that purpose, high output coupling was used, keeping the energy level still suitable to saturate the absorber.

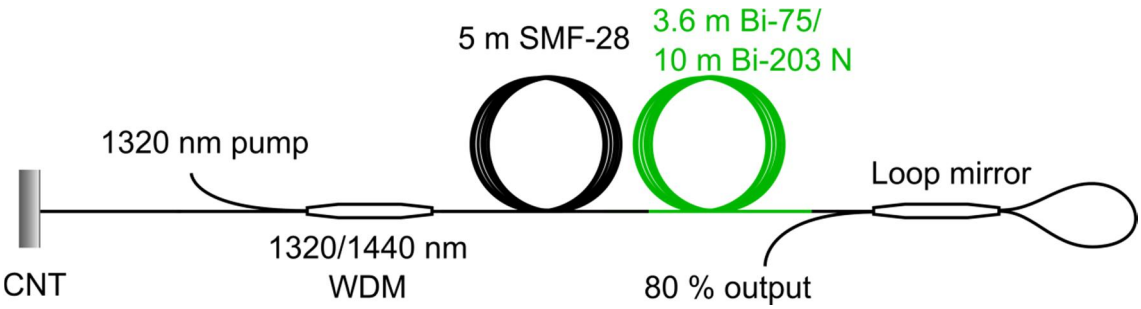

Figure 4.7: *The schematic illustration of the linear anomalous dispersion cavity. The length of the gain fiber was 3.6 m and 10 m for high- and low-absorption fibers, respectively. About 5 meters of SMF-28 was added to provide sufficient anomalous cavity dispersion.*

For high-absorption fiber (Bi-75) the length of the active fibers was 3.6 m. About 7 meters of standard telecom fiber SMF-28 was added inside the cavity to ensure sufficient net cavity dispersion value of 0.22 ps/nm. The fundamental repetition rate of the laser was 9 MHz corresponding to the total cavity length of 11.5 m. However, the fundamental repetition rate was not observed when the laser operated in stable mode-locked regime, instead the laser showed a strong tendency to multiple pulse operation even at the mode-locking threshold. The spectrum and the corresponding autocorrelation trace for the laser operating in the anomalous dispersion regime are shown in Figure 4.8. The laser delivered 525 fs pulses with 250 mW threshold pump power. The bandwidth of the pulse spectrum equaled to 6.98 nm and centered at 1450 nm, yielding to a time-bandwidth product of 0.52 indicating a slightly chirped pulse. The chirp is acquired in a relatively long output fiber incorporating two spectral filters for unabsorbed pump power. The achieved output power of the laser was 2.5 mW with 320 mW of pump power. Multiple pulse regime negatively affected on energy and peak power reducing their value in comparison to single pulse operation.

The low-absorption fiber Bi-203N was used as a gain media as well. In this case, active fiber length of 10 m was used to compensate the lower absorption per meter value of the fiber. The extra SMF-28 was removed from the cavity, since sufficient anomalous dispersion value could be achieved using the active fiber only. With this fiber, the laser demonstrated comparable output pulse quality as shown in Figure 4.9. However, the output power and efficiency of the laser performance with Bi-203N as gain medium was improved. The average output power reached up to 11.3 mW by using 170 mW of pump power. Again, multiple pulses with relatively chaotic pulse dynamics were observed, as seen from Figure 4.9 (c).

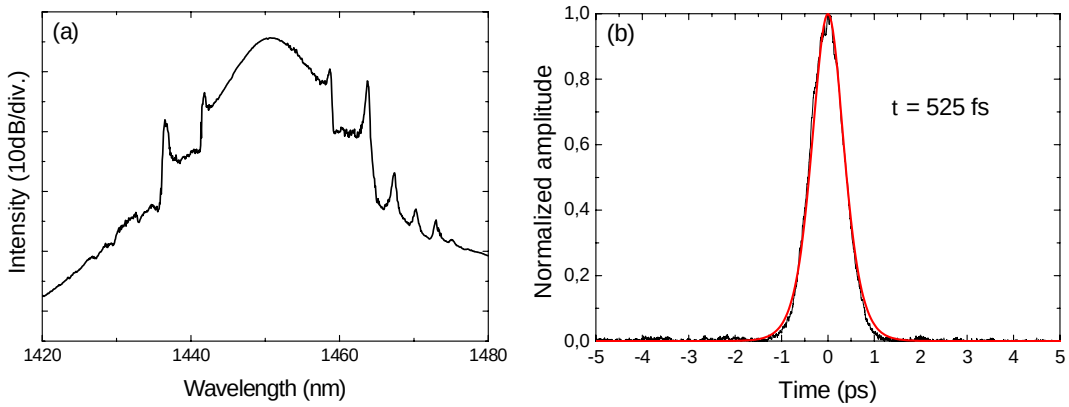

Figure 4.8: *The spectrum and autocorrelation trace of the output pulse. The gain fiber was high-absorption fiber Bi-75.*

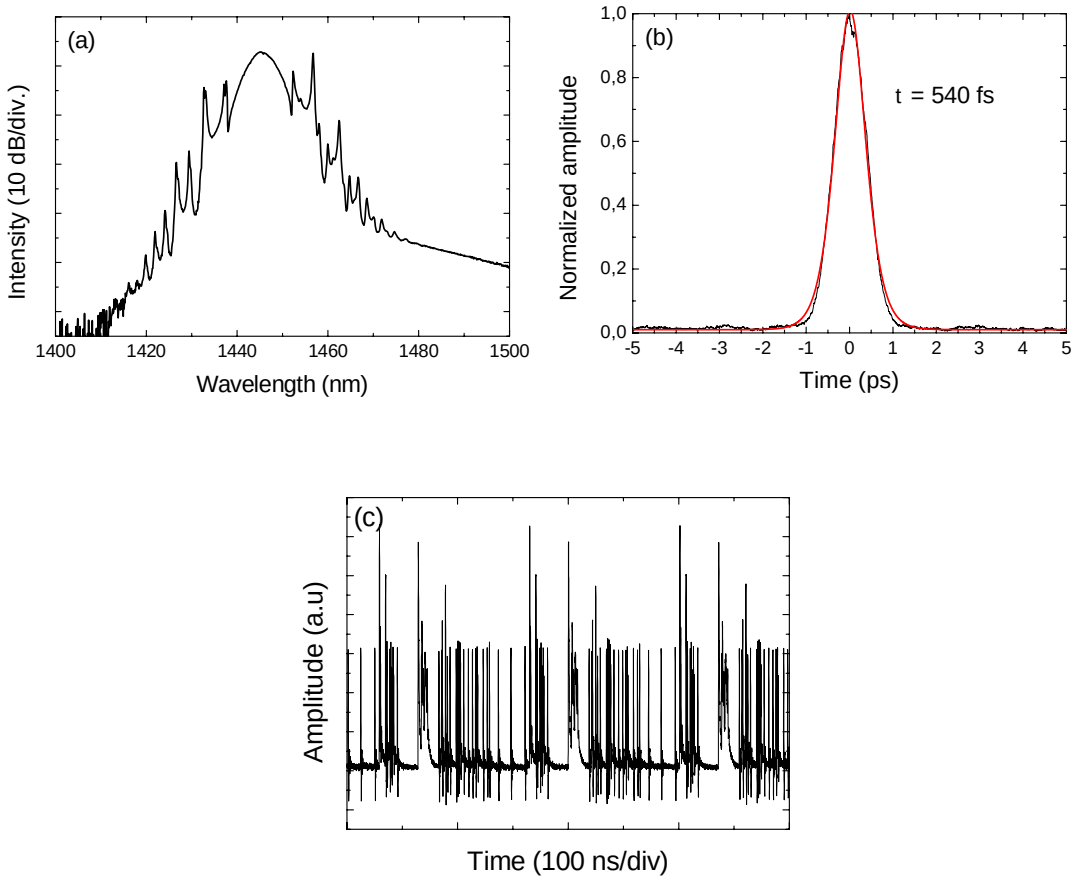

Figure 4.9: *(a) The spectrum and (b) the autocorrelation trace of the output pulse for low-absorption fiber Bi-203N. (c) The output pulse train recorded by a fast digital oscilloscope and a photodetector. Both of the fibers showed strong tendency to multiple pulse instability in anomalous dispersion regime.*

In conclusion, both of the bismuth-doped fibers delivered mode-locked operation in anomalous dispersion regime at ~1440 nm wavelength with comparable parameters of the output pulse. The laser suffered from pulse breaking as common for mode-locked lasers operating in anomalous dispersion regime. With bismuth-doped fibers the pulse breaking was very pronounced, and single-pulse operation of the laser was not observed in anomalous dispersion regime within the whole pump range. The results are in comparable with [44], where the pulse grouping effect was studied in more detail.

4.2.3 Mode locking in normal dispersion regime

To suppress the multiple pulsing and increase the pulse energy and peak power of the laser, the cavity dispersion was changed to the normal dispersion by removing additional SMF-28 and adding 0.9 m/2.4 m of dispersion compensation fiber (DCF) inside the cavity for Bi-75/Bi-203N fibers, respectively [P1]. The normal dispersion regime

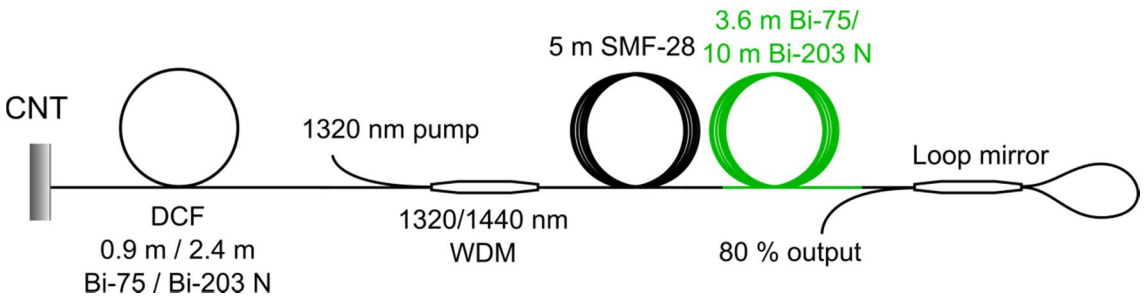

Figure 4.10: *The schematic illustration of the linear net normal dispersion cavity. DCF was added to change the dispersion value to -0.16 ps/nm (normal dispersion). Different length of the DCF was needed depending on the length of the active fiber.*

supports dissipative solitons, preventing the formation of multiple pulses prominent for lasers operating in the anomalous dispersion regime and therefore increasing the energy of a single pulse. Both active fiber lengths remained same than for anomalous dispersion regime. The DCF had -0.09 ps/nm·m normal dispersion, changing the net cavity dispersion to value of ~ -0.16 ps/nm. The schematic of the net normal dispersion cavity is shown in Figure 4.10.

With Bi-75 fiber as a gain medium the laser delivered single-pulse output at 20 MHz fundamental repetition rate corresponding to ~5 m of total cavity length. The mode-locking threshold was 200 mW, what is comparable to the threshold in anomalous dispersion regime with the same fiber. No sign of pulse breaking instability was observed in this dispersion regime. However, the average output power of the laser was lower than in anomalous dispersion regime. The laser delivered only 1.5 mW of average power using 320 mW of pump power, almost 50 % lower than the value in anomalous dispersion regime. The decrease in the output power was because of the high splice losses between DCF and SMF-28. This is a well-known disadvantage of DCFs and decreasing the splice loss between the standard telecom fibers and DCFs is of the technical interest [75]. The losses inside the cavity were minimized by placing the DCF before the absorber and butt-coupling DCF to the absorber. This enabled the use of only one SMF-DCF splice. The remaining SMF-DCF splice loss was separately measured to be ~1 dB when using optimized splicing parameters for direct splicing without using any intermediate fibers.

The spectrum and autocorrelation trace of the output pulse are shown in Figure 4.11. The pulse duration was 2.1 ps and a 20 nm spectral bandwidth corresponds to a time-bandwidth product of 6.1. The large value of the product is indicative of a large chirp acquired during the cavity roundtrip, which is typical for dissipative solitons generated in cavities operated in normal net cavity dispersion regime. In normal dispersion regime, the laser operated at the fundamental repetition rate determined by the cavity

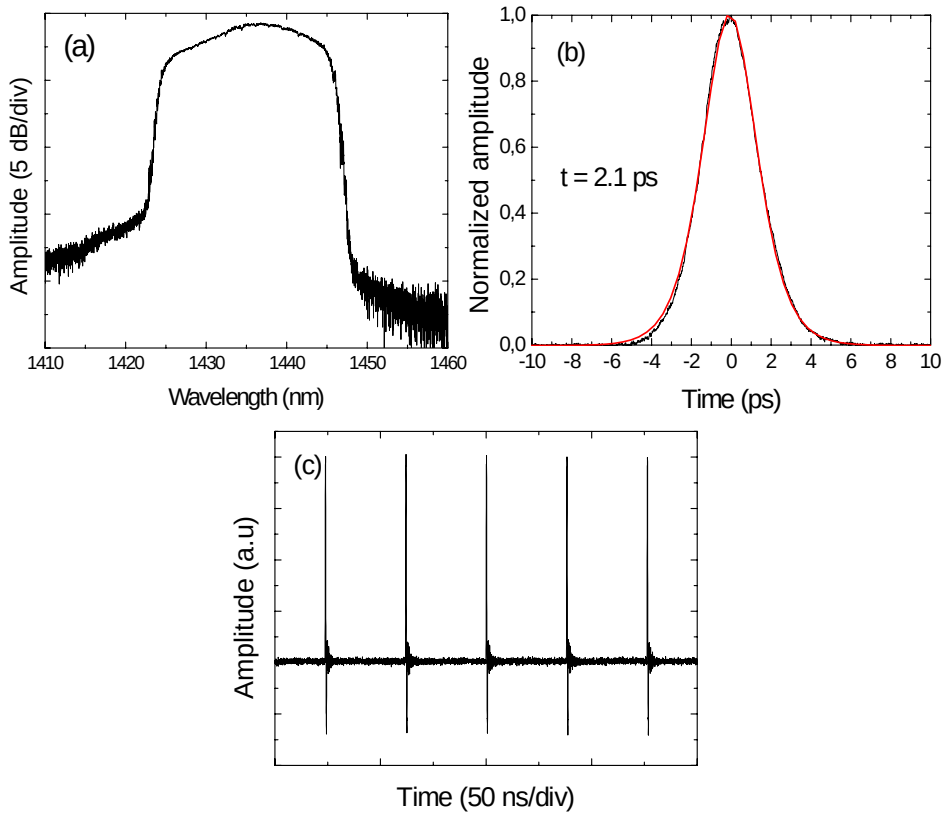

Figure 4.11: *(a) The spectrum, (b) the autocorrelation and (c) the oscilloscope trace of the output pulse train in normal dispersion regime. The gain fiber was Bi-75. Reprinted with permission from [P1], © 2015 Optical Society of America*

length, and no sign of pulse breaking instability was observed. The laser delivered 1.5 mW average output power using 320 mW of pump power.

The other gain fiber, Bi-203 N was then switched the in place of Bi-75 (Figure 4.10). Because of the longer active fiber length the length of DCF was increased to 2.4 m to compensate the increase in anomalous dispersion. Other parameters of the laser remained constant. The output characteristics of the laser are presented in Figure 4.12. The laser delivered 23 mW of average power when the pumping power was 380 mW. This is a clear improvement compared to results with Bi-75.

The laser operated at a fundamental repetition rate of 6.25 MHz (Figure 4.12 (c)), corresponding to pulse energy of 3.7 nJ. However, the spectrum deviated from the conventional spectrum for normal dispersion regime mode-locking, showing additional modulation. Moreover, from autocorrelation (Figure 4.12 (b)) it is noticed that the pulse is superimposed on a large pedestal, which is a clear indication of bad pulse quality and/or poor stability of the mode-locking. Careful analysis of the oscilloscope picture could reveal multiple pulse bunch within the same envelope. The exotic pulse interaction within the group could result in spectrum modulation, pedestal being the evidence in the autocorrelation trace.

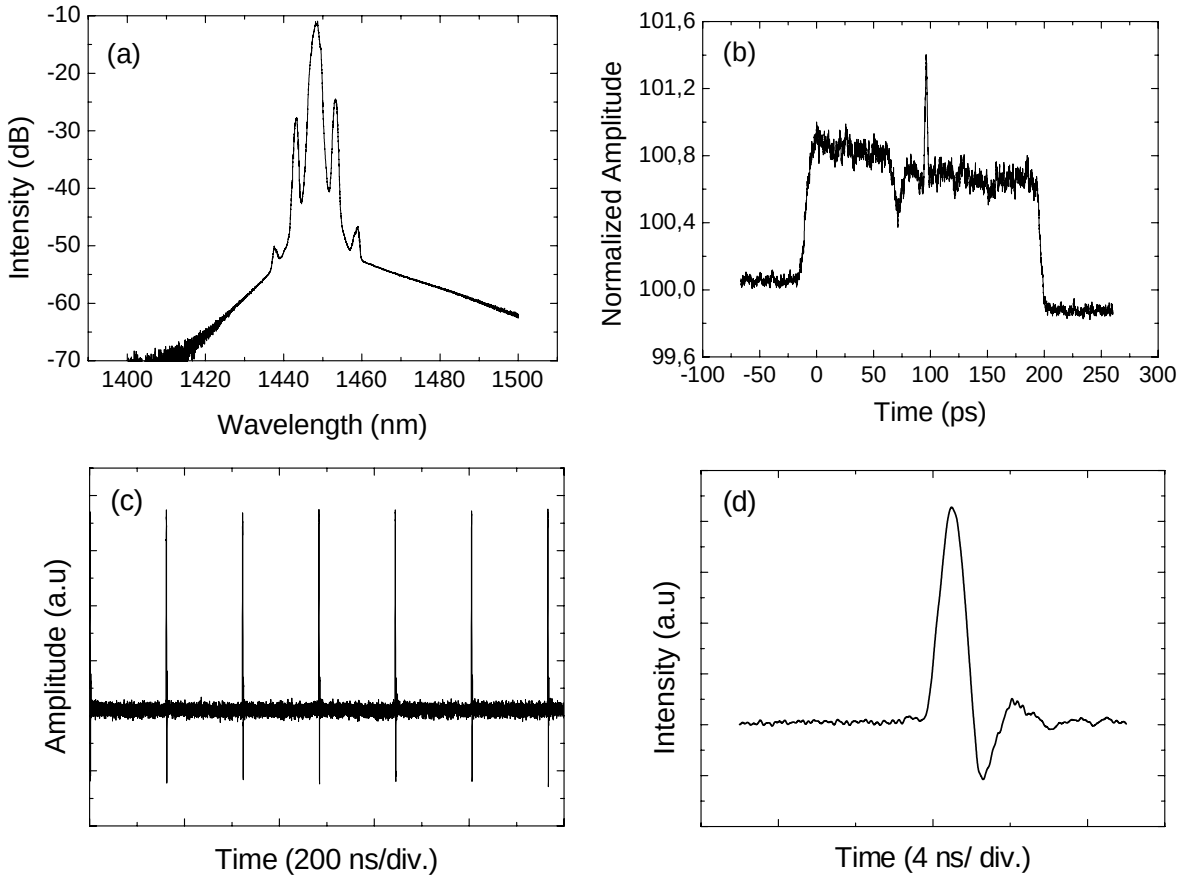

Figure 4.12: *(a) The spectrum, (b) the autocorrelation and (c) the oscilloscope trace of the output pulse train in normal dispersion regime. (d) The oscilloscope trace of a single pulse. The gain fiber was 203N.*

However, the existence of the sub-pulses inside the pulse envelope could not be directly confirmed because of the limited resolution of the photodetector. The autocorrelator on the other hand could resolve pulses of few tens of femtoseconds, but it requires the pulses to be static in time domain. If the sub-pulses under the envelope are jittering fast in time-domain the autocorrelator sees them as a pedestal because of measurement averaging. Therefore, the exact nature of the pulses emitted by the normal dispersion laser using gain fiber Bi-203N remains unclear.

4.2.4 MOPA-system

To exploit the best elements of both bismuth gain fibers, a master oscillator – power amplifier (MOPA) architecture was used to increase the output performance of 1450 nm bismuth-doped fiber lasers operated in the net normal dispersion regime [P1].

The master oscillator was assembled using Bi-75 as a gain fiber, since the pulse quality using Bi-75 inside the laser outperformed the quality achieved with Bi-203N. Unfortunately, using Bi-75 resulted in penalty with achievable output power as described be-

fore. This was compensated by using high-efficient Bi-203N fiber inside the fiber amplifier.

The schematic illustration of the MOPA-system is shown in Figure 4.13. 35 meters of low-absorption fiber Bi-203N was used as a gain medium of the amplifier. The output of the pump SDL was shared between the amplifier and the master oscillator. The dispersion of the Bi-203N fiber was anomalous, and therefore the fiber amplifier acted both as a power amplifier and a pulse compressor, efficiently dechirping the pulses provided by the master oscillator. Essentially, the system was a fiber based CPA, where the stretched pulses provided by the master oscillator were amplified and simultaneously compressed to restore the high peak power of the pulse.

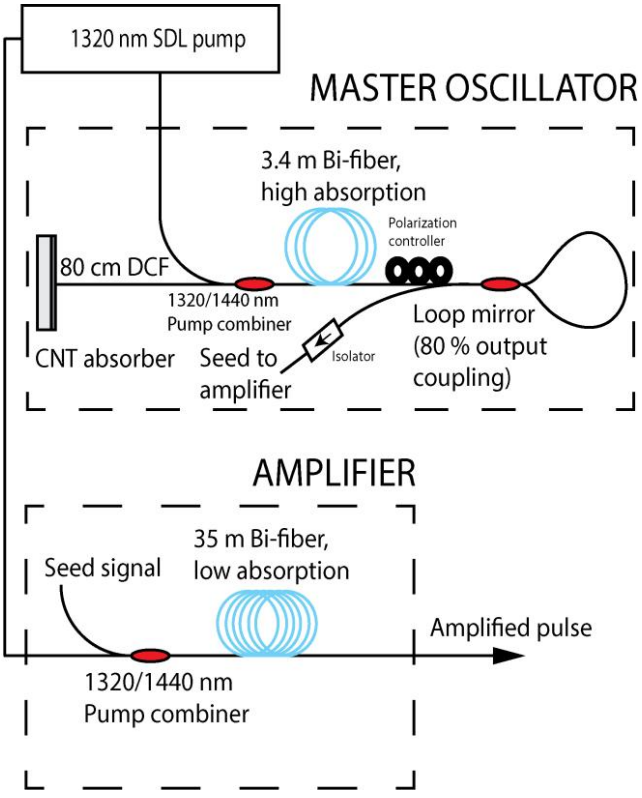

Figure 4.13: *The schematic of the MOPA-system. Reprinted with permission from [P1], © 2015 Optical Society of America*

The autocorrelation and the spectrum of the pulse after the amplification are shown in Figure 4.14. A substantial spectral broadening occurred inside the amplifier, creating a continuum with bandwidth of 175 nm. This is due to the nonlinear effects, such as four wave mixing (FWM), modulation instabilities, stimulated Raman scattering (SRS) and cross- and self-phase modulation (XPM, SPM) inside the amplifier fiber. This can be exploited in supercontinuum generation, [76].

Average output power of 15 mW was achieved by using 320 mW and 400 mW of pump power for the master oscillator and the amplifier, respectively. The FHWM pulse duration after the dechirping inside the fiber amplifier was as short as 240 fs, corresponding to peak power of 3.1 kW. The 240 fs pulses produced by the fiber system are the shortest pulses reported for any bismuth fiber based laser system to date.

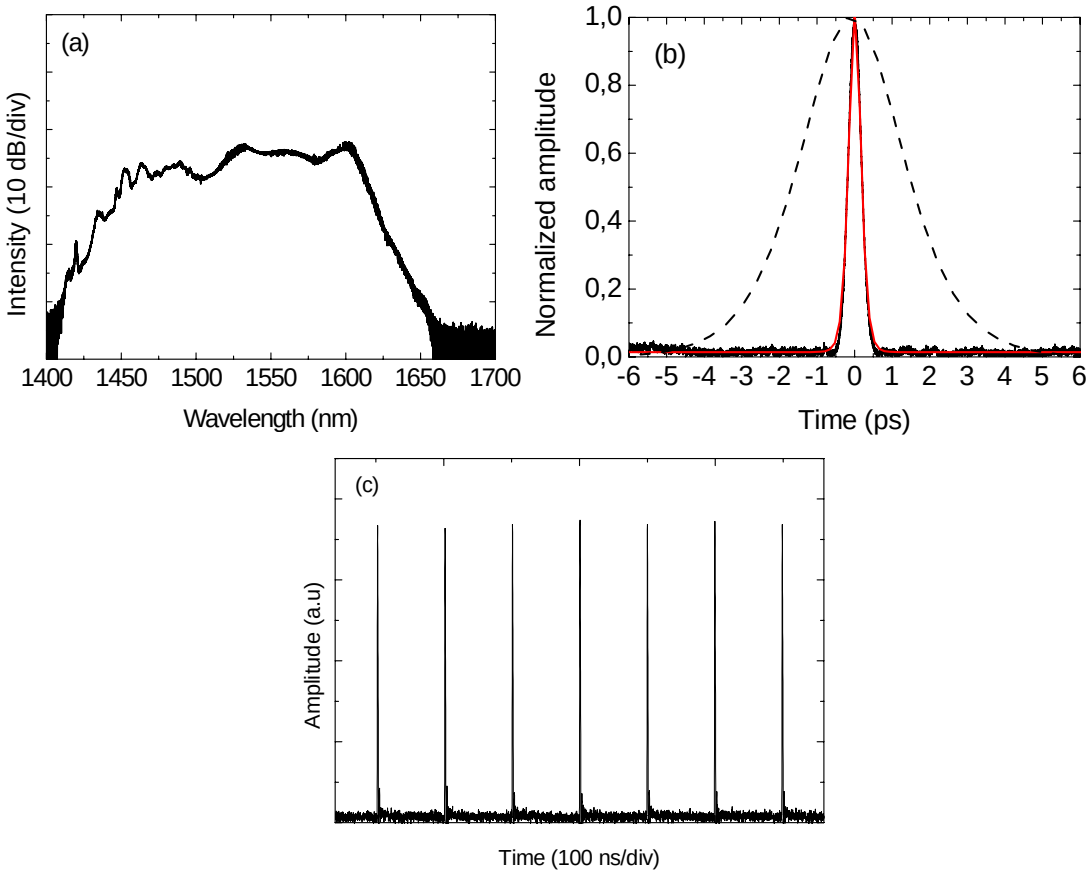

Figure 4.14: *(a) The spectrum, (b) the autocorrelation and (c) the oscilloscope trace of the output pulse train in normal dispersion regime after the amplification. The dashed line in (b) is the pulse before the compression inside the fiber amplifier. Reprinted with permission from [P1], © 2015 Optical Society of America*

4.3 Bismuth fiber laser at 1730 nm

After studying the bismuth doped fibers emitting at 1450 nm, the experimental research was extended to even longer wavelength, using novel bismuth fibers providing gain at 1700 nm. The experimental work at 1730 nm wavelength included the study of both anomalous and normal dispersion regimes and MOPA-system, similar to the experimental work completed at 1400 nm wavelength region [P2].

4.3.1 Fiber characterization

Single-mode gain fiber for 1700 nm was composed of a bismuth-doped fiber with an equal content of GeO_2 and SiO_2 in a core. The fiber preform was fabricated by a standard modified chemical vapor deposition (MCVD) process. The fiber with 125-µm diameter and cutoff wavelength of 1.2 µm was drawn from the preform after additional jacketing made at the same drawing speed. Bismuth concentration in the fiber core glass was ~0.02 wt.%.

The absorption spectrum of bismuth-doped fiber with two characteristic bands is presented in Figure 4.15. The absorption bands peaked at 1.4 and 1.65 µm caused by the formation of bismuth-related active centers are associated with Si and Ge, respectively. The optical properties of these bismuth-related active centers can be found in detail in [77], where the study is focused on investigation of the bismuth-doped fiber primarily for the spectral range between 1.6-1.8 µm.

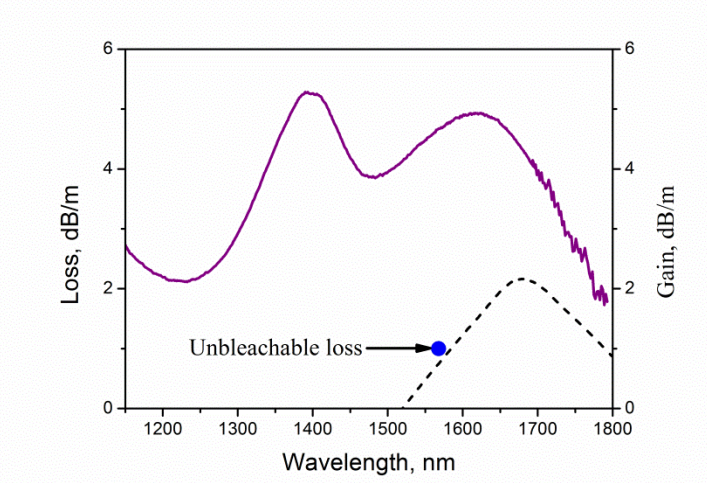

Figure 4.15: *The absorption and net gain of the used bismuth gain fiber for 1700 nm wavelength region. The unbleachable loss was measured at 1560 nm and is indicated as a dot.*

The loss of the fiber was measured at 1.56 µm as a function of pump power. The residual loss level shown in Figure 4.15 is ~1 dB/m, corresponding to the small signal absorption of 22%. The high level of unbleachable loss was due to the relatively high concentration of bismuth ions required for a laser with short cavity length. Figure 4.15 illustrates the gain spectrum of bismuth-doped fiber pumped at 1.46 µm. The highest small-signal gain of ~2 dB/m was observed at the wavelength 1.7 µm for pump power of ~200 mW.

Similar to the measurements with 1400 nm mode-locked bismuth fiber laser, the transient behavior of 1700 nm bismuth gain fiber was studied by examining the relaxation oscillations. Figure 4.16 shows the relaxation oscillation frequency measured at different wavelengths. The slope of the linear fitting reveals quite significant frequency dependence with wavelengths from which it can be concluded that 1700 nm bismuth gain fiber is acting as a three-level system based on the equation (5).

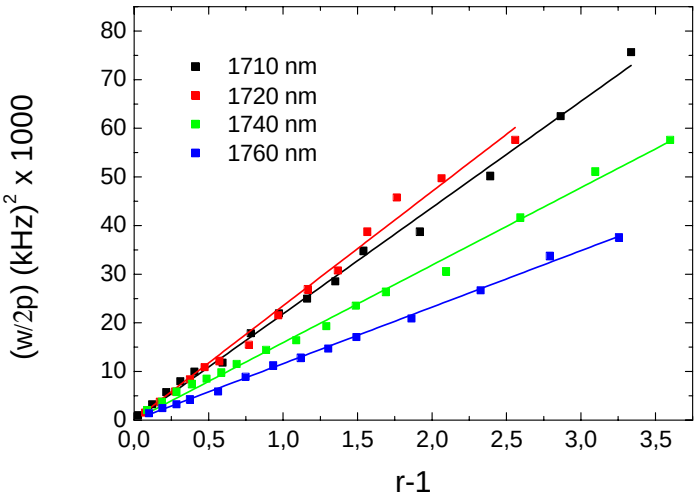

Figure 4.16: *The relaxation oscillations in 1700 nm bismuth-doped fiber. The change of the slope for different wavelengths indicates that 1700 nm bismuth acts as a three-level system.*

4.3.2 Mode-locking in anomalous dispersion regime

Similar to the experiments at 1400 nm, first an anomalous dispersion cavity supporting conventional soliton operation of the laser was designed and assembled. The schematic of the laser cavity is shown in Figure 4.17. The laser was pumped by a 1560 nm commercial fiber laser unit, capable of providing up to 5 W of pump power coupled to a single mode fiber. The pump light was coupled to the cavity using a 1560/1730 nm pump combiner. The active fiber length was 5 m. The 35 % output was taken through a loop mirror acting as an output coupler. The other end of the cavity was terminated by a CNT saturable absorber mirror, which enabled the passive mode-locked operation of the laser. The CNT saturable mirror used in anomalous dispersion regimes was equipped with two layers of CNT-film described in Section 4.1. To compensate the relatively high normal dispersion of the active fiber 19 meters of SMF-28 commercial telecommunication fiber was added inside the laser cavity, resulting in net cavity length of ~25 meters. The total cavity dispersion was equal to ~0.35 ps/nm.

Above 300 mW of pump power, a stable mode-locked operation was observed. The spectrum and autocorrelation of the output pulses are shown in Figure 4.18. The spectrum was centered at 1730 nm with a bandwidth of 2.91 nm. The pulse duration was 1.65 ps ($sech^2$-fitting is assumed), giving a time-bandwidth product of 0.48. This indicates a nearly transform limited pulse. A strong tendency for multiple pulse operation of the laser was observed with an increase of pump power. The laser exhibited a strong hysteresis behavior, maintaining the mode-locked operation until the pump power was decreased down to 75 mW. Below this pump power level the laser switched to CW-regime.

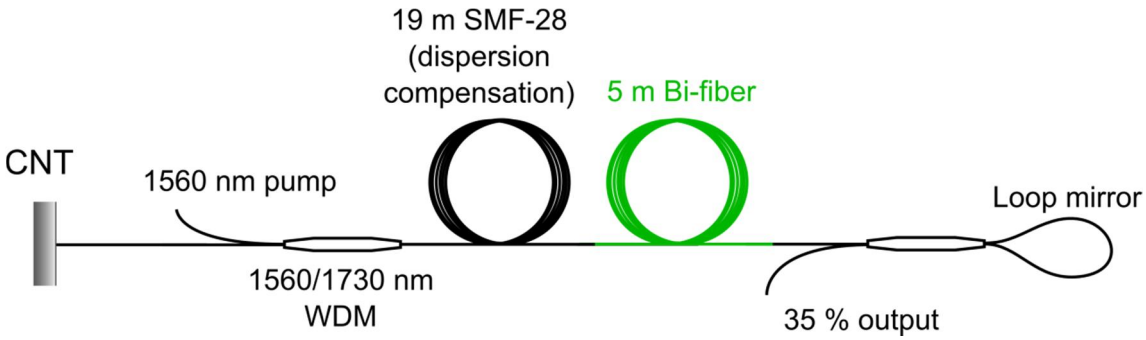

Figure 4.17: *The schematic of the bismuth fiber laser operating in anomalous dispersion regime.SMF-28 fiber (19 meters) was added to change the total dispersion of the cavity to anomalous regime.*

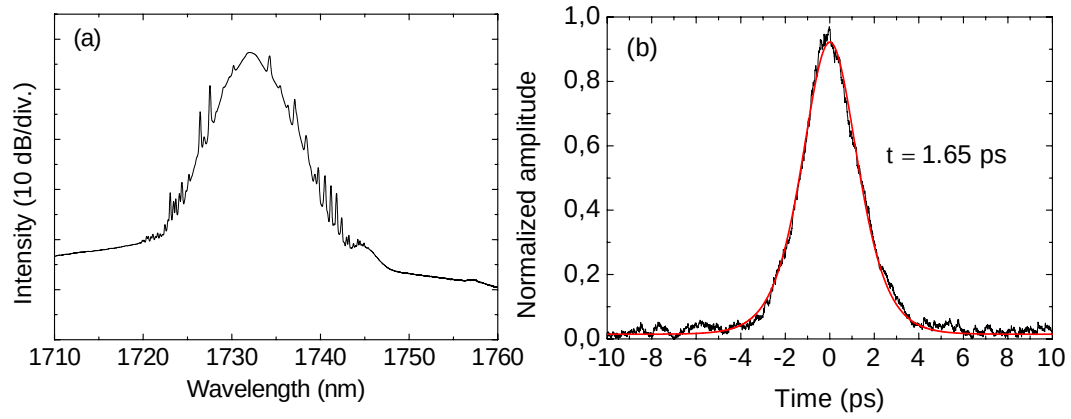

Figure 4.18: *The spectrum and the autocorrelation trace of the 1700 nm mode-locked bismuth fiber laser operating in anomalous dispersion regime.*

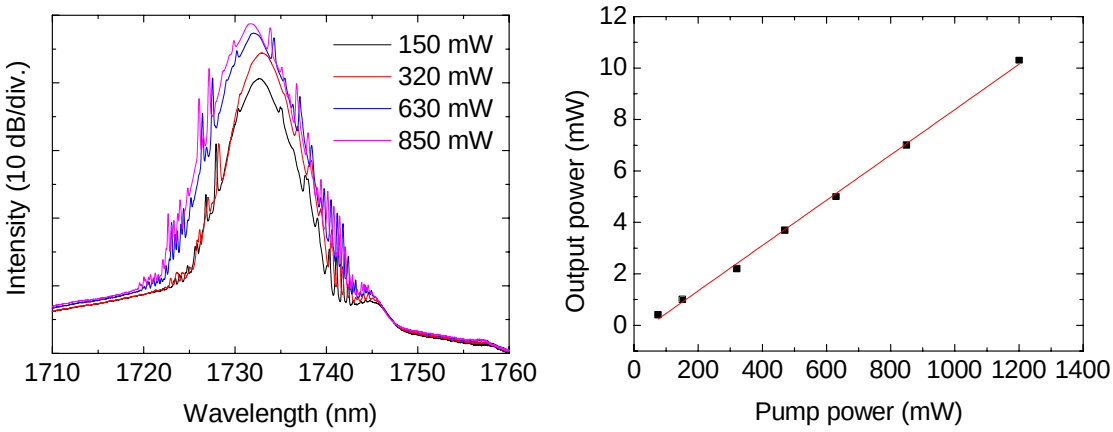

Figure 4.19: *(a) The spectrum recorded with different values of pump power (b) the slope efficiency of the laser.*

The spectrum was recorded for different pump powers, and only small deviations were observed in anomalous dispersion regime, as shown in Figure 4.19 (a). The slope efficiency of the laser was only 1 % as can be seen from Figure 4.19 (b). The modest efficiency was caused by a sum of different factors, such as a high splice loss between the active and passive fibers, relatively high linear absorption of the CNT-absorber, and relatively short length of the active fiber. The length of active fiber was determined by its high value of dispersion, to compensate which long length of SMF-28 was required.

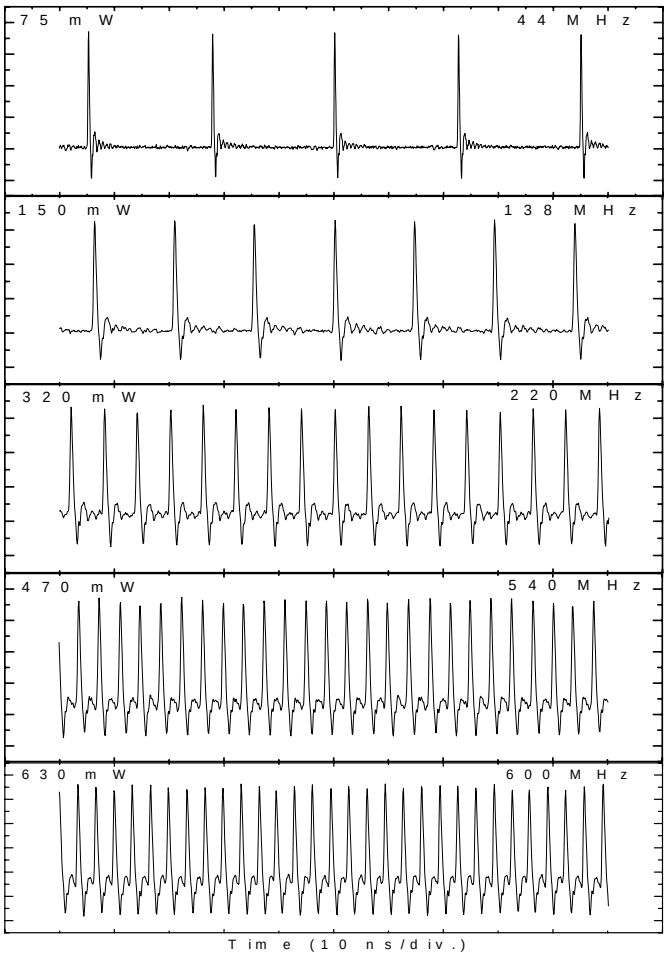

***Figure 4.20**: (a) The oscilloscope trace of the pulse train recorded for different values of pump power. For the values of 75 mW and 150 mW the traces were recorded by triggering the mode-locked operation at 300 mW pump power and then decreasing down to the desired value.*

Multiple pulse regime is a typical observation for an anomalous dispersion laser operating in conventional soliton regime, where it is the fundamental and dominant mechanism limiting the achievable pulse energy. Similar to the mode-locking at 1450 nm, bismuth laser operated in soliton regime at 1700 nm showed a strong tendency to multiple pulsing even at the threshold of the mode-locked regime. This might be because of the relatively high ground losses in bismuth-doped fibers, resulting in increase of threshold level. Consequently, the energy inside the cavity can exceed the fundamental energy limit of a single soliton, leading to pulse breaking even at the operation start point. The laser demonstrated high repetition rate with high harmonic count. The repetition rate at higher pump powers exceeded the resolution of the used photodetector. The pulse trains recorded for different values of pump power are shown in Figure 4.20.

Exploiting normal dispersion has been regularly used to overcome the constraints in anomalous dispersion regime providing the soliton shaping. It was noticed that multiple pulsing in soliton regime in mode-locked bismuth lasers is even more pronounced compared to their well-established rare-earth doped counterparts. However, bismuth fiber laser operating at 1700 nm demonstrated harmonic mode-locking with well-defined pulse separation, in contrast to the relatively chaotic pulse dynamics observed in case of 1450 nm laser.. The harmonic mode-locking is the way to achieve high repetition rate without shortening the cavity, and it is of great interest for some applications where high repetition rate with modest pulse energy are required.

4.3.3 Mode-locking in normal dispersion regime

After the detailed research in net anomalous dispersion regime, the cavity dispersion was then changed to net normal dispersion regime by reducing the length of the intracavity SMF-28 fiber to 10 meters. This changed the total cavity dispersion to value of ~ -0.1 ps/nm. In order to achieve the mode-locked operation of the laser in normal dispersion regime, it was observed that the absorption of the saturable absorber had to be increased. This was done by using a CNT saturable absorber mirror equipped with one additional layer of CNT-film compared to the absorber used in anomalous dispersion cavity, i.e. an absorber with three layers of CNT-film. This increased both the linear and nonlinear absorption of the absorber, after which the mode-locking was triggered in normal dispersion regime as well.

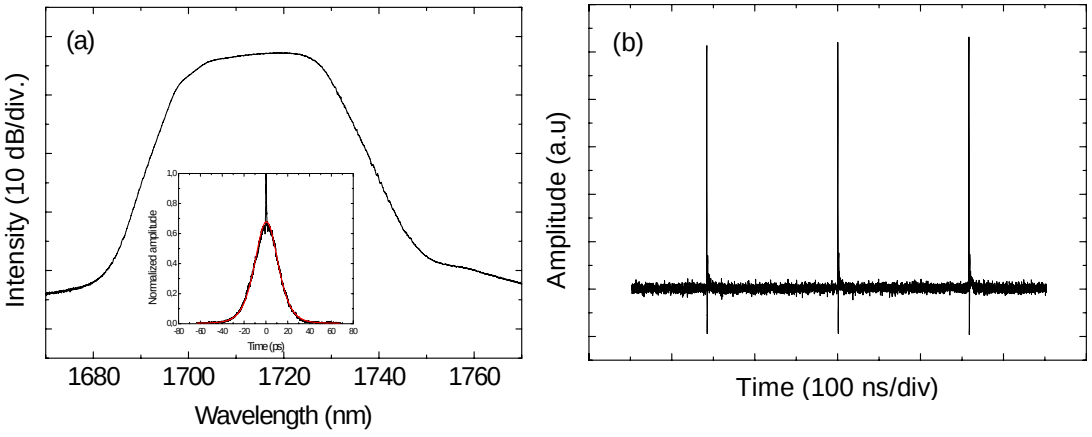

***Figure 4.21**: (a) The spectrum and the autocorrelation (inset) corresponding to an unstable pulse regime at the mode-locking threshold. (b) The oscilloscope trace of the output pulse train at fundamental repetition rate of 6.3 MHz.*

In normal dispersion regime, the 1700 nm bismuth fiber laser operated at 6.3 MHz fundamental repetition rate (Figure 4.21 (b)). The mode-locking threshold was 300 mW, similar to anomalous dispersion regime. At the pump power corresponding to the mode-locking threshold or above it, the pulse operation was always unstable similar to the regime illustrated in Figure 4.21. (a), which presents the spectrum and autocorrelation for the pump power of ~450 mW. The shape of the spectrum resembles conventional normal dispersion regime spectrum, but the edges of the spectrum are distorted. In the autocorrelation trace a strong coherence spike is observed on top of a broad background. This is a clear indication of bad pulse quality, possible multiple chaotically fluctuating sub-pulses inside one envelope. This is suggested also by the oscilloscope trace, where the tips of the pulses appeared blurred. This behavior is not clear from Figure 4.21 (b) because the oscilloscope data taken for figures includes only one acquisition, and this specific behavior is seen only when monitoring the pulse train in-situ.

When the pump power is decreased to 170 mW the laser shifts to stable mode-locked regime. The spectrum edges become steeper, and the spike in the autocorrelation trace disappears. The laser maintained stable pulse operation only at low pump power level of ~170 mW, whereas a substantial spectral broadening and distortion was observed when the pump power was increased again. The reason for the development of the instability and spectral broadening is most likely the lack of suitable spectral filtering. The stable mode-locking in normal dispersion regime requires a delicate balance between multiple parameters, one of which is the spectral bandwidth [78]. In case of 1700 nm bismuth gain fiber the 3 dB bandwidth of the gain exceeds 150 nm, and the gain filtering is not strong enough to stabilize the mode-locking at high pump levels.

In the stable mode-locked regime the laser produced 14.8 ps pulses with 20 nm bandwidth, equaling to time-bandwidth product of 28. The value of time-bandwidth product is an indication of a high chirping of the pulse, as common for the pulses in normal dispersion cavities and similar to what was observed in bismuth laser operating at 1400 nm. The spectrum and autocorrelation trace in stable mode-locking regime are shown in Figure 4.22. The low pump power needed for maintaining the stable single pulse regime limited the average output power of the laser to 0.7 mW at the fundamental 6.3 MHz repetition rate.

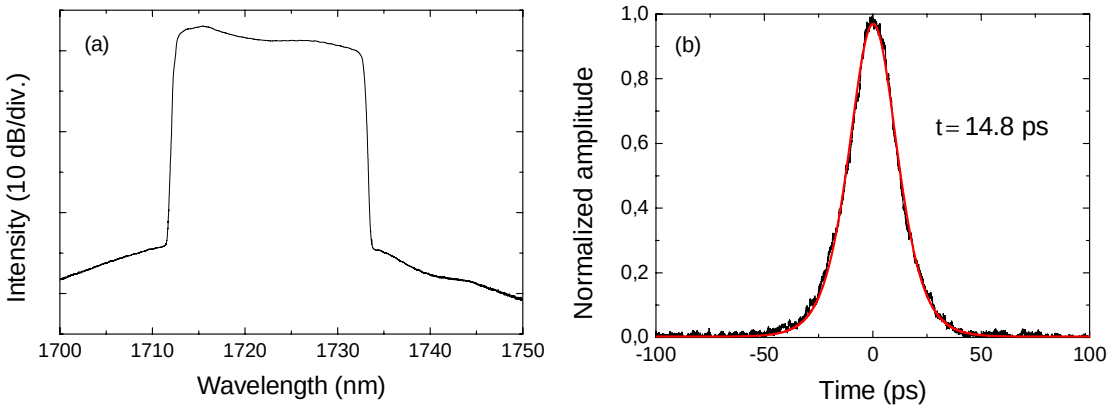

Figure 4.22: *(a) The spectrum and (b) the autocorrelation corresponding to the stable pulse regime of the normal dispersion bismuth fiber laser operating at 1700 nm.*

Finally, the compressibility of the pulse was tested by adding external 70 m of SMF-28 fiber after the output of the laser. The compression was studied only for low-power regime with stable pulse operation. The spectrum and the autocorrelation of the pulse after propagating through the compressing fiber are shown in Figure 4.23. The bandwidth of the pulse was 16 nm and the pulse duration was compressed to 1.05 ps assuming sech2-fitting. This equaled to a time-bandwidth product of 1.69, considerably lower than the value before the compressing fiber, indicating efficient dechirping of the pulse. However, the time-bandwidth product still exceeds the fundamental limit of 0.315 corresponding to the transform limited pulse quality. Transform-limited pulse corresponding to the duration of ~160 fs could be approached with optimized length of the compression fiber. However, the ultimate limit of the pulse width is determined by the possible nonlinearity of the chirp superimposed on the pulse and timing jitter induced by the cavity and pumping instabilities

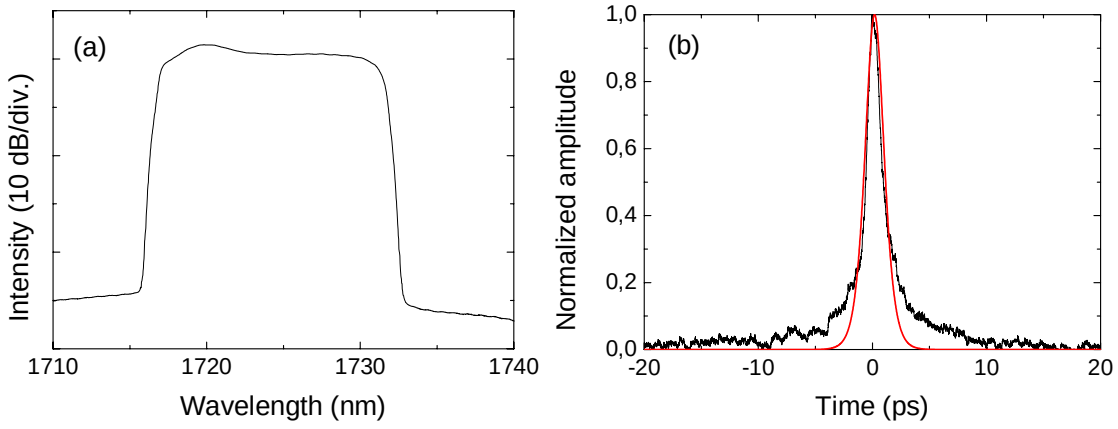

Figure 4.23: *(a) The spectrum and (b) the autocorrelation after external fiber compressor.*

5. CONCLUSIONS AND FUTURE WORK

In this thesis it was shown, that bismuth-doped fibers can be exploited for generation of ultrashort pulses at 1450 nm and 1730 nm. The operating wavelength is determined by the bismuth-doped fibers with different host glass compositions and by using a suitable pump wavelength. In the experiments a CNT absorber was used to trigger the mode-locked operation of the lasers, owing to broadband absorption characteristics of carbon-based mode-lockers. Therefore, bismuth-doped fiber lasers equipped with a CNT or graphene absorbers have notable potential as a broadband pulsed light source in the future.

At 1450 nm, generation of 245 fs pulses with peak power of 3.1 kW was demonstrated using a MOPA-system. These are to the best of the author's knowledge the shortest and most powerful pulses performed for any bismuth-doped fiber device to date. Moreover, generation of solitary pulses at 1450 nm were demonstrated using CNT as a saturable absorber for the first time in bismuth-doped fiber lasers operating at ~1450 nm wavelength. This wavelength region is extremely interesting, as it extends the wavelengths covered by well-established erbium-doped fiber devices, and could be used for advanced optical fiber communication in the future.

At 1730 nm, ultrashort pulse generation was obtained for both anomalous and normal dispersion regimes. This spectral region is novel and to date pulsed fiber devices at this wavelength have not been demonstrated at all to the best of authors knowledge. However, this spectral region is very attractive for many applications, including tomography [79], gas sensing [80] and remote control. Moreover, human tissues containing lipids show a peak of absorption at ~1720 nm, absorption by fat exceeding the absorption caused by water at this wavelength. This allows selective targeting of tissues containing lipids, and could be exploited for example in different skin treatments [81].

In this work, generation of 1.65 ps and 1.04 ps pulses at 1730 nm were demonstrated in anomalous and normal dispersion regimes, respectively. In anomalous dispersion regime the laser operated in harmonic mode-locking, increasing the repetition rate to 600 MHz. In normal dispersion regime, fundamental repetition rate of 6.3 MHz was observed.

Although novel mode-locked systems have successfully been demonstrated, developing of mode-locked bismuth fiber lasers is relatively challenging. One of the challenges is the relatively low absorption of the bismuth doped fibers. The non-saturable losses of bismuth-doped fibers are proportional to the doping level and as a result it should be low for fiber efficiency to be maximized. For CW applications the long fiber length is

not an issue, but in case of mode-locked lasers the long active fiber length is requiring additional efforts in dispersion management. For the mode-locked devices the sign and magnitude of the cavity dispersion has a significant impact on the pulse dynamics. In case of mode-locked bismuth fiber lasers, a trade-off between the laser efficiency and sufficient value of dispersion has to be often made, since the additional dispersive elements, such as gratings or dispersion compensation fibers are unavoidably introducing additional losses to the cavity.

In addition to dispersion, longer cavity length increases the nonlinearity. In case of anomalous dispersion regime and soliton pulse shaping the generation of multiple pulses is caused by the accumulation of the nonlinear phase-shift during the cavity round-trip, and therefore shorter cavity length is generally preferred. On the other hand, long cavity length could have potential to generate energetic pulses with low repetition rate if the single pulse operation can be maintained for example by exploiting the mode-locking in normal dispersion regime. This was demonstrated successfully for both 1450 nm and 1730 nm lasers.

In conclusion, this work summarizes the development work done for obtaining pulsed laser sources at 1450 and 1730 nm using bismuth-doped fibers. The research focus on bismuth-doped fibers is continuing intensively, and further improvement of the devices is assumed after the detailed origin of the near infrared emission of bismuth-doped glasses is confirmed. Therefore, bismuth-doped fiber is a promising candidate for ultra-fast fiber communication and laser systems in the future.

REFERENCES

[1] A. E. Siegman, “Lasers”, *University Science Books*, Palo Alto, CA, USA, 1283 p (1986).

[2] R. Paschotta, “Encyclopedia of laser physics and technology”, *Wiley-VCH*, 856 p (2008).

[3] T. H. Maiman, “Stimulated optical radiation in ruby”, *Nature* **187,** 493-494 (1960).

[4] A. C. S. van Heel, “A new method of transporting optical images without aberrations”, *Nature*, **173**, 39 (1954).

[5] G. Argawal, Nonlinear Fiber Optics, Academic Press (2001).

[6] R. Paschotta, J. Nilsson, A. C. Tropper and D. C. Hanna, “Ytterbium-doped fiber amplifiers”, *IEEE Journal of Quantum Electronics* **33,** 1049-1056 (1997).

[7] H. W. Etzel, H. W. Gandy and R. J. Ginther, “Stimulated emission of infrared radiation from ytterbium activated silicate glass”, *Applied Optics* **1,** 534-536 (1962).

[8] D. C. Hanna, R. M. Percival, I. R. Perry, R. G. Smart, P. J. Suni, J. E. Townsend and A. C. Tropper, “Continuous-wave oscillation of a monomode ytterbium-doped fibre laser”, *Electronics Letters* **24,** 1111-1113 (1988).

[9] H. M. Pask, Robert J. Carman, David. C. Hanna, Anne C. Tropper, Colin J. Mackechnie, P. R. Barber and J. M. Dawes, “Ytterbium-doped silica fiber lasers: versatile sources for the 1-1.2 μm region”, *IEEE Journal of Selected Topics in Quantum Electronics* **1,** 2-13, (1995).

[10] S. B. Poole, D. N. Payne and M. E. Ferman, “Fabrication of low-loss optical fibres containing rare-earth ions”, *Electronics Letters* **21,** 737-738 (1985).

[11] R. J. Mears, L. Reekie, I. M. Jauncey, D. N. Payne, “Low-noise erbium-doped fibre amplifier operating at 1.54 μm”, *Electronics Letters* **23,** 1026-1028 (1987).

[12] O. G. Okhotnikov, V. V. Kuzmin and J. R. Salcedo, “General intracavity method for laser transition characterization by relaxation oscillations spectral analysis”, *IEEE Photonics Technology Letters* **6,** 362-364 (1994).

[13] W. J. Miniscalco, “Erbium-doped glasses for fiber amplifiers at 1500 nm”, *Journal of Lightwave Technology* **9,** 234-250 (1991).

[14] D. C. Hanna, I. M. Jauncey, R. M. Percival, I. R Perry, R. G. Smart, P. J. Suni, J. E. Townsend and A. C. Tropper, “Continuous-wave oscillation of a monomode thulium-doped fibre laser”, *Electronics Letters* **24,** 1222-1223 (1988).

[15] K. Oh, T. F. Morse, A. Kilian, L. Reinhart and P. M. Weber, “Continuous-wave oscillation of thulium-sensitized holmium-doped silica fiber laser”, *Optics Letters* **19,** 278-280 (1994).

[16] S. D. Jackson, F. Bugge and G. Erbert, “Directly diode-pumped holmium fiber lasers”, *Optics Letters* **32,** 2496-2498 (2007).

[17] L. Wetenkamp, “Efficient CW-operation of a 2.9 μm Ho^{3+} -doped fluorozirconate fibre laser pumped at 640 nm”, *Electronics Letters* **26,** 883-884 (1990).

[18] S. W. Henderson, P. J. M. Suni and C. P. Hale, “Coherent laser radar at 2 μm using solid-state lasers, *IEEE Transactions on Geoscience and Remote Sensing* **31,** 4-15 (1993).

[19] M. Nathaniel, M. Fried and K. E. Murray, “High-power thulium fiber laser ablation of urinary tissues at 1.94 μm”, *Journal of Endourology* **19,** 25-31 (2005).

[20] K. Bremer, A. Pal, S. Yao, E. Lewis, R. Sen, T. Sun and K. T. V. Grattan, “Sensitive detection of CO_2 implementing tunable thulium-doped all-fiber laser”, *Applied Optics* **52,** 3957-3963 (2013).

[21] K. Murata, Y. Fujimoto, T. Kanabe, H. Fujita and M. Nakatsuka,”Bi-doped SiO2 as a new laser material for an intense laser”, *Fusion Eng. Design* **44,** 437-439 (1999).

[22] Y. Fujimoto and M. Nakatsuka “Optical amplification in bismuth-doped silica glass”, *Applied Physics Letters* **82,** 3325-3326 (2003).

[23] V. V. Dvoyrin, V. M. Mashinsky, E. M. Dianov, A. A. Umnikov, M. V. Yashkov and A. N. Guryanov, “Absorption, fluorescence and optical amplification in MCVD bismuth-doped silica glass optical fibres”, *ECOC 2005, 31st European Conference on Optical Communication*, Glasgow, UK, 25-29 September 2005, Volume **4,** 949-950.

[24] T. Haruna, M. Kakui, T. Taru, S. Ishikawa and M. Onishi, ”Silica-based bismuth-doped fiber for ultra broad band light-source and optical amplification around 1.1 μm”, *Proc. Opt. Amplifiers Appl. Top. Meet.* Budapest, Hungary, 7-10 August 2005, paper MC3.

[25] E. M. Dianov, V. V. Dvoyrin, V. M. Mashinsky, A. A. Umnikov, M. V. Yashkov and A. N. Gur'yanov, "CW bismuth fibre laser", *Quantum Electronics* **35,** 1083-1084 (2005).

[26] E. M. Dianov, "Bismuth-doped optical fibers: a challenging active medium for near-IR lasers and optical amplifiers", *Light: Science & Applications* **1** (2012), e12, doi:10.1038/lsa.2012.12. Published online 25 May 2012.

[27] S. Firstov, S. Alyshev, M. Melkumov, K. Riumkin, A. Shubin and E. Dianov, "Bismuth-doped optical fibers and fiber lasers for a spectral region of 1600-1800 nm", *Optics Letters* **39,** 6927-6930 (2014).

[28] M. Duelk and M. Zirngibl, "100 Gigabit Ethernet – applications, features, challenges" *INFOCOM 2006, 25th IEEE International Conference on Computer Communications,* Barcelona, Spain, 23-29 April 2006, pp. 1-5.

[29] M. Peng, G. Dong, L. Wondraczek, L. Zhang, N. Zhang, J. Qiu, "Discussion on the origin of NIR emission from Bi-doped materials", *Journal of Non-Crystalline Solids* **357,** 2241-2245 (2011).

[30] L. F. Mollenauer, N. D. Vieira and L. Szeto, "Optical properties of the $Tl^0(1)$ center in KCl", *Physical Review B* **27,** 5332-5346 (1983).

[31] M. Fockele, F. J. Ahlers, F. Lohse, J-M Spaeth and R. H. Bartram, "Optical properties of atomic thallium centres in alkali halides" *Journal of Physics C: Solid State Physics* **18,** 1963 (1985).

[32] I.A. Bufetov, M. A. Melkumov, V. F. Khopin, S. V. Firstov, A. V. Shubin, O. I. Medvedkov, A. N. Guryanov and E. M. Dianov, "Efficient Bi-doped fiber lasers and amplifiers for the spectral region 1300-1500 nm", *Proc. SPIE* 7580, Fiber Lasers VII: Technology, Systems, and Applications, 758014 (February 17, 2010); doi:10.1117/12.840666.

[33] M. A. Melkumov, I. A. Bufetov, A. V. Shubin, S. V. Firstov, V. F. Khopin, A. N. Guryanov and E. M. Dianov, "Laser diode pumped bismuth-doped optical fiber amplifier for 1430 nm band", *Optics Letters* **36,** 2408-2410 (2011).

[34] E. M. Dianov, A. V. Shubin, M. A. Melkumov, O. I. Medvedkov and I. A. Bufetov, “High-power cw bismuth-fiber lasers”, *Journal of the Optical Society of America B* **24,** 1749-1755 (2007).

[35] A. B. Rulkov, A. A. Ferin, S. V. Popov, J. R. Taylor, I. Razdobreev, L. Bigot and G. Bouwmans, “Narrow-line, 1178 nm CW bismuth-doped fiber laser with 6.4W output for direct frequency doubling”, *Optics Express* **15,** 5473-5476 (2007).

[36] I. A. Bufetov, M. A. Melkumov, S. V. Firstov, K. E. Riumkin, A. V. Shubin, V. F. Khopin, A. N. Guryanov and E. M. Dianov, “Bi-doped optical fibers and fiber lasers”, *IEEE Journal of Selected Topics in Quantum Electronics* **20,** 0903815 (2014).

[37] A. V. Shubin, I. A. Bufetov, M. A. Melkumov, S. V. Firstov, O. I. Medvedkov, V. F. Khopin, A. N. Guryanov and E. M. Dianov, “Bismuth-doped silica-based fiber lasers operating between 1389 and 1538 nm with output power of up to 22 W”, *Optics Letters* **37,** 2589-2591 (2012).

[38] S. V. Firstov, S. V. Alyshev, K. E. Riumkin, M. A. Melkumov, O. I. Medvedkov and E. M. Dianov, “Watt-level, continuous-wave bismuth-doped all-fiber laser operating at 1.7 μm”, *Optics Letters* **40,** 4360-4363 (2015).

[39] E. M. Dianov, A. A. Krylov, V. V. Dvoyrin, V. M. Mashinsky, P. G. Kryukov, O. G. Okhotnikov and M. Guina, “Mode-locked Bi-doped fiber laser”, *Journal of Optical Society of America B* **24,** 1807-1808 (2007).

[40] S. Kivistö, R. Gumenyuk, J. Puustinen, M. Guina, E. M. Dianov and O. G. Okhotnikov, ”Mode-locked Bi-doped all-fiber laser with chirped fiber Bragg grating”, *IEEE. Photon. Technol. Lett.* **21,** 599-601 (2009).

[41] E. J. R. Kelleher, J. C. Travers, Z. Sun, A. C. Ferrari, K. M. Golant, S. V. Popov and J. R. Taylor, “Bismuth fiber integrated laser mode-locked by carbon nanotubes” *Laser Physics Letters* **7,** 790-794 (2010).

[42] A. –P. Luo, Z. –C. Luo, W. –C. Xu, V. V. Dvoyrin, V. M. Mashinsky and E. M. Dianov, “Tunable and switchable dual-wavelength passively mode-locked Bi-doped all-fiber ring laser based on nonlinear polarization rotation”, *Laser Phys. Lett.* **8,** 601-605 (2011).

[43] R. Gumenyuk, J. Puustinen, A. V. Shubin, I. A. Bufetov, E. M. Dianov and O. G. Okhotnikov, “1.32 μm mode-locked bismuth-doped fiber laser operating in anomalous and normal dispersion regimes”, *Optics Letters* **38,** 4005-4007 (2013).

[44] R. Gumenyuk, M. A. Melkumov, V. F. Khopin, E. M Dianov and O. G. Okhotnikov, “Effect of absorption recovery in bismuth-doped silica glass at 1450 nm on soliton grouping in fiber laser”, *Scientific Reports* **4,** 7044 (2014).

[45] M. M. Ivanenko, S. Fahimi-Weber, T. Mitra, W. Wierich and P. Hering, ”Bone tissue ablation with sub-μs pulses of a Q-switch CO_2 laser: Historical examination of thermal side effects”, *Lasers in Medical Science* **17,** 258-264 (2002).

[46] J. E. Nettleton, B. W. Schilling, D. N. Barr and J. S. Lei, “Monoblock laser for a low-cost, eyesafe, microlaser range finder”, *Applied Optics* **39,** 2428-2434 (2000).

[47] Rofin Group, CW- and Q-swithced lasers. Available at (26.11.2015) http://www.rofin.com/en/products/solid-state-lasers/cw-and-q-switched-lasers/

[48] U. Keller, “Recent developments in compact ultrafast lasers”, *Nature* **424,** 831-838 (2003).

[49] B. C. Collings, K. Bergman, S. T. Cundiff, S. Tsuda, J. Nathan Kutz, J. E. Cunningham, W. Y. Jan, M. Koch and W. H. Knox, “Short cavity erbium/ytterbium fiber lasers mode-locked with a saturable Bragg reflector”, *IEEE Journal of Selected Topics in Quantum Electronics* **3,** 1065-1075 (1997).

[50] X. Li, X. Liu, X, Hu, L. Wang, H. Lu, Y. Wang and W. Zhao, “Long-cavity passively mode-locked fiber ring laser with high-energy rectangular-shape pulses in anomalous dispersion regime”, *Optics Letters* **35,** 3249-3251 (2010).

[51] M. Hofer, M. E. Fermann, F. Haberl, M. H. Ober and A. J. Schmidt, “Mode locking with cross-phase and self-phase modulation”, *Optics Letters* **16,** 502-504 (1991).

[52] M. E. Fermann, M. J. Adrejco, Y. Silberberg and M. L. Stock, “Passive mode locking by using nonlinear polarization evolution in a polarization maintaining erbium-doped fiber”, *Optics Letters* **18,** 894-896 (1993).

[53] U. Keller, K. J. Weingarten, F. X. Kärtner, D. Kopf, B. Braun, I. D. Jung, R. Fluck, C. Hönninger, N. Matuschek and J. Aus der Au, “Semiconductor saturable absorber mirrors (SESAM’s) for femtosecond to nanosecond pulse

generation in solid-state lasers", *IEEE Journal of Selected Topics in Quantum Electronics* **2,** 435-453 (1996).

[54] S. Y. Set, H. Yaguchi, Y. Tanaka, M. Jablonski, "Mode-locked fiber lasers based on saturable absorber incorporating carbon nanotubes", *Optical Fiber Communications Conference*, Atlanta, Georgia, United States, 2003, PD44-P1-3 vol.3, doi:10.1109/OFC.2003.1248625.

[55] S. Y. Set, H. Yaguchi, Y. Tanaka and M. Jablonski, "Laser mode locking using a saturable absorber incorporating carbon nanotubes", *Journal of Lightwave Technology* **22,** 51-56 (2004).

[56] A. Martinez and Z. Sun, "Nanotube and graphene saturable absorbers for fibre lasers", *Nature Photonics* **7,** 842-845 (2013).

[57] R. Saito, G. Dresselhaus, M.S. Dresselhaus, "Physical Properties of Carbon Nanotubes", *Imperial College Press*, London, 259p (1998).

[58] K. S. Novoselov, A. K. Geim, S. V. Morozov, D. Jiang, Y. Zhang, S. V. Dubonos, I. V. Grigorieva and A. A. Firsov, "Electric field effect in atomically thin carbon films", *Science* **306,** 666-669 (2004).

[59] T. Hasan, Z. Sun, F. Wang, F. Bonaccorso, P. H. Tan, A. G. Rozhin and A. C. Ferrari, "Nanotube-polymer composites for ultrafast photonics", *Advanced Materials* **21,** 3875-3899 (2009).

[60] Q. Bao, H. Zhang, Y. Wang, Z. Ni, Y. Yan, Z. X. Shen, K. P. Loh and D. Y. Tang, "Atomic-layer graphene as a saturable absorber for ultrafast pulsed lasers", *Advanced Functional Materials* **19,** 3077-3083 (2009).

[61] K. S. Novoselov, V. I. Fal'ko, L. Colombo, P. R. Gellert, M. G. Schwab and K. Kim, "A roadmap for graphene", *Nature* **490,** 192-200 (2012).

[62] Y.-W. Song, S.-Y. Jang, W.-S. Han and M.-K. Bae, "Graphene mode-lockers for fiber lasers functioned with evanescent field interaction", *Applied Physics Letters* **96,** 051122 (2010).

[63] Z. Q. Luo, J. Z. Wang, M. Zhou, H. Y. Xu, Z. P. Cai and C. C. Ye, "Multiwavelength mode-locked erbium-doped fiber laser based on the interaction of graphene and fiber-taper evanescent field", *Laser Physics Letters* **9,** 229-233 (2012).

[64] F. Bernard, H. Zhang, S.-P. Gorza and P. Emplit, "Towards mode-locked fiber laser using topological insulators", *Nonlinear Photonics 2012*, Colorado

Springs, Colorado, United States, 17-21 June 2012, paper NTh1A.5, doi:10.1364/NP.2012.NTh1A.5.

[65] C. Zhao, Y. Zou, Y. Chen, Z. Wang, S. Lu, H. Zhang, S. Wen and D. Tang, "Wavelength-tunable picosecond soliton fiber laser with topological insulator: Bi_2Se_3 as a mode locker" *Optics Express* **20,** 27888-27895 (2012).

[66] C. Zhao, H. Zhang, X. Qi, Y. Chen, Z. Wang, S. Wen and D. Tang, "Ultra-short pulse generation by a topological insulator based saturable absorber", *Applied Physics Letters* **101,** 211106 (2012).

[67] A. M. Heidt, J. P. Burger, J.-N. Maran and N. Traynor, "High power and high energy ultrashort pulse generation with a frequency shifted feedback fiber laser", *Optics Express* **15,** 15892-15897 (2007).

[68] J. M. Sousa and O. G. Okhotnikov, "Short pulse generation and control in Er-doped frequency-shifted-feedback fibre lasers", *Optics Communications* **183,** 227-241 (2000).

[69] F. X. Kärtner, I. D. Jung and U. Keller, "Soliton mode-locking with saturable absorbers", *IEEE Journal of Selected Topics in Quantum Electronics* **2,** 540-556 (1996).

[70] Datasheet for SMF-28 fiber by Corning. Available at (27.11.2015) http://ece466.groups.et.byu.net/notes/smf28.pdf

[71] S. M. J. Kelly, "Characteristic sideband instability of periodically amplified average soliton", *Electronics Letters* **28,** 806-808 (1992).

[72] P. Grelu and N. Akhmediev, "Dissipative solitons for mode-locked lasers", *Nature Photonics* **6,** 84-92 (2012).

[73] D. Strickland and G. Mourou, "Compression of amplified chirped optical pulses", *Optics Communications* **56,** 219-221 (1985).

[74] Lawrence Livermore National Laboratory, "Multilayer dielectric gratings: increasing the power of light", Science & Technology review, September 1995. Available (accessed on 16.5.2016): https://str.llnl.gov/str/pdfs/09_95.2.pdf.

[75] A. D Yablon, "Optical fiber fusion splicing", *Springer, 245-248, 308p.* (2005)

[76] P. H. Pioger, V. Couderc, P. Leproux and P. A. Champert, “High spectral power density supercontinuum generation in a nonlinear fiber amplifier”, *Optics Express* **15,** 11358-11363 (2007).

[77] S. V. Firstov,. V. F. Khopin, I. A. Bufetov, E. G. Firstova, A. N. Guryanov and E. M. Dianov, “Combined excitation-emission spectroscopy of bismuth active centers in optical fibers” *Optics. Express* **19,** 19551-19561 (2011).

[78] A. Chong, W. H. Renninger and F. W. Wise, “Properties of normal-dispersion femtosecond lasers”, *Journal of Optical Society of America. B* **25,** 140-148 (2008).

[79] H. Kawagoe, S. Ishida, M. Aramaki, Y. Sakakibara, E. Omoda, H. Kataura and N. Nishizawa, “Development of a high power supercontinuum source in the 1.7 μm wavelength region for highly penetrative ultrahigh-resolution optical coherence tomography”. *Biomedical Optics Express.* **5**, 932–943 (2014).

[80] P. Chambers, E. A. D. Austin and J. P. Dakin, “Theoretical analysis of a methane gas detection system, using the complementary source modulation method of correlation spectroscopy”, *Measurement Science and Technoogy.* **15**, 1629–1636 (2004).

[81] R. R. Anderson, W. Farinelli, H. Laubach, D. Manstein, A. N. Yaroslavsky, J. Gubeli, K. Jordan, G. R. Neil, M Shinn, W. Chandler, G. P. Williams, S. V. Benson, D. R. Douglas and H. F. Dylla, “Selective photothermolysis of lipid-rich tissues: a free electron laser study”, *Lasers in Surgery and Medicine* **38,** 913-919 (2006).

LIST OF PUBLICATIONS

[P1] T. Noronen, M. Melkumov, D. Stolyarov, V. F. Khopin, E. Dianov and O. G. Okhotnikov, ”All-bismuth fiber system for femtosecond pulse generation, compression and energy scaling”, *Optics Letters* **40,** 2217-2220 (2015).

[P2] T. Noronen, S. Firstov, E. Dianov and O. G. Okhotnikov, “1700 nm dispersion managed mode-locked bismuth fiber laser”, *Sci. Rep*. **6,** 24876 (2016).

APPENDIX 1

Publication 1

Teppo Noronen, Mikhail Melkumov, Dmitrii Stolyarov, Vladimir F. Khopin, Evgenii Dianov and Oleg. G. Okhotnikov, “All-bismuth fiber system for femto-second pulse generation, compression and energy scaling”, Optics Letters 40, 2217-2220. Reprinted with permission.

May 15, 2015 / Vol. 40, No. 10 / OPTICS LETTERS 2217

All-bismuth fiber system for femtosecond pulse generation, compression, and energy scaling

Teppo Noronen,[1,*] Mikhail Melkumov,[2] Dmitrii Stolyarov,[3] Vladimir F. Khopin,[4] Evgenii Dianov,[2] and Oleg G. Okhotnikov[1,3]

[1]*Optoelectronics Research Centre, Tampere University of Technology, Korkeakoulunkatu 3, Tampere 33720, Finland*

[2]*Fiber Optics Research Center, Russian Academy of Sciences, 38 Vavilov Street, Moscow 119333, Russia*

[3]*Ulyanovsk State University, 42 Leo Tolstoy Street, Ulyanovsk 432017, Russia*

[4]*Institute of Chemistry of High-Purity Substances, Russian Academy of Sciences, 49 Tropinin Street, Nizhny Novgorod 603600, Russia*

[*]*Corresponding author: teppo.noronen@tut.fi*

Received March 6, 2015; revised April 16, 2015; accepted April 16, 2015;
posted April 17, 2015 (Doc. ID 235665); published May 6, 2015

We demonstrate a 1.44-μm bismuth-doped master oscillator–power amplifier (MOPA) system for generating femtosecond pulses. The cavity of master oscillator comprises dispersion-compensating fiber for detuning the total dispersion to the normal regime and a carbon nanotube saturable absorber for triggering the mode-locked operation. The described multifunction bismuth fiber amplifier performs energy scaling, large spectral broadening, and pulse compression. The results show that the large chirp superimposed on the pulses in the bismuth oscillator with normal dispersion can be effectively suppressed in a subsequent bismuth power amplifier with anomalous dispersion and high nonlinearity, resulting in high-quality pulses with record duration of 240 fs. An all-fiber design provides a practical solution that avoids the need for supplementary pulse stretching and compression.

OCIS codes: (140.3510) Lasers, fiber; (140.4050) Mode-locked lasers; (320.5520) Pulse compression.
http://dx.doi.org/10.1364/OL.40.002217

The fiber lasers based on Yb^{3+}, Er^{3+}, Nd^{3+}, and Tm^{3+} rare-earth materials cover a 0.9–2.1-μm spectral range with an exception for a 1.1–1.5-μm wavelength gap that occurred due to the lack of appropriate doping elements. This wavelength range is, however, valuable for broadband data transmission, medical applications, and for high-brightness frequency-doubled visible sources. Bismuth-doped fibers are considered to be promising candidates for providing gain in this spectral range [1]. Indeed, continuous wave lasers around the 1.18-μm wavelength with output power up to several watts have been demonstrated [2,3]. Mode-locked bismuth-doped lasers have also been reported at this wavelength using either semiconductor saturable absorber mirrors (SESAMs) [4,5] or carbon nanotubes (CNTs) [6]. Recently, long-wavelength mode-locked bismuth-doped fiber lasers operating at 1.32 μm [7] and 1.45 μm [8] were reported. The ultrashort pulse regime in these lasers was accompanied by a soliton grouping effect due to anomalous dispersion of the fiber cavity. Although the soliton shaping is routinely used to produce transform-limited pulses directly from mode-locked oscillators, this pulse shaping strategy can, however, raise numerous effects that may limit practical value of the method. The most detrimental consequence is associated with energy quantization and multiple pulse generation.

Considerable scaling of pulse energy has been demonstrated with ultrafast lasers operating in a normal-dispersion regime [7]. These oscillators support so-called dissipative solitons that prevent the multiple pulse instability and result in a superior performance compared to lasers with anomalous dispersion of the cavity. The conservative dispersion-managed solitons require the balance only between dispersion and nonlinearity, while in a laser supporting dissipative solitons, the dispersion is one among several parameters determining the laser dynamics, i.e., group-velocity dispersion, self-phase modulation, saturable absorption, and spectral filtering. The dissipative soliton regime can be achieved from an all-normal dispersion cavity or the cavity with segments of normal dispersion that ensure their dominant contribution to the cavity dispersion. While pulse energies from a conservative soliton laser are limited by accumulation of nonlinear phase shift, dissipative soliton lasers have demonstrated the highest femtosecond pulse energies produced to date [9,10].

In this work, we report a 1.44-μm all-bismuth fiber master oscillator–power amplifier (MOPA) system for generating femtosecond pulses combining their potentials for compression and energy scaling. The bismuth fiber is pumped by a 1.32-μm low-noise semiconductor disk laser with output power launched into the core of single-mode fiber up to 1.5 W. Diffraction-limited quality of the disk laser beam allows efficient core-pumping and is an essential attribute of the proposed method that allows avoiding cladding pumping of bismuth fiber exhibiting low pump absorption [11]. Net normal dispersion of the laser cavity is implemented to maintain high-energy single pulse operation. The pulse compression down to 240-fs record duration for bismuth fiber system results in peak power of 3.1 kW, which in turn originates from a substantial spectral broadening achieved with modest pump power. This characteristic of bismuth amplifier was accomplished by designing an active fiber combining an appropriate amount of nonlinearity and dispersion at the signal wavelength of 1440 nm.

Two bismuth fibers with different doping levels of bismuth centers were fabricated for use as gain elements in the master oscillator and power amplifier. Both fiber preforms were made by the standard modified chemical vapor deposition (MCVD) process using vapor deposition of Bi-compound on F300 pure silica tube (Heraeus). The tubes were further consolidated into the rods and jacketed with the same F300 silica to adjust the cutoff

0146-9592/15/102217-04$15.00/0

wavelength. Next the bismuth fibers were drawn from the preforms.

High-absorption fiber used in the master oscillator has higher bismuth weight concentration of ≈0.3% in the fiber core compared to the low-absorption fiber used in the amplifier (≈0.031%). The different doping level of the fibers used in a master oscillator and power amplifier allows the separate optimization of the seed pulses and saturation parameters of the power amplifier. Particularly, the overall efficiency and output pulse energy of the MOPA-system exploiting highly doped fiber in a short-length laser cavity and low-absorption fiber in the amplifier with adiabatic spatial gain distribution demonstrate the superior performance compared to the system built of the bismuth fiber with the same doping level. Fibers have step index profiles with $\Delta n \approx 7 \times 10^{-3}$ and $\Delta n \approx 9 \times 10^{-3}$ formed by adding of 5 and 6.5 mol. % of germanium in high- and low-absorption fibers, respectively. The remaining material of the core for each fiber is pure SiO_2 with 94.7 and 93.5 mol. %, correspondingly. The cut-off wavelength is ≈0.9 μm in both fibers. Absorption and gain spectra observed for excitation wavelength of 1320 nm are presented in Fig. 1. The highest net gain 4.4 dB/m for high-absorption fiber and 0.7 dB/m for low-absorption fiber peaked at 1420–1430 nm was measured for 350 mW of pump power at 1320 nm. Further details of spectroscopic and lasing properties of germanosilicate bismuth-doped fibers and the origin of bismuth active centers can be found in [12–14].

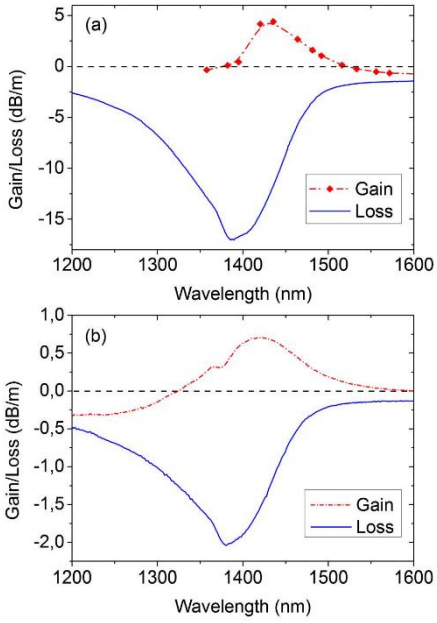

Fig. 1. Optical gain and loss in (a) high-absorption and (b) low-absorption bismuth fiber.

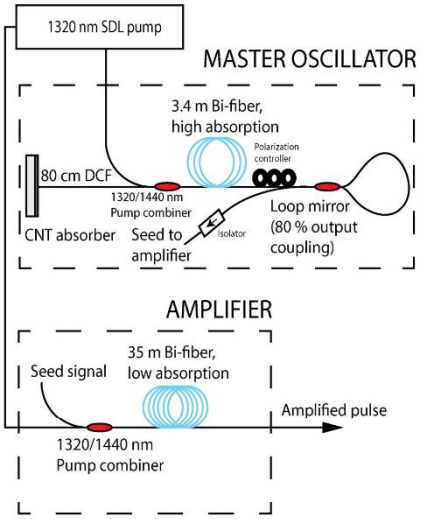

Fig. 2. Schematic of the MOPA-system.

The setup for the bismuth MOPA is shown in Fig. 2. The active medium of the laser cavity was a 3.4-m-long high-absorption bismuth-doped fiber, which was pumped through a 1320/1440-nm pump combiner. The pump source was a 1.32-μm semiconductor disk laser (SDL), delivering near diffraction-limited beam quality. The SDL characteristics are given in [15]. The linear laser cavity was terminated by a loop mirror with ~80% of output coupling. The relatively high output coupling provides an increased output power of the master oscillator and could prevent sporadic parasitic continuous wave oscillations. A butt-coupled carbon nanotube (CNT) saturable absorber deposited onto a silver mirror supports the mode-locked operation. A CNT-absorber equipped with a silver mirror terminating the laser cavity ensures a large bandwidth compared to monolithic semiconductor saturable absorbers grown in a single epitaxial run. The estimated modulation depth of CNT-absorber is 3%–6%.

The bismuth-doped fiber and the standard telecom fiber used in passive sections of the laser cavity each exhibit a relatively low anomalous dispersion at the signal wavelength. The estimation for dispersion of bismuth silica-based fibers provides the value below 0.01 ps/nm × m. The cavity dispersion was tuned to the net normal dispersion regime by incorporating 80 cm of dispersion compensation fiber (DCF) with the normal dispersion of −0.09 ps/nm × m. The resulted net normal dispersion regime of ≈ −0.14 ps/nm supports the dissipative solitons, prevents the formation of multiple pulses prominent for lasers operating in the anomalous dispersion regime, and consequently, allows the energy scaling. The nonlinearity of active fibers should be close to the value known for standard silica fiber because the doping level of bismuth is relatively low.

For pump power above 200 mW, the seed laser exhibits stable mode-locked operation at a fundamental repetition rate of 20 MHz. The autocorrelation and spectrum of the seed laser are shown in Fig. 3. The laser delivers 1.5 mW of average power for 320 mW of pump power with 2.1-ps pulse duration. A 20-nm spectral bandwidth corresponds to a time-bandwidth product of 6.1. The large value of the product is indicative of a large chirp, which is typical for dissipative solitons generated from a cavity with normal dispersion.

The signal from oscillator is further amplified in a 35-m-long low-absorption bismuth-doped fiber. Both the oscillator and amplifier are pumped by the same 1.32-μm disk laser. The output of the pump SDL is shared nearly equally between the master source (320 mW) and the amplifier (400 mW). The signal from the oscillator is scaled in the bismuth amplifier to an average power of 15 mW. It was observed that the bismuth power amplifier provides an efficient chirp removal resulting in pulse duration of 240 fs with peak power of 3.1 kW corresponding to the shortest pulses reported for bismuth-doped fiber lasers. The pulse parameters at the amplifier output are shown in Fig. 4.

A presence of an intensive spectral broadening provided by bismuth amplifier should be noted, as seen from Fig. 4(a). Indeed, a broad continuum with bandwidth of 175 nm has been observed for the average power of only 15 mW.

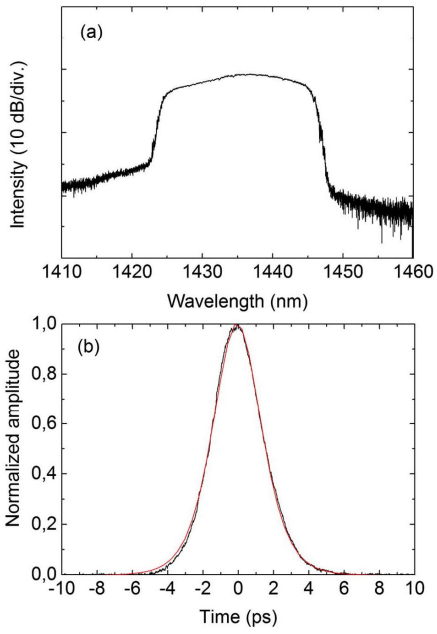

Fig. 3. (a) Spectrum and (b) autocorrelation of the pulses from the master oscillator reveal the spectral bandwidth of 20 nm and the corresponding duration of 2.1 ps ($sech^2$ fitting).

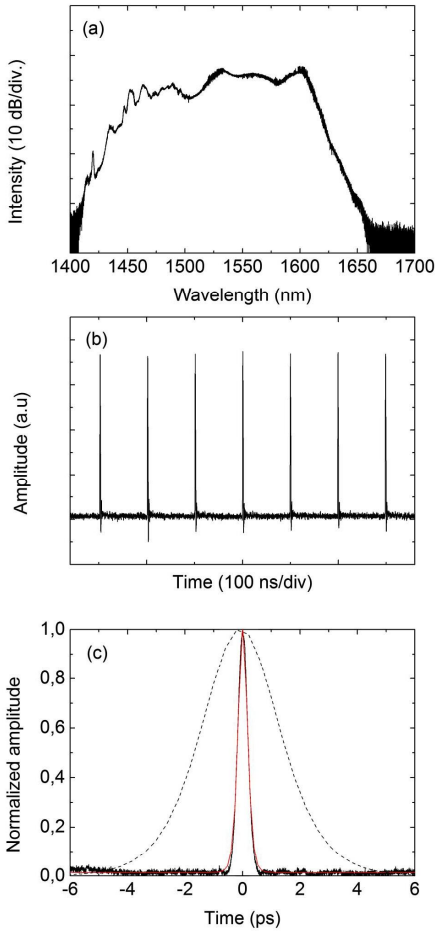

Fig. 4. (a) Spectrum, (b) pulse train, and (c) autocorrelation observed at the output of bismuth MOPA-system. The dashed line in (c) shows the pulse before the compression in bismuth fiber amplifier.

In summary, we have reported continuous-wave mode-locking of a bismuth-doped fiber laser, using a carbon nanotube-based saturable absorber and auxiliary bismuth fiber amplifier/compressor. The laser generates 2.1-ps pulses at the repetition rate of 20 MHz with an average output power of 1.5 mW. A 1.44-μm bismuth-doped fiber laser operates with the net normal dispersion regime and is used as a seed source for a bismuth-doped fiber amplifier for further pulse energy scaling and compression. 240-fs pulses with 3.1-kW peak power were achieved at the amplifier output. The unique multifunction bismuth power amplifier provides simultaneously large spectral broadening and subsequent efficient pulse

compression. The apt combination of dispersion and gain/absorption of bismuth fibers demonstrates the high potential of bismuth technology for all-fiber MOPA systems. The fiber system generates, to the best of our knowledge, the shortest pulses reported to date with bismuth-doped lasers.

This work was supported in part by the Grant Program of the Presidium of Russian Academy of Sciences No. 24.

References

1. E. M. Dianov, Light Sci. Appl. **1**, e12 (2012)
2. A. B. Rulkov, A. A. Ferin, S. V. Popov, J. R. Taylor, I. Razdobreev, L. Bigot, and G. Boucmans, Opt. Express **15**, 5473 (2007).
3. E. M. Dianov, A. V. Shubin, M. A. Melkumov, O. I. Medvedkov, and I. A. Bufetov, J. Opt. Soc. Am. B **24**, 1749 (2007).
4. E. M. Dianov, A. A. Krylov, V. V. Dvoyrin, V. M. Mashinsky, P. G. Kryukov, O. G. Okhotnikov, and M. Guina, J. Opt. Soc. Am. B **24**, 1807 (2007).
5. S. Kivistö, J. Puustinen, M. Guina, R. Herda, S. Marcinkevicius, E. M. Dianov, and O. G. Okhotnikov, Opt. Express **18**, 1041 (2010).
6. E. J. R. Kelleher, J. C. Travers, Z. Sun, A. C. Ferrari, K. M. Golant, S. V. Popov, and J. R. Taylor, Laser Phys. Lett **7**, 790 (2010).
7. R. Gumenyuk, J. Puustinen, A. V. Shubin, I. A. Bufetov, E. M. Dianov, and O. G. Okhotnikov, Opt. Lett. **38**, 4005 (2013).
8. R. Gumenyuk, M. A. Melkumov, V. F. Khopin, E. M. Dianov, and O. G. Okhotnikov, Sci. Rep. **4**, 7044 (2014).
9. P. Grelu and N. Akhmediev, Nat. Photonics **6**, 84 (2012).
10. A. Chong, W. H. Renninger, and F. W. Wise, J. Opt. Soc. Am. B **25**, 140 (2008).
11. O. G. Okhotnikov, *Semiconductor Disk Lasers: Physics and Technology* (Wiley, 2010).
12. I. A. Bufetov, M. A. Melkumov, S. V. Firstov, K. E. Riumkin, A. V. Shubin, V. F. Khopin, A. N. Guryanov, and E. M. Dianov, IEEE J. Sel. Top. Quantum Electron. **20**, 111 (2014).
13. M. Peng, G. Dong, L. Wondraczek, L. Zhang, N. Zhang, and J. Qiu, J. Non-Cryst. Solids **357**, 2241 (2011).
14. V. O. Sokolov, V. G. Plotnichenko, and E. M. Dianov, Opt. Mater. Express **3**, 1059 (2013).
15. J. Heikkinen, R. Gumenyuk, A. Rantamäki, T. Leinonen, M. Melkumov, E. M. Dianov, and O. G. Okhotnikov, Opt. Express **22**, 11446 (2014).

APPENDIX 2

Publication 2

T. Noronen, S. Firstov, E. Dianov and O. G. Okhotnikov, “1700 nm dispersion managed mode-locked bismuth fiber laser”, Sci. Rep. 6, 24876 (2016). Reprinted with permission.

www.nature.com/scientificreports

SCIENTIFIC REPORTS

OPEN

1700 nm dispersion managed mode-locked bismuth fiber laser

Teppo Noronen[1], Sergei Firstov[2], Evgeny Dianov[2] & Oleg G. Okhotnikov[1,3]

Received: 30 November 2015
Accepted: 06 April 2016
Published: 21 April 2016

We demonstrate the first 1.7 μm bismuth-doped fiber laser generating ultrashort pulses via passive mode-locking. Pulse operation has been achieved for both anomalous and normal dispersion of the laser cavity owing to broadband characteristics of carbon nanotube saturable absorber. The laser delivered 1.65 ps pulses in net anomalous dispersion regime. In normal dispersion regime, the laser delivered 14 ps pulses which could be compressed to 1.2 ps using external fiber compressor.

Bismuth-doped fibers as new type of laser medium are attracting attention due to their unique optical properties, which provide a way for the development of efficient optical devices (lasers, optical amplifiers, etc.) operating in broad spectral region from 1.1 to 1.8 μm[1]. Excluding wavelengths near 1550 nm, this spectral region remains rather uncovered because of the absence of optical transitions in fibers doped with rare-earth ions and other dopants[2]. Although at ~1550 nm there exist a great variety of efficient fiber lasers and amplifiers based on erbium-doped fibers, the practical gain in these fibers is limited to a relatively narrow spectral window between 1530–1560 nm. Outside of this region, the efficiency of the devices is decreased significantly. To date there has been significant progress in the field of development of Bi-doped fibers which has led to fabrication of the fibers producing gain in a broad wavelength range. As a result, continuous-wave (CW) fiber lasers, optical amplifiers and superluminescent sources based on bismuth fibers operating in the wavelength range from 1.15 to 1.55 μm have been successfully developed (see e.g.[3] and references therein). The efficiency and output power of this type of fiber lasers could reach higher than 60% and 20 W, respectively.

Recently it was shown that using of high-GeO_2 silica-based fiber doped with bismuth the spectral range of amplification could be extended to long-wavelength region from 1.6 to 1.8 μm[4]. Thereafter, CW bismuth-doped fiber lasers operating in 1.625–1.775 μm and providing a watt-level power output have been demonstrated[5]. This spectral region is very attractive for many applications, including tomography[6], gas sensing[7] and remote control. Moreover, human tissues containing lipids show a peak of absorption at ~1720 nm, absorption by fat exceeding the absorption caused by water at this wavelength. This allows selective targeting of tissues containing lipids, and could be exploited for example in different skin treatments[8].

In addition to CW bismuth-doped fiber lasers, mode-locked lasers operating at all major wavelengths covered by CW bismuth fiber lasers have been demonstrated. Most of the demonstrations have been based on passive mode-locking using semiconductor saturable absorber mirrors (SESAMs) as mode-lockers[9–12]. Moreover, mode-locking at 1180 nm using a carbon nanotube (CNT) absorber has been demonstrated in[13], where the authors reported generation of 558 ps and 4.7 ps pulses in anomalous and normal dispersion regimes, respectively. Recently, we demonstrated a 1.45 μm pulsed bismuth fiber system operating in normal dispersion regime and producing 240 fs pulses, using carbon nanotubes as a saturable absorber[14]. In this paper, we report the first mode-locked bismuth-doped fiber laser operating at 1.7 μm, extending the mode-locked operation of bismuth fiber lasers to cover the long-wavelength gain region of bismuth-doped fibers. CNT saturable absorber has been used successfully to obtain pulse generation in both anomalous and normal cavity dispersion regimes.

Results

Single-mode active medium was composed of a bismuth-doped fiber with an equal content of GeO_2 and SiO_2 in a core. The fiber preform was fabricated by a standard modified chemical vapor deposition (MCVD) process. The fiber with 125-μm diameter and cutoff wavelength of 1.2 μm was drawn from the preform after additional jacketing made at the same drawing speed. Bismuth concentration in the fiber core glass was ~0.02 wt.%. The absorption spectrum of bismuth-doped fiber with two characteristic bands is presented in Fig. 1. The absorption bands peaked at 1.4 and 1.65 μm caused by the formation of bismuth-related active centers are associated with

[1]Optoelectronics Research Centre, Tampere University of Technology, Korkeakoulunkatu 3, 33720 Tampere, Finland. [2]Fiber Optics Research Center, Russian Academy of Sciences, 38 Vavilov Street, 119333 Moscow, Russia. [3]Ulyanovsk State University, L. Tolstoy str. 42, 432017 Ulyanovsk, Russia. Correspondence and requests for materials should be addressed to T.N. (email: teppo.noronen@tut.fi)

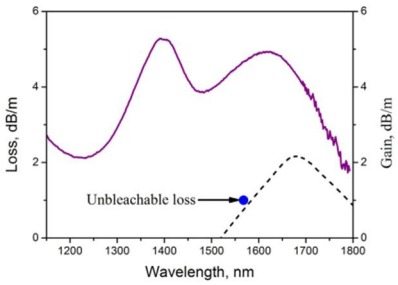

Figure 1. Absorption and gain spectra of bismuth-doped fiber are plotted by solid and dashed lines, respectively. Unbleachable loss level at 1.55 μm is indicated as a point.

Si and Ge, respectively. The optical properties of these bismuth-related active centers can be found in detail in[15], where the study is focused on the optical properties of the bismuth-doped fiber primarily for a spectral range of 1.6–1.8 μm. First, the loss measurements were carried out at 1.56 μm as a function of pump power. The residual loss level shown in Fig. 1 is ~1 dB/m, corresponding to the small signal absorption of 22%. The high level of unbleachable loss is due to the relatively high concentration of bismuth ions required for laser with a short cavity length. Figure 1 illustrates the gain spectrum of bismuth-doped fiber pumped at 1.46 μm. The highest small-signal gain of ~2 dB/m was observed at the wavelength 1.7 μm for pump power of ~200 mW.

Two single-walled carbon nanotube (SWNT) saturable absorbers were prepared for the mode-locking experiments. The carbon nanotubes were produced by thermal composition of ferrocene in the presence of carbon monoxide at ambient pressure[16]. SWNTs were collected onto a nitrocellulose filter during the fabrication, so that a thin SWNT-film was formed onto the filter surface. The carbon nanotube film was then transferred onto a silver mirror by pressing the filter and SWNT-film (SWNT-film side down) against the mirror surface. The carbon nanotube film was strongly adhered on the mirror surface as a result of applied pressure, after which the remaining filter was peeled off leaving a pure SWNT-film on the mirror surface. The other saturable absorber mirror was fabricated by stacking two layers of SWNT-film onto a mirror, whereas the other absorber consisted of three layers of SWNT-film. As it is well known, major drawbacks of CNT-absorbers are their relatively high non-saturable losses and low ratio of modulation depth to the non-saturable loss[17]. Particularly in case of fiber lasers, a stable mode-locking needs sufficient value of modulation depth, whereas the fiber lasers can often tolerate considerable amount of non-saturable losses because of usually high values of gain. Therefore, multiple layers of carbon nanotube film were needed to increase the modulation depth of the absorber, although this unavoidably increased the non-saturable losses of the absorber as well. At least two layers of SWNT-film were found to be vital in order to achieve stable mode-locked operation and suppress the parasitic continuous wave oscillations, which were encountered when using an absorber with just one layer of SWNT-film.

The optical properties of carbon nanotubes are dependent on the diameter of the nanotubes[18]. The diameter of the used nanotubes ranged from about 1.2 nm to 1.8 nm, meaning that the nanotubes were slightly larger than often used for absorbers for pulsed lasers at ~1500 nm wavelength[19,20]. The linear absorption of a SWNT-film was measured by transferring a single layer of carbon nanotube film onto a quartz glass substrate, and the absorption spectrum was recorded by a spectrometer which covered the working wavelength range from 175 to 3300 nm. An uncoated substrate was used as a reference to exclude the effect of the substrate and light source. The linear absorption of a one SWNT-film is shown in Fig. 2(a). For used CNT-absorbers exploiting two/three layers of carbon nanotube film, the linear absorption is about two/three times the absorption of a one layer, respectively. This leads to linear absorption values of about 10% and 15% at 1700 nm for the two used absorbers.

The nonlinear optical properties were measured at 1700 nm wavelength by using pump-probe spectroscopy[21]. The normalized nonlinear reflectivity of the absorber equipped with two layers of CNT is presented in Fig. 2(b) showing the modulation depth of ~3.7%. The nonlinear reflectivity of the second absorber is estimated to be slightly higher. Compared for example to recent work in[19] and[22], the modulation depth of the absorber is lower compared to the previously reported value of ~11%. Moreover, the authors report saturation intensities considerably lower than that of the absorbers used in this work.

After the fabrication of fibers and preparation of saturable absorbers, a mode-locked bismuth fiber laser operating at 1.7 μm was studied for two dispersion regimes. The cavity is shown schematically in Fig. 3. In anomalous dispersion regime the cavity comprises 5 m long active fiber with normal dispersion and 19 meters of standard telecom fiber used for dispersion compensation. The dispersion management ensures the operation in net anomalous dispersion regime with a total cavity dispersion of ~0.35 ps/nm. The pump radiation at 1565 nm from continuous-wave erbium fiber laser is launched through a dichroic 1560/1730 nm pump coupler. One end of the cavity is terminated by a saturable absorber with two layers of CNT-film, while another cavity end is terminated by a fiber loop mirror directing 35% of the signal to the output. Residual pump is filtered out using two selective couplers placed at the output port of the laser. Above 300 mW of pumping power, a stable mode-locked operation of the laser has been regularly observed. The spectra and corresponding autocorrelation in anomalous-dispersion soliton regime are presented in Fig. 4.

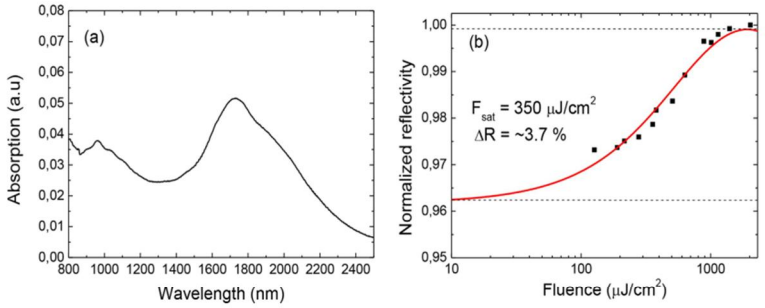

Figure 2. (**a**) The linear absorption of a single SWNT layer. The fabricated two saturable absorber mirrors exploited two and three layers of SWNT layers stacked one on another, increasing the both the linear and nonlinear absorption of the absorber. (**b**) The normalized nonlinear reflectivity of the absorber equipped with two layers of SWNT film.

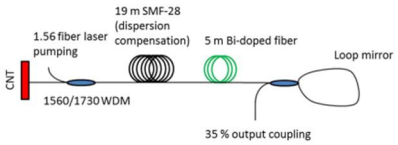

Figure 3. The schematic of the mode-locked bismuth fiber laser operating in the anomalous dispersion regime.

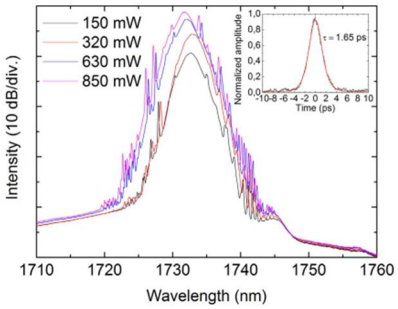

Figure 4. The spectra at different pump powers and the autocorrelation trace (inset) of the output pulse for the cavity operating in anomalous dispersion regime.

The pulse spectrum centered at 1730 nm has the bandwidth of 2.91 nm, as seen from Fig. 4. The laser produces 1.65 ps sech^2-pulses with time-bandwidth product of 0.48 indicating nearly transform-limited pulse quality. The slight deviation from the transform limited quality is because of the chromatic dispersion in relatively long fiber pigtails at the laser output. With an increase of pump power, the laser demonstrates a strong tendency to multiple-pulse operation, which is a typical dynamics of a soliton laser operating with net anomalous dispersion cavity. The multiple pulse instability is a dominant mechanism limiting the pulse energy scaling in conservative soliton systems. For the start-up of the pulse operation corresponding to the pump power of 300 mW ("on-threshold" of mode-locking), the pulse repetition rate is ~200 MHz, though the fundamental repetition rate is only ~4 MHz. The laser exhibits a large hysteresis of pulse operation, since the mode-locking is switched off only after the pump power is decreased to below 75 mW, which is marked as "off-threshold" in Fig. 5. With increasing the pump power, the laser tends to produce stable harmonic mode-locked operation with well-defined pulse periods (Fig. 6), contrary to soliton bunching and grouping phenomena often observed in fiber lasers operating

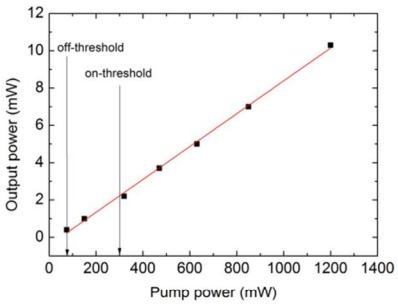

Figure 5. The average output power versus pump power. The pulsed operation develops when pump power is increased to 300 mW ("on-threshold"). When decreasing the pump power, the pulsed operation is maintained until the pump power is decreased below 75 mW ("off-threshold").

Figure 6. The pulse trains for different pump powers.

in anomalous dispersion regime. Regarding the stability of the pulse train, for many applications the property known as timing jitter is important, since it describes the deviations in temporal pulse positions compared to a perfectly regular pulse train. Timing jitter of the laser was not measured. However, we note that timing jitter is provoked by the cavity and pumping instabilities, and therefore in case of free-running passively mode-locked laser timing jitter can be relatively high compared to laser systems where special care has been taken to reduce the timing jitter.

The cavity dispersion was then changed to normal dispersion regime by reducing the length of additional intracavity anomalous dispersion fiber from 19 meters down to 10 meters, resulting in the net normal dispersion of −0.1 ps/nm. It was found that larger value of modulation depth and absoprtion was required to maintain stable pulse operation in normal dispersion regime. Thus, a mirror comprising three layers of CNT-film was used as a saturable absorber for the normal dispersion cavity, while the modulation depth of two layers was sufficient for the net anomalous dispersion cavity. We note that it is possible to use the same absorber for triggering mode-locking in both anomalous and normal dispersion regimes, as demonstrated for example in[23]. Indeed, it was observed that the absorber with higher nonlinearity was capable of triggering mode-locking in anomalous dispersion regime as well. However, the performance of the laser was optimized by using an absorber with lower absorption value in anomalous dispersion regime.

For the normal dispersion, a single pulse operation was observed after increasing the pump power over "on-threshold" of pulse regime. The pulse operation could be maintained until the pump power was decreased below the "off-threshold" value, showing hysteresis behavior comparable to the anomalous dispersion regime. The hysteresis phenomenon and multiple pulse formation in cavities with normal dispersion have been observed and are discussed more detailed for example in[24]. In our laser the threshold for possible multiple pulse operation was not reached in normal dispersion regime. Figures 7 and 8 present characteristics of the single pulse train,

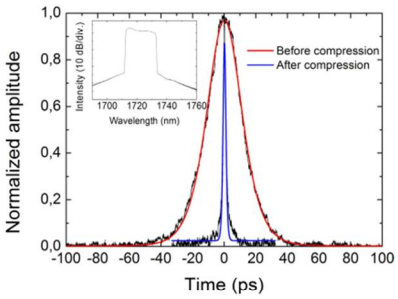

Figure 7. The autocorrelation traces of the pulse with normal cavity dispersion before the compression (red) and after the external pulse compression (blue). The spectrum is shown as an inset. The pump power is 170 mW.

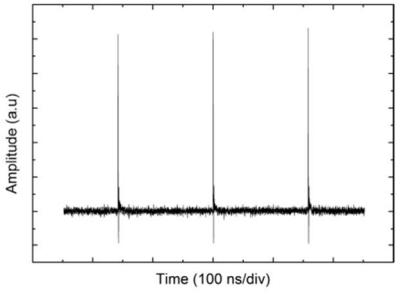

Figure 8. The single-pulse train from the normal dispersion cavity.

revealing 14-ps pulses with ~20 nm spectral bandwidth. The pulses are highly chirped as expected for a cavity with normal dispersion. With further increase of the pump power, the optical spectrum exhibits essential broadening and some instability of the pulse train was developed.

Finally, the compressibility of the pulse was studied by adding standard telecom fiber (SMF-28) to the output of the laser. Figure 7 shows the pulse characteristics before compression (red curve) and after propagation through 70 m of SMF-28 fiber (blue curve). The output pulse width of 1.2 ps assuming $sech^2$-fitting indicates an efficient compression of the pulse. Further compression of the pulse would require optimization of the compressor and transform-limited pulse width of ~160 fs could be approached with optimized length of the fiber. However, in practice the shortest pulse duration is limited by the chirp nonlinearity.

Conclusion

In conclusion, we have demonstrated a mode-locked bismuth doped fiber laser operating in 1.7 μm spectral range. Pulse operation has been demonstrated using carbon nanotube (CNT) as a broadband saturable absorber for the laser cavity with both anomalous and normal dispersion. In anomalous dispersion regime nearly transform limited pulses with pulse duration of 1.65 ps were achieved; however, the pulse energy was limited by the multiple pulsing developed with increasing pump power. In normal dispersion regime the laser operated in a stable single-pulse regime producing 14 ps pulses, which could be compressed down to 1.2 ps using an external fiber compressor. It can be therefore concluded that the mode-locked bismuth-doped fiber lasers are capable to operate at long-wavelengths of 1.75 μm, representing an attractive pulse source suitable for numerous applications.

References

1. Dianov, E. M. Bismuth-doped optical fibers: a challenging active medium for near-IR lasers and optical amplifiers. *Light Sci. Appl.* **1,** e12 (2012).
2. Dussardier, B. & Blanc, W. Novel dopants for silica-based fiber amplifiers. *Optical Fiber Communication Conference and Exposition and The National Fiber Optic Engineers Conference*, Mar 2007, Anaheim, United States, Optical Society of America, paper OMN1 (2007).
3. Bufetov, I. A. *et al.* Bi-doped optical fibers and fiber lasers. *IEEE J. Sel. Topics Quantum Electron.* **20,** 0903815 (2014).

4. Firstov, S. V. *et al.* Bismuth-doped optical fibers and fiber lasers for a spectral region of 1600–1800 nm. *Opt. Lett.* **39,** 6927–6930 (2014).
5. Firstov, S. V. *et al.* Watt-level, continuous-wave bismuth-doped all-fiber laser operating at 1.7 μm. *Opt. Lett.* **40,** 4360–4363 (2015).
6. Kawagoe, H. *et al.* Development of a high power supercontinuum source in the 1.7 μm wavelength region for highly penetrative ultrahigh-resolution optical coherence tomography. *Biomed. Opt. Express.* **5,** 932–943 (2014).
7. Chambers, P., Austin, E. A. D. & Dakin, J. P. Theoretical analysis of a methane gas detection system, using the complementary source modulation method of correlation spectroscopy. *Meas. Sci. Technol.* **15,** 1629–1636 (2004).
8. Anderson, R. R. *et al.* Selective photothermolysis of lipid-rich tissues: a free electron laser study. *Lasers Surg. Med.* **38,** 913–919 (2006).
9. Dianov, E. M. *et al.* Mode-locked Bi-doped fiber laser. *J. Opt. Soc. Am. B* **24,** 1807–1808 (2007).
10. Kivistö, S. *et al.* Pulse dynamics of a passively mode-locked Bi-doped fiber laser. *Opt. Express* **18,** 1041–1048 (2010).
11. Gumenyuk, R. *et al.* 1.32 μm mode-locked bismuth-doped fiber laser operating in anomalous and normal dispersion regimes. *Opt. Letters* **38,** 4005–4007 (2013).
12. Gumenyuk, R. *et al.* Effect of absorption recovery in bismuth-doped silica glass at 1450 nm on soliton grouping in fiber laser. *Sci. Rep.* **4,** 7044 (2014).
13. Kelleher, E. J. R. *et al.* Bismuth fiber integrated laser mode-locked by carbon nanotubes. *Laser Phys. Lett.* **7,** 790–794 (2010).
14. Noronen, T. *et al.* All-bismuth fiber system for femtosecond pulse generation, compression and energy scaling. *Opt. Lett.* **40,** 2217–2220 (2015).
15. Firstov, S. V. *et al.* Combined excitation-emission spectroscopy of bismuth active centers in optical fibers. *Opt. Express* **19,** 19551–19561 (2011).
16. Moisala, A. *et al.* Single-walled carbon nanotube synthesis using ferrocene and iron pentacarbonyl in a laminar flow reactor. *Chem. Eng. Sci.* **61,** 4393–4402 (2006).
17. Martinez, A. & Sun, Z. Nanotube and graphene saturable absorbers for fibre lasers. *Nature Photon.* **7,** 842–845 (2013).
18. Weisman, R. B. & Bachilo, S. M. Dependence of optical transition energies on structure for single-walled carbon nanotubes in aqueous suspension: an empirical Kataura plot. *Nano Lett.* **3,** 1235–1238 (2003).
19. Han, D. *et al.* Simultaneous picosecond and femtosecond solitons delivered from a nanotube-mode-locked all-fiber laser. *Opt. Lett.* **39,** 1565–1568 (2014).
20. Hasan, T. *et al.* Nanotube-polymer composites for ultrafast photonics. *Adv. Mater.* **21,** 3874–3899 (2009).
21. Fleischhaker, R., Krauß, N., Schättiger, F. & Dekorsy, T. Consistent characterization of semiconductor saturable absorber mirrors with single-pulse and pump-probe spectroscopy. *Opt. Express* **21,** 6764–6766 (2013).
22. Liu, X. & Cui, Y. Flexible pulse-controlled fiber laser. *Sci. Rep.* **5,** 9399 (2015).
23. Cui, Y. & Liu, X. Graphene and nanotube mode-locked fiber laser emitting dissipative and conventional solitons. *Opt. Express* **21,** 18969–18974 (2013).
24. Liu, X. Hysteresis phenomena and multipulse formation of a dissipative system in a passively mode-locked fiber laser. *Phys. Rev. A* **81,** 023811 (2010).

Acknowledgements

The research was partly supported by the Technopark Mordovia and by Academy of Finland under project 269121. Ulyanovsk State University support through joint project is acknowledged. The authors would like to thank Albert Nasibulin for providing the carbon nanotube samples.

Author Contributions

T.N. and O.G.O. designed the experimental setup and analyzed the data. T.N. made the actual laser measurements. S.F. and E.D. contributed to the development and characterization of this type of Bi-doped fiber, T.N., O.G.O. and S.F. wrote the manuscript, which all authors reviewed.

Additional Information

Competing financial interests: The authors declare no competing financial interests.

How to cite this article: Noronen, T. *et al.* 1700 nm dispersion managed mode-locked bismuth fiber laser. *Sci. Rep.* **6**, 24876; doi: 10.1038/srep24876 (2016).